NASA Contractor Report 4693

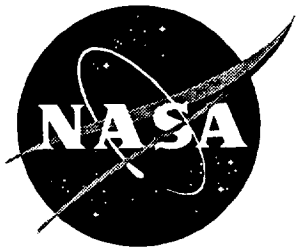

Analysis of Systems Hardware Flown on LDEF—New Findings and Comparison to Other Retrieved Spacecraft Hardware

Harry Dursch and Gail Bohnhoff-Hlavacek
Boeing Defense & Space Group • Seattle, Washington

Donald Blue
Georgia Tech Research Institute • Atlanta, Georgia

Patricia Hansen
NASA Goddard Space Flight Center • Greenbelt, Maryland

National Aeronautics and Space Administration
Langley Research Center • Hampton, Virginia 23681-0001

Prepared for Langley Research Center
under Contract NAS1-19247

September 1995

Printed copies available from the following:

NASA Center for AeroSpace Information
800 Elkridge Landing Road
Linthicum Heights, MD 21090-2934
(301) 621-0390

National Technical Information Service (NTIS)
5285 Port Royal Road
Springfield, VA 22161-2171
(703) 487-4650

FOREWORD

This report describes the work accomplished under "LDEF Systems Special Investigation Group Support" contract NAS1-19247, Task 18 (October 1994 through February 1995). Sponsorship for this program was provided by National Aeronautics and Space Administration, Langley Research Center, Hampton, Virginia.

Ms. Joan Funk, NASA Langley Research Center (LaRC), was the NASA Contracting Officer's Technical Monitor. Dr. James Mason, Goddard Space Flight Center (GSFC), was both the System Special Investigation Group (SIG) Chairman and the NASA Task Technical Monitor. Mr. Harry Dursch, Boeing Defense & Space Group (BD&SG), was Program Manager. The following BD&SG personnel provided support during this program:

Harry Dursch	Program Manager
Gail Bohnhoff-Hlavacek	Optics, Optical Scatter, and Optical Database
Dr. Gary Pippin	Materials
Dr. Peter Gruenbaum	Solar Cells and Electronics
Brenda Wilson	LDEF Archive Office

The Systems SIG funded NASA GSFC personnel to perform a Long Duration Exposure Facility (LDEF) contamination study. Dr. Philip Chen, NASA GSFC, managed this activity and Ms. Patricia Hansen and Ms. Katherine Southall performed the study. A summary of their findings is presented in this document.

The Systems SIG also funded Dr. Donald Blue, Georgia Tech Research Institute (GTRI), to update his previous findings on the effects of the LDEF environment on optical materials. His report, titled "Degradation of Optical Materials in Space," is presented in this document.

TABLE OF CONTENTS

TABLE OF CONTENTS
(continued)

FIGURES

TABLES

ACRONYM LIST

AO	Atomic Oxygen
AR	Anti-Reflection
BD&SG	Boeing Defense & Space Group
BRDF	Bi-directional Reflection Distribution Function
BTDF	Bi-directional Transmittance Distribution Function
CAA	Chromic Acid Anodize
CCD	Charge Coupled Device
CCHP	Constant Conductance Heat Pipe
CIRRIS	Cryogenic InfraRed Radiance Instrument for the Shuttle
COSTAR	Corrective Optics Space Telescope Axial Replacement
DHP	Diode Heat Pipe
EECC	Environment Exposure Control Canisters
ESA	European Space Agency
EOIM-III	Energetic Oxygen Interactions with Materials
EPS	Electrical Power Systems
FRECOPA	French Cooperative Passive Payload
GSFC	Goddard Space Flight Center
GTRI	Georgia Technical Institute of Research
HEPP	Low Temperature Heat Pipe Experiment Package
HRSM	High Resolution Scatter Mapping
HST	Hubble Space Telescope
ISS	International Space Station
JSC	Johnson Space Center
KSC	Kennedy Space Center
LaRC	Langley Research Center
LDEF	Long Duration Exposure Facility
LED	Light Emitting Diode
LEO	Low Earth Orbit
M/D	Meteoroid and Debris
MMH	MonoMethyl Hydrazine
MSFC	Marshall Space Flight Center
MSX	Midcourse Space Experiment
NASA	National Aeronautics and Space Administration
NCSA	National Center for Supercomputing Applications
NDI	Normalized Detector Irradiance
NVR	Non-Volatile Residue
PEARLSS	Particulate Effects Analysis Response Levels Spaceborne Sensors
PI	Principal Investigator
QCM	Quartz Crystal Microbalance
SADE	Solar Array Drive Electronics
SAEF-II	Spacecraft Assembly and Encapsulation Facility
SBV	Space Based Visible
SEM	Scanning Electron Microscope
SIG	Special Investigation Group
SMM	Solar Maximum Mission
SP-HVDE	Space Plasma - High Voltage Drainage Experiment
SPQCM	Superpolished Quartz Crystal Microbalance
SS	Stainless Steel
SSM	Second Surface Mirror
TGS	Triglycine Sulphate
ULE	Ultra Low Expansion
WF/PC	Wide Field Planetary Camera
XPS	X-ray Photoelectron Spectroscopy

1.0 EXECUTIVE SUMMARY

The Systems Special Investigation Group (Systems SIG) was chartered to investigate the effects of the extended mission on both the Long Duration Exposure Facility (LDEF) systems and experiment systems and to coordinate and integrate all systems analysis. In April 1992, the Systems SIG published a summary report titled "Analysis of Systems Hardware Flown on LDEF - Results of the Systems Special Investigation Group." The 1992 300-page report described LDEF and the LDEF mission, the various space environments seen by LDEF, and all systems related findings through 1991 (ref. 1). A 5-page excerpt from reference 1's Executive Summary discussing the status of systems findings through 1991 is reprinted in Appendix A of this document. In addition, an electronic LDEF Optical Experiments Database was also created that contained a file for each of the LDEF experiments that possessed optical hardware. Each file contains various fields that identify the optical hardware flown, describes the environment seen by the hardware, summarizes experimenter findings, and lists references for further information. A paper copy of the Optical Materials database was contained in the 1992 report.

The Systems SIG was funded in FY 1994 to update the 1992 report with any new system-related findings. This report, titled "Analysis of Systems Hardware Flown on LDEF - New Findings and Comparison to Other Retrieved Spacecraft Hardware," is a result of this activity. Over the past 3 years additional LDEF systems related information has become available from a wide variety of sources including information presented at the NASA Langley Research Center (LaRC)-sponsored 2nd and 3rd LDEF Post-Retrieval Symposiums and the NASA Marshall Space Flight Center (MSFC) sponsored LDEF Materials Results for Spacecraft Applications Conference. In addition, an ongoing literature search was being conducted by Boeing Library Technical Services so that any publication with LDEF related information was identified and abstracts obtained.

Dr. Donald Blue, GTRI, was funded by the Systems SIG to further document recent LDEF optical findings and to compare these findings to findings from analysis of other retrieved spacecraft optical hardware. Dr. Blue was principal investigator (PI) for the LDEF experiment, titled "Effects of Long Duration Exposure on Active Optical System Components," and author of several papers on the effects of the low-Earth-orbit (LEO) environment on LDEF optical hardware. His report titled "Degradation of Optical Materials in Space" is presented in Section 6.0.

A report titled "Effect of Long Duration Space Exposure on Optical Scatter" in Section 7.0 discusses the effect of space environmental effects on induced optical scatter. Although a great deal of work has gone into analyzing individual LDEF experiments by LDEF PIs, the optical scatter information is spread throughout several published reports, related ground simulation tests, and Special Investigation Group studies, and has never been reviewed in its entirety. This report, formatted as a stand-alone document, summarizes the published data and included related optical scatter work from more recent space missions.

NASAGoddard Space Flight Center (GSFC) personnel were funded to perform a molecular and particle contamination survey of LDEF and compare their findings to predicted values using existing contamination modeling codes. A summary of GSFC's findings are presented in Section 8.0.

The Optical Materials Electronic Database was also updated to include the most recent findings on LDEF experiments that contained optical materials. The database is current, with published experimental findings through the end of 1994, including the Third LDEF Symposium. An electronic copy, along with an users guide, is available by contacting the LDEF Archive Office. The increased size of the database precluded including a paper copy with this document.

The following paragraphs summarize the latest System SIG findings. Also included is comparison of LDEF system findings to results from other retrieved hardware including Hubble Space Telescope (HST) and optical materials flown on Shuttle experiments. Findings presented in this Executive Summary are discussed in more detail in Sections 3.0 through 8.4.

General Observations

Analysis of the more recent LDEF system results, along with post-flight test results from retrieved HST hardware, continue to show the primary cause of on-orbit system anomalies or inadequate system performance to be poor design, poor workmanship, and/or lack of adequate pre-flight testing. With the exception of on-orbit contaminated optics, effects of the LEO space environment on system performance has proven to be negligible. However, this finding should be tempered by the fact both spacecraft received relatively low radiation dosages. The higher charged-particle exposure associated with higher inclination orbits (such as International Space Station's 51.6° inclination) could have an impact on systems. These impacts include an increase in the frequency of single event upsets (for similar shielding thicknesses) and accelerating the degradation of solar cell/solar array power outputs.

With the exception of one heat pipe thermal/vacuum test, all mechanical, electrical, and thermal system and subsystem testing was completed in time to be documented in the April 1992 Systems SIG summary report (see Appendix A and ref. 1 for previous results). The vast majority of new LDEF systems related findings involve the analysis of optical hardware and the study of the effects of molecular and particulate contamination on optical hardware. Over the last 3 years several LDEF PIs have continued their investigation into determination of optical degradation mechanisms.

Mechanical

Previous Systems SIG findings showed that no structural related metallic adhesion had occurred on LDEF (refs. 1 & 2). Over the last 3 years, two minor cases of metallic seizure have been reported by LDEF PIs. One instance involve indium washers cold-flowing into adjoining aluminum and/or glass surfaces. This occurred on 16 flight assemblies but no assembled ground control specimens existed for comparison (ref. 3). Because of indium's low melting temperature and solubility, it is expected that this adhesion would have occurred on ground assemblies subjected to the same temperatures and contact pressures as the assemblies flown on LDEF. The second case of adhesion involved seizure between steel springs and aluminum backing plates (ref. 4). Microscopy revealed transfer of aluminum to the spring. It is speculated that the adhesion was caused by fretting of the two mating surfaces which was induced by launch vibrations and/or thermal cycling. While neither of the two cases of adhesion were critical, they both point out the need to select the correct mating materials and surface treatments.

Previously reported loss of MoS_2 dry film lubricant exposed on a trailing edge tray proved to be erroneous. More detailed examination of pre-flight documentation showed that the lubricant was never applied to the stainless steel substrates.

Electrical

Testing and analysis of solar cells and solar array materials comprised the majority of new electrical hardware information generated over the last 3 years. Results continue to show the robustness of covered silicon and gallium arsenide cells in low-inclination LEO environments. LDEF results have verified the selection of solar array materials planned for use on international Space Station (ISS). Two documents (refs. 5 & 6) were recently published summarizing all LDEF solar cell findings.

A concept for a large area space based phased array antenna was evaluated on LDEF's space end. In addition to passively exposing potential antenna materials, the experiment was designed to study the issue of the interaction between high voltage and LEO plasma. This was accomplished by recording discharges initiated across high voltage electrodes. Very few discharge events were recorded with only one 3 kV discharge and eleven 1.5 kV discharges being recorded. There was no evidence of any single-event upsets and there was no charring of the Kapton or other damage visible at the electrode gaps (ref. 7).

Thermal

The most extensive post-flight LDEF system functional test was performed on the LDEF experiment, "Low Temperature Heat Pipe Flight Experiment" (HEPP) in December 1992. The HEPP was removed from its tray, installed into a test fixture, and underwent thermal/vacuum testing. This test was performed to simulate actual flight conditions, enabling the acquisition of temperature data for comparison with orbital data and correlation with thermal model predictions. Results show that the hardware performed as it had 14 years ago. The failure of the HEPP to obtain the desired on-orbit temperatures was attributed to an apparent error in the the original thermal model that overestimated the HEPP radiator's cooling capacity.

Optics

Significant progress has been made in understanding the various degradation mechanisms associated with optical materials flown on LDEF. Over the last 3 years numerous papers have been published containing analysis of LDEF optical material results. These findings have been added to the LDEF Optical Database and collated by Dr. Blue for the Systems SIG in his report titled "Effects of Long Duration Exposure on Active Optical System Components" (printed in its entirety in Sec. 6.0). Findings continue to show that most optical components survived quite well, and space-induced degradation was not a significant influence on most post-retrieval properties. Molecular contamination of exposed optical surfaces by outgassed material was the major influence on optical property degradation, leading to significant transmission loss in the ultraviolet spectral region.

The effects of optical scatter, caused by micrometeoroid and debris impacts, atomic oxygen (AO), ultraviolet (UV) radiation, and contamination, are discussed in Sec. 7.0 in a report titled "Effect of Long Duration Space Exposure on Optical Scatter." This report includes results from LDEF, other recent missions such as HST, and ground based testing. Results show off-axis optical scatter due to contamination increased by about a factor of 10 on mirror surfaces. The potential exists for large increases in optical scatter for unshielded optics on the leading edge (ram) from meteoroid and debris impacts, but only small increases for Earth-looking cases. Recent ground based experiments and modeling have increased understanding concerning the effects of space exposure on optical scatter and have become important spacecraft design tools.

Contamination

There are many theories proposed to explain the sources and mechanisms of the contamination observed on LDEF. While no one theory has explained all the contamination effects observed on LDEF, many of the theories correlate well with the modeling results to explain the sources of contamination on LDEF and the effects of AO and UV radiation. The actual contamination observed on LDEF is due to complex interactions with the space environment and LDEF materials. Analytical modeling results, in many cases, confirm actual effects shown on many of the LDEF experiments. Section 8 consists of a report discussing the molecular and particle contamination that occurred on LDEF

Hubble Space Telescope

The return of HST hardware has also added to the understanding of the effects of long term LEO exposure on spacecraft systems hardware. HST was deployed at an altitude of 331.6 nautical miles and 28.5° inclination on April 25, 1990. In December 4, 1993 the Shuttle rendezvoused with the HST at an altitude of 317 nautical miles to service and repair its faulty optical system. The mission included retrieval of several pieces of hardware after over 42 months in LEO. The Wide Field Planetary Camera-I (WF/PC-I) instrument was replaced with an updated version of the same instrument called WF/PC-II. The High Speed Photometer was replaced by the Corrective Optics Space Telescope Axial Replacement (COSTAR) which was designed to correct the spherical aberration in HST's primary mirror. The original solar arrays were replaced with new arrays and one array was returned to Earth. Two rate sensing units (with two gyroscopes each) and two electronic control units were also replaced.

While the WF/PC I was operational at the time of its replacement, several optical surfaces had degraded optical properties (ref. 7). Three components of the WF/PC I underwent spectral transmittance and reflectance testing; the pick-off mirror, aperture window, and the external M1 mirror (see figure 1-1). The pick-off mirror, mounted on an arm that was exposed to the center of HST's interior, showed significant reflectance loss in the vacuum UV region. The aperture window showed the same effect, although not quite so drastic. The MI mirror, located outside the HST near the WF/PC radiator, did not optically degrade. The observed degradation on both the pick-off mirror and aperture window was attributed to a thick molecular contamination layer. The pick-off mirror and aperature window surface facing HST's interior had a measured contaminant layer of 450 and 150 Angstroms, respectively. While the specific source of the contaminant is still unknown, it appears to be a UV-deposited organic with soluble and non-soluble components. The source of the UV is believed to be the Earth's albedo.

Postflight testing of the returned solar array at the European Space Agency revealed that despite thousands of particle impacts there was no indication that any meteoroid or debris impact caused any of the observed anomalies or any power degradation. Electrical related anomalies were observed in both solar array wings. Two were within solar cell strings, but both recovered (annealed) while on-orbit leaving behind burn marks. Another short was traced to a sharp edge on the deployment drum. Postflight testing of the returned array's deployment mechanisms showed nominal operating characteristics. One of the two Solar Array Drive Electronics (SADE) units required replacement due to non-functioning transistors. These units were not designed for on-orbit replacement. During replacement of SADE-1, the astronauts experienced difficulty in handling the small fasteners used to attach the SADE to Hubble's exterior surface. This included having to recapture fasteners that had floated away. Unlike the initial SADEs, the replacement unit was re-designed for future on-orbit servicing.

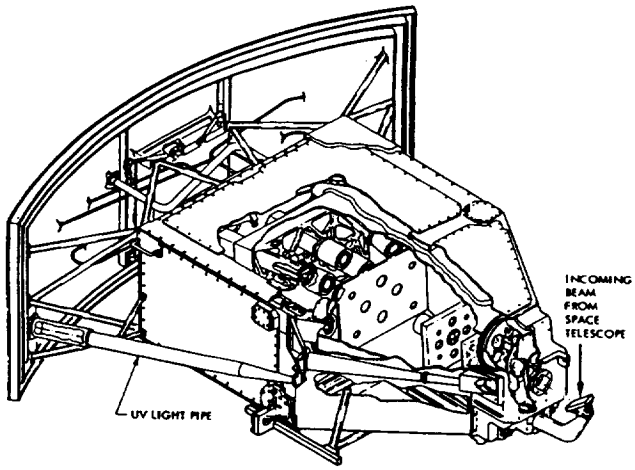

Figure 1-1. The WF/PC-I pick-off mirror and aperture window are in the lower right hand corner.

2.0 LDEF MISSION

LDEF was developed by NASA's Office of Aeronautics and Space Technology and the Langley Research Center to provide a means of exposing a variety of experiments to the LEO environment. LDEF was designed and fabricated at Langley in the late 1970s as a passive satellite which was reusable for planned repeat missions. It was a 14-ft-diameter by 30-ft-long aluminum structure with the cylindrical cross-section of a 12-sided regular polygon. LDEF, weighing 21,400 lb, was placed in orbit by the Space Shuttle Challenger on April 7, 1984 at a 257-nmi nearly-circular orbit with a 28.4° inclination. LDEF was gravity-gradient stabilized and mass loaded so that one end of the LDEF was always pointed at Earth and one side (leading edge, row 9) was always oriented into the orbit path (ram) direction and one side (trailing edge, row 3) was always oriented 180° from ram. Because this orientation remained constant throughout the entire mission, LDEF provided an excellent opportunity to study the effects of the various space environments on materials and systems.

A total of 57 different experiments were flown on LDEF and the experiment objectives ranged from the study of the LEO environment to determining the effect of long-term space exposure on tomato seeds. Because of schedule changes and the loss of Space Shuttle Challenger, LDEF was not retrieved until January 12, 1990 after spending 69 months in LEO. Figure 2-1 is an on-orbit photo of LDEF after being grappled by the Space Shuttle Columbia. During these 69 months, LDEF completed 32,422 orbits of Earth and traveled almost 750,000,000 nmi. The levels of exposure to atomic oxygen and solar ultraviolet radiation as functions of experiment locations on LDEF are shown in figures 2-2 and 2-3, respectively. Following the Shuttle landing at Edwards Air Force Base and the ferry flight to Kennedy Space Center, the deintegration process began. This process was initiated with the removal of LDEF from the Space Shuttle Columbia on January 27, 1990 and ended 4 months later with the LDEF structure being placed in storage.

The extended duration of the LDEF mission, constant orientation to ram, and the successful retrieval presented a unique opportunity to study the long-term effects of space exposure on the more than 10,000 specimens carried on the 57 different experiments. Because of the extended mission length, the science and engineering interest extended beyond the original individual experiment objectives. Four Special Investigation Groups were formed by the LDEF Science Office to assist in the deintegration of LDEF and post-flight analysis of hardware. These four SIGs were the Induced Radiation, Material, Systems, and Meteoroid and Debris SIGs.

The hardware of interest to the Systems SIG included an enormous diversity of systems, subsystems, and components. The management of this hardware was facilitated by division into the four major engineering disciplines represented by LDEF hardware: mechanical, electrical, thermal, and optical. In order to assist the post-flight testing and analysis of LDEF hardware, the Systems SIG developed a set of standardized test plans for each of the four engineering disciplines (ref. 8). These plans were designed to be used by both the Systems SIG or the experimenters in their testing and analysis of systems hardware. These test plans, available through the LDEF Archive Office, have been used in assisting in the post-flight inspection of the retrieved HST hardware.

Beginning with on-site support of the de-integration of LDEF at Kennedy Space Center (KSC), Systems SIG personnel have supported the testing of active system related testing of experiments either at KSC, experimenters facilities, or at Boeing Defense & Space Group (BD&SG) facilities. BD&SG was funded by the Systems-SIG to provide the necessary personnel and facilities required to meet the Systems SIG objectives.

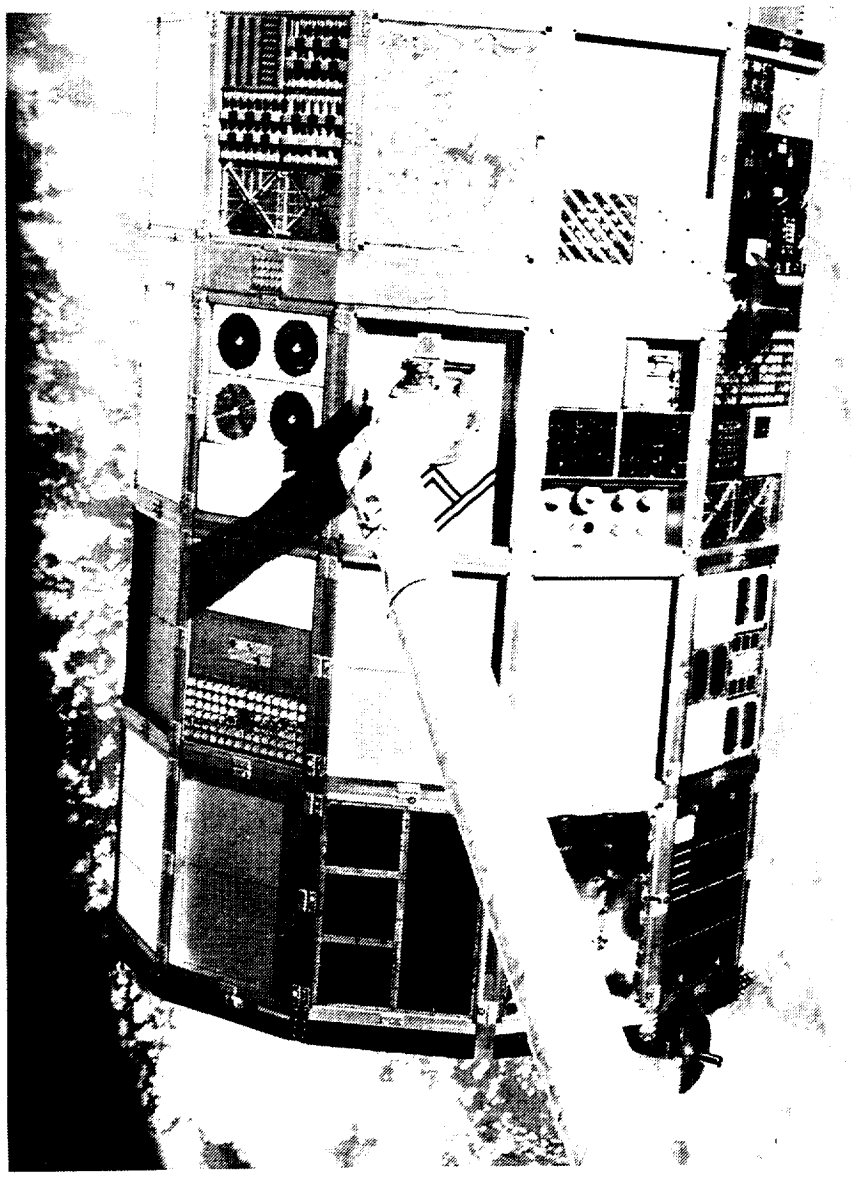

Figure 2-1. On-Orbit Photo of LDEF Being Retrieved by the Space Shuttle Columbia

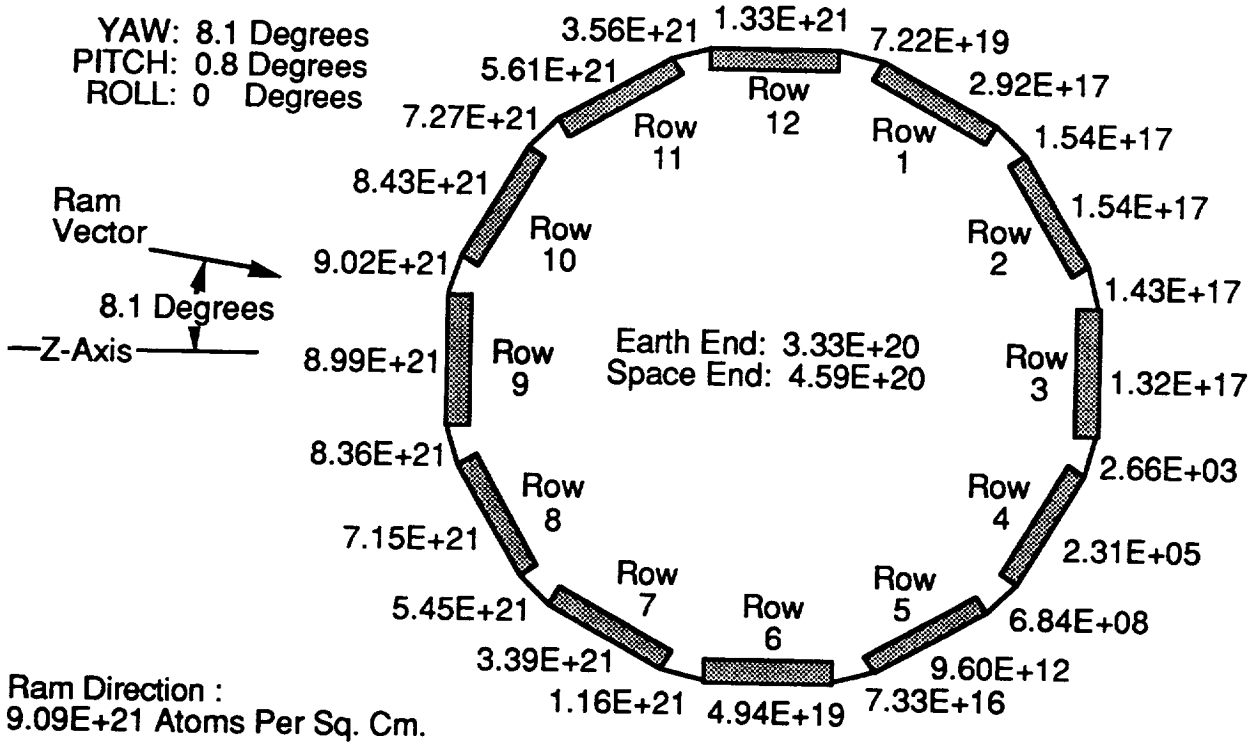

Figure 2-2. Total Atomic Oxygen Dose as a Function of LDEF Experiment Location

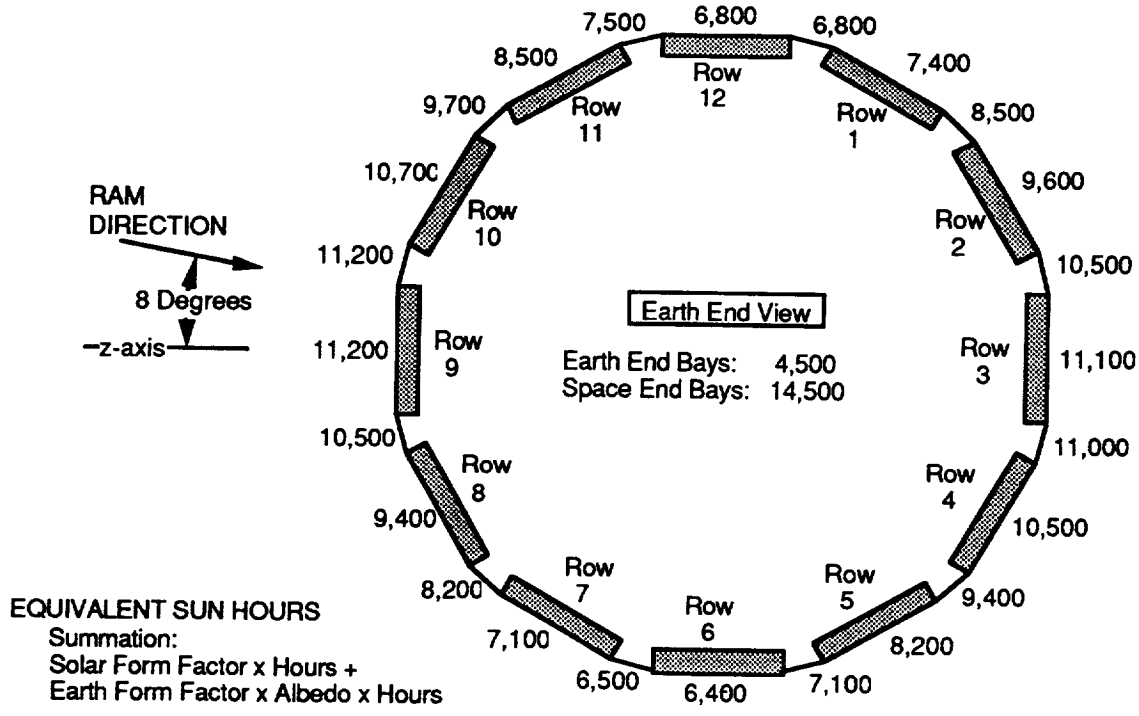

Figure 2-3. Total Equivalent Sun Hours as a Function of LDEF Experiment Location

In April 1992 the Systems SIG distributed a report titled "Analysis of Systems Hardware Flown on LDEF - Results of the Systems Special Investigation Group" (ref. 1). This 300-page report summarized the major Systems SIG findings through 1991. The report contained sections describing LDEF and the LDEF mission, brief summaries of the various LEO environments seen by LDEF, all major findings discussed by the four engineering disciplines, paper copy of the Optical Materials Database, and over 140 references for further details. This document is also available by contacting the LDEF Archive Office.

The Systems SIG was funded in FY94 to update the April 1992 report with all new systems related findings. This report is a result of this activity and provides the final status of the continuing investigation into the effects of the 69-month exposure of LDEF systems to the LEO environment.

2.1 LDEF ARCHIVE SYSTEM

The LDEF Archive System has been designed to provide spacecraft designers and space environment researchers single-point access to all available LDEF related resources (ref. 9). This includes data, photographs, technical reports, and LDEF hardware. The archive system is comprised of two parts. The first part is the physical contents of the archive such as LDEF hardware, documentation, and photographs. The second part is the electronic on-line system available through Internet using public domain, NCSA Mosaic, software. It contains data files, both numerical and graphical image files, micrograph and photograph image files, technical report abstracts, and full text files. Access to the on-line system is through the Internet World Wide Web using the following address:

http://blearg.larc.nasa.gov/org/see/ldef.html

For further information contact the LDEF Archive Office, Hampton, VA at 804-766-8973.

3.0 MECHANICAL HARDWARE

Sections 3.0 through 7.0 document the final status of the investigation into the effects of the 69-month exposure of LDEF systems hardware to the LEO environment. Reference 1 discusses the results obtained during the first 2 years of the LDEF investigations. Sections 3.0 through 7.0 discuss any additional information obtained in the following 3 years of LDEF systems related investigations. Other retrieved spacecraft hardware results, such as HST, and selected ground based test results are also presented.

Mechanical hardware flown on LDEF included the primary structure, fasteners, canisters, grapples, viscous damper, lubricants, seals, and composites. The following paragraphs describe the additional information gathered during the last three years including non-LDEF information that validates LDEF fastener findings

3.1 FASTENERS

The Systems SIG investigated all reported instances of LDEF fastener removal difficulties and in all cases the difficulties were attributed to galling during installation or post-flight removal. The results of the following MIT Lincoln Laboratories test program validated LDEF findings that installation practices were responsible for the galling that led to high removal torques and occasional fastener breakage.

MIT Lincoln Laboratories undertook a test program to minimize creation and spread of metallic particles generated from use of the nearly 1000 fasteners required on the Space Based Visible (SBV) instrument package (ref. 10). This experiment was initially scheduled to be launched in October 1993 but now is scheduled for May 1995. Mission requirements include high stray light rejection and low BRDF optics, a type of design which is extremely sensitive to particulate contamination. The following paragraph summarizes Lincoln Lab's findings:

Testing of precision cleaned series 300 stainless steel (SS) fasteners mounted in non-locking SS key inserts showed creation of appreciable contamination during installation. The contamination level significantly increased upon shaking the same bolting arrangement at flight qualification vibration levels. During post-test removal, 30 percent of the fasteners seized and broke. In comparison, SS fasteners electroplated with gold and silver showed light particulate contamination and were easily removed. Two classes of fastener lubrication were also investigated: solids and low-outgassing liquids. Results showed a 10 percent solution of oil in freon performed the best at preventing galling and minimizing particle contamination (after immersion of a fastener in the solution, the freon evaporates leaving behind a thin film of oil). Other forms of lubrication provided similar results but were quite expensive compared to the oil/freon solution. In addition, the SS fastener alloy was changed from the 300 series to A286 which is harder and stronger resulting in fewer contamination particles. The inserts were nonlocking (locking inserts generated excessive particles), therefore a locking mechanism was required. The least contaminating design was found to be elongated strips of KEL-F thermoplastic material embedded in the fastener threads. The authors state that in-flight measurements will be available to assess the low BRDF performance on the SBV primary mirror. These measurement will provide a sense of whether the effort to minimize particulates have been successful.

3.2 LUBRICANTS, GREASES, AND SEALS

Several lubricants, greases, and seals had their characterization completed over the last 3 years. The following paragraphs summarize these new findings. Reference 11, titled "Evaluation of Seals and Lubricants Used on LDEF," June 1994, discusses the description and findings for all the seals and lubricants flown on LDEF.

Everlube 620C (Dry Film MoS_2). Initial findings led us to believe the six 0.5" dia x 0.25" thick stainless steel buttons, flown on tray D3, had been coated with Everlube 620C. Post-flight testing and analysis had determined that no 620C existed on the 0.5" dia buttons. This apparent loss of lubricant in an exposed trailing edge environment was reported to the LDEF community in several reports (including the 1992 Systems Report) and presentations. More detailed examination of pre-flight documentation and photographs show the buttons were never coated with the Everlube 620C.

Braycote 601. Castrol Braycote 601 was used to lubricate the four drive shafts which opened and closed the AO187-1 canisters. The drive shafts were located on tray A3's exterior surface but saw minimal UV exposure due to canister shadowing. As reported in the '92 Systems Report, initial post-flight chemical analysis suggested changes in the 601 had occurred including degradation of the PTFE filler, lowering of the base oil viscosity, and a change in endotherms. However, further analysis showed the initial analysis had included residual solvent used to extract the Braycote from drive shafts. It has been determined that some slight differences had occurred between flight and non-flight material, but were likely caused by traces of moisture and/or contamination. Castrol reported no significant change in the temperature at which decomposition begins or in the relative levels of base oil to thickener, indicating the Braycote 601 was unchanged.

Molykote Z and Vapor Deposited MoS_2. LDEF experiment AO138-10 (located trailing edge tray B3) was a static experiment consisting of stacks of 1"-dia washers machined from various metals representative of spacecraft mechanisms. Eight columns of six pairs of washers (total of 48 washer pairs) were loaded together with various contact pressures. Three of the washer pairs had one mating surface with Molykote Z (Dow Corning product) and another three pairs had one mating surface coated with vapor deposited MoS_2. Ground based specimens were kept loaded under vacuum throughout LDEF's mission. The experimenter's objective was to evaluate the tendency of various metals to coldweld and to the determine the effect of MoS_2 lubricants on coldwelding. No coldwelding occurred on any flight or ground specimens. No additional lubricant results have been reported. Additional experiment details are found in refs. 1 & 11.

Air-Cured MoS_2 (per MIL-L-23398). This lubricant was used on several components on each of the five NASA provided Environmental Exposure Control Canister (EECC). The lubricant was applied to the Belleville washers, drive shafts, and linkages of each canister. No visual changes were noted for the lubricant on the drive shafts and linkages. Sixteen of the washers were removed from a trailing edge EECC for evaluation. Results showed burnished areas and areas of buildup. No abnormal wear was observed. Areas of lubricant thinning, often to bare metal, were present on some of the convex surfaces. However, none of these effects were attributed to the 69-month exposure to the LEO trailing edge environment (ref. 11).

Butyl Seals Used on the EECCs. Butyl seals were used to seal the drawers on the five EECCs. Except for the first 9 months the drawers were open and the seals were shielded from the external spacecraft environment. Analysis consisted of comparing post-flight leak rates to pre-flight values. Increased rates were noted for two of the three canisters analyzed. However, it is unlikely that atomic oxygen was the cause for the increased rates for the two leading edge canisters as the atomic oxygen (AO) fluence for the first nine months was only 2.3×10^{20} atoms/cm^2. Results discussed in detail in reference 11 suggest that outgassing contaminants might have interfered with the on-orbit resealing of the drawers.

3.3 METALLIC SEIZURE

Indium/Aluminum. Indium washers were used for thermal transfer between the rear filter and an aluminum holding plate on Experiment AO147. Figure 3-1 shows a cross-section of the filter assemblies and the location of the indium washers (item 7 in figure 3-1). Sixteen of these assemblies were flown on the leading edge tray E-9. Difficulty was experienced in trying to remove the filters from their aluminum mounts (ref. 3). Initially it was thought that the epoxy used on the perimeter of the filters to bond two filters together had flowed, resulting in holding the filters in place. However, it was found that the indium washers had formed a bond between the bottom of the glass filter and aluminum mount. Machining of the aluminum was required to remove the glass filters.

Reference 12 notes that metals such as aluminum and copper can diffuse rapidly into indium at normal temperatures because of indium's low melting point. Molten indium readily adheres to many materials, including nonmetals such as aluminum oxide and quartz. Indium is soft and ductile and forms large contact areas, and it flows more readily than other metals under compressive force. It is speculated that the indium, which was under pressure from the spring washer holding the filters in place, had cold-flowed into both glass and aluminum forming a low tensile strength bond. No assembled ground controls existed to determine whether the indium adhesion would have occurred in a terrestrial environment. Indium solders are used for bonding nonmetallic materials. They will coat glass and other non-metallic materials when the molten solder is gently rubbed against the surface of the nonmetallic. These solders have melting temperatures as low as 250°F. Pure indium has a melting point of 315°F. The actual indium content of the washers is unknown. The PI also noted evidence of high temperatures within the filter stacks which would have contributed to the flow/adhesion of the indium washer. It is expected that this phenomenon would have occurred on ground based assemblies subjected to the same temperatures and contact pressures as the 16 assemblies flown of Experiment AO147.

Aluminum/Steel Seizure. During the continued examination of the French Cooperative Passive Payload (FRECOPA) LDEF experiment hardware, it was found that several steel springs had become stuck to adjoining small aluminum plates (ref. 4). Steel springs were used to hold an aluminum plate in position (the aluminum plates were used as specimen backing plates). A total of 57 spring/backing plate assemblies were used on this trailing edge experiment. The FRECOPA deintegration team noted that several (4 or 5) of these assemblies had adhered to each other. Both the steel and aluminum were untreated and neither alloy is known. The experimenters noted the force needed to separate the two materials was slight and could not be measured. Electronic microscopy revealed a transfer of matter with aluminum being found on the spring (figure 3-2). No ground control assemblies exist.

It is speculated by BD&SG personnel that this steel/aluminum adhesion was caused by fretting of the two mating surfaces. Fretting is a wear phenomenon that can occur between two tight-fitting surfaces subjected to a cyclic relative motion of extremely small amplitude. This motion could have been caused by launch induced vibrations and/or thermal cycling. One stage of the fretting process is adhesion between fretting surfaces by the formation of bonded junctions between asperities of the mating surfaces. If the two mating surfaces are of dissimilar metals, the softer metal's oxide film will be disrupted resulting in transfer of the softer material to the harder material. This explains the transfer of the aluminum to the steel spring. A study on aluminum showed that if the oxide coating remained intact, adhesion would not occur in vacuum (ref. 13). As soon as the oxide coating was removed, a metallic bond with a strength of approximately 25 percent of the applied compressive stress was formed. If coatings and/or oxide films can remain intact through on-orbit cycling, adhesion between the two mating surfaces should not occur. *While the intermetallic adherence of the steel/aluminum assemblies flown on FRECOPA was not critical, it does point out the importance of the correct surface treatment of mating surfaces.*

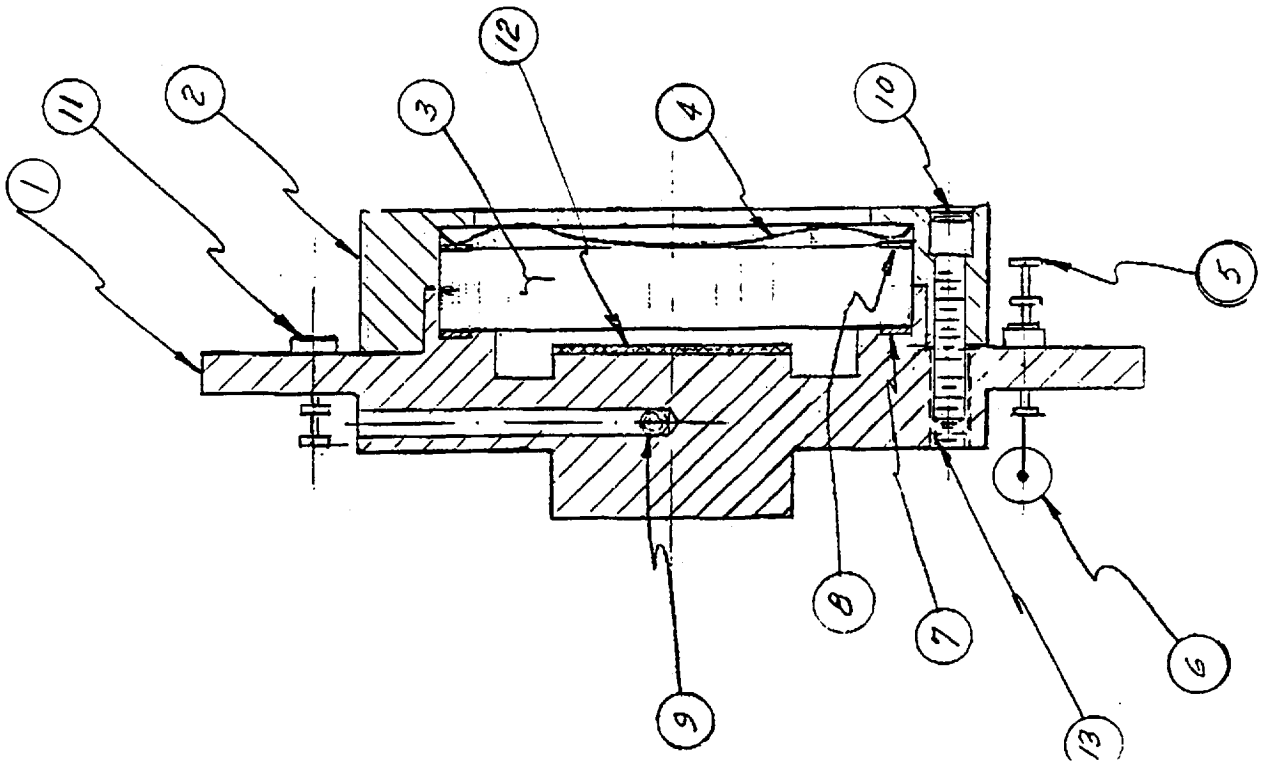

Figure 3.1 Cross-Section of AO147 Filter Assembly - Item #7 is the Indium Washer, #3 the Glass Filter, and #1 the Aluminum Base Plate.

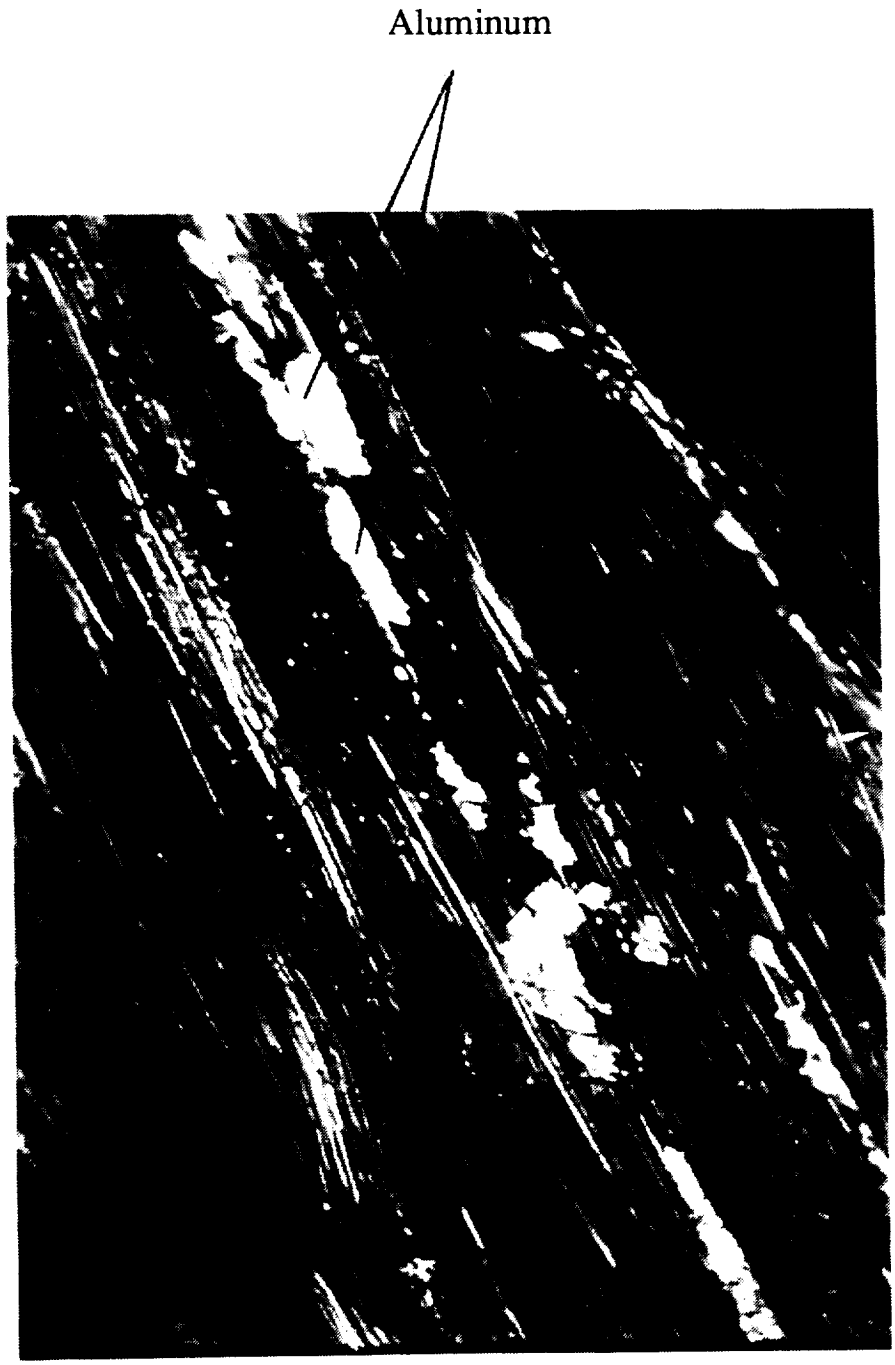

Figure 3.2 Photomicrograph Showing Transfer of Aluminum to Steel Spring (Photograph Courtesy of Christian Durin)

4.0 ELECTRICAL HARDWARE

A wide variety of electrical and electronic systems and hardware were used on LDEF. NASA provided certain guidelines and design review requirements, but success or failure of the individual experiments was the responsibility of the PIs. The vast majority of electrical systems and hardware was characterized during the first couple of years following LDEF's return to Earth. The following paragraphs contain any additional findings that have occurred during the last 3 years.

4.1 DIELECTRIC MATERIALS

The Space Plasma - High Voltage Drainage LDEF Experiment (SP-HVDE) consisted of two identical experimental trays located on near leading and near trailing edges (trays B10 and D4, respectively). The objective was to compare the effects of ram and wake spacecraft environments on dielectric materials and solar cells. Kapton samples of varying thicknesses (2 to 5 mils) were maintained at ±300, ±500, and ±1000 volts, and the leakage current through the cells was measured; in addition, each tray carried two solar cell strings, each biased at either 300 volts or -300 volts (ref. 14).

The Kapton experiments were set up as follows: a voltage was placed across the Kapton films, and this was connected to a coulombmeter that measured the overall charge that passed through the film. By dividing by the battery lifetime (233 days), an average leakage current was obtained. One would expect lower currents for thicker films, and higher currents for high voltages, but in general, this pattern was not observed. For the positively-biased samples, only the 3-mil samples showed the trend of higher currents with higher voltages, whereas the 5-mil samples showed a decreased current at 1000 volts, and there was no clear trend for sample thicknesses. For the negatively-biased samples, the leakage currents are lower by a factor of 3 than for the positively-biased samples. These samples showed only small variations of leakage current with bias voltage and film thickness. The authors suggested that with negative bias the current may be caused by localized electro-discharged events.

The flown solar cells were compared to identical control cells. Both the leading and trailing edge solar cell modules showed less than 2 percent overall degradation, except for one module which was damaged by a micrometeoroid/debris impact, and showed a 10 percent loss. During flight, the metal interconnect strips between the cells of each module were exposed to the space plasma and provided a path for leakage current. This current was measured with coulombmeters in a similar fashion to the Kapton samples, but no conclusions were drawn from the data.

In summary, the SP-HVDE results show no clear trend for positively-biased Kapton films exposed to space plasma under voltage. Negatively-biased samples had less leakage current than positively-biased samples, and showed little variation with respect to film thickness and bias voltage. Solar modules showed very little degradation, except when damaged by a micrometeoroid/debris impact.

4.2 SPACE-BASED PHASE ARRAY ANTENNA CONCEPT

The primary objective of the LDEF experiment titled "Effect of Space Environment on Space Based Radar Phased Array Antenna", located on LDEF's space end, was to determine the performance of materials chosen for large area space antenna concepts (ref. 7). The principal material was Kapton which had been selected for the load-bearing dimensionally critical structure in the phased-array antenna plane. Roughly one-half of this LDEF experiment was occupied by tension assemblies containing panels of Kapton and glass/Kapton maintained at one of four stress levels. The remainder of the tray contained a portion of the proposed antenna plane

and active electronic components. The components included a high voltage power supply, timing control circuitry, and a memory system. This part of the experiment was designed to determine discharges triggering across high voltage electrodes and to determine the effects of the subsequent high voltage discharge events on the Kapton of the antenna plane. The electrodes (two each at 1.5 and 3.0 kV) were formed from knife-edge cuts in copper diode elements bonded to the outer antenna plane.

The experiment was designed to record discharges initiated across the spark gaps by environmental interactions, such as contaminant transport and/or coupling to the space plasma. Very few discharge events were recorded during the time the experiment was active (day 32 to day 243). One 3kV discharge and 11 1.5 kV discharges were recorded. There was no evidence of any single-event upsets and there was no charring of the Kapton or other damage visible at the electrode gaps. Creep measurements of the Kapton and glass Kapton showed little or no significant differences between flight space specimens and the flight control specimens. As was expected, the exposed Kapton surfaces were degraded due to the space end atomic oxygen environment.

4.3 SOLAR CELLS

Analysis of solar cells and solar array materials flown on LDEF continued over the last 3 years with several LDEF PIs published papers (refs. 16 through 18). Continued comparison of post-flight current-voltage characteristics with pre-flight data for covered silicon and gallium-arsenide solar cells continue to show little or no changes. The vast majority of meteoroid and debris impactors were typically of small size and of high energy but their impacts resulted in minimal electrical degradation. Results continued to show that cells covered with polymer-type materials exhibited higher cell performance degradation than cells mounted with more conventional glass covers. In addition, the glass covers appeared to provide additional protection against incident micrometeoroid or debris (ref. 17).

Reference 5 discusses the results from analysis of all published LDEF solar cell data. The data are compared to each other as well to other published solar cell flight data. The results from LDEF support the selection of solar cells and solar array material for ISS. Although the exact type of silicon solar cell being used by ISS was not flown on LDEF, similar silicon cells performed well, and the wrap-through contacts should avoid the problems that some of the wrap-around cells had on LDEF. Copper interconnects were a good choice because they will not be eroded in the same way as exposed silver interconnects. It should be noted that ISS's higher inclination of 51.6° (compared to LDEF's and HST's inclination of 28.5°) will result in a higher charged particle exposure that is very sensitive to altitude. The 5-mil thick coverglass will absorb protons of energy less than 4 MeV; the number of protons greater than 4 MeV is expected to be higher by a factor of two to eight at a 60° inclination, depending on the altitude. Only the low energy electrons will be affected by the 5-mil coverglass; the total number of electrons is expected to be higher by a factor of two to ten at a 60° inclination, again depending on altitude.

An excellent source for all LDEF solar cell data is contained in reference 6. This document provides detailed solar cell descriptions and comparison of pre-flight and post-flight electrical characteristics for all published data.

Applicability of LDEF solar cell and solar array data to the design of ISS's Electrical Power System (EPS) components and materials selection is discussed in reference 19. The conclusions reached by this 1991 study included (1) most of the anomalies associated with related EPS hardware (batteries, relays, solar cells, solar array materials, etc.) flown on LDEF were design limitations and were not component or material failures; (2) major emphasis must be placed on atomic oxygen protection; and (3) effects of synergistic contamination/atomic oxygen/ultraviolet/thermal cycling environment place an emphasis on contamination control.

One of the most significant findings from the investigation into returned HST hardware and the post-flight analysis of the Eureca spacecraft is the robustness of the solar arrays. ESA reports no power loss on either HST or Eureca arrays that is associated with meteoroid or debris (M/D) impacts. The returned HST array contained over 25,000 solar cells. Post-retrieval inspection showed 22 additional coverglass cracks not associated with M/D impacts. Particle impact counts were performed by ESA personnel on the HST array. A total of 3862 impact features greater than 100 to 200 microns were recorded. These impacts resulted in 1316 cracked coverglasses and 738 damaged silicon solar cells. Despite these numerous impacts and resulting physical damage, the overall array power degradation of 3 percent was less than expected. ESA personnel did notice an interesting phenomena associated with increased discoloration (contamination?) on the array surface associated with increased current collection.

5.0 THERMAL HARDWARE

The following heat pipe discussion summarizes the only thermal system component testing that has occurred over the last 3 years.

5.1 HEAT PIPES

Constant Conductance Heat Pipes. The LDEF experiment, "Low Temperature Heat Pipe Experiment Package (HEPP)," located on tray F12, was designed to evaluate the performance of two different heat pipes and a low-temperature (182K) phase change material. The HEPP did not cool below 188.6K during the LDEF mission. As a result, the preprogrammed transport test sequence which initiates when the phase change material (n-heptane) temperature drops below 180K was never activated. Therefore, in-flight transport tests with both heat pipes, and the diode reverse test could not be run. Because n-heptane has a melt temperature of 182K, its freeze/thaw behavior could not be evaluated on-orbit.

The heat pipes were an axially grooved aluminum constant conductance heat pipe (CCHP) and a stainless steel axially grooved liquid trap diode heat pipe (DHP). Both heat pipes use ethane as the working fluid for operation in the range of 150K to 250K. N-heptane was the phase change material. Reference 20 contains (1) a detailed experiment description and (2) on-orbit, post-flight, and post-flight thermal-vacuum test results. A summary of these test results, including the cause of HEPP not cooling below the desired temperature, follows:

Both flight and ambient post-flight testing showed all electrical systems were functioning properly after retrieval and that the mechanical and thermal integrity of the HEPP were intact. Following the functional test at KSC during deintegration, HEPP was removed from its LDEF tray and underwent thermal vacuum testing at NASA GSFC. This experiment was the only known LDEF hardware to undergo post-flight thermal vacuum testing. These results showed the n-heptane canister, constant conductance heat pipe, and the diode heat pipe were all performing as they had 14 years ago. The phase change material froze at a temperature only 1K higher than was measured 15 years ago, well within instrumentation accuracy. The failure of the HEPP to obtain the desired temperatures was attributed to an apparent error in the original thermal model that overestimated the HEPP radiator's cooling capacity due to "radiative parasitics from the LDEF's interior not properly coupled to the HEPP's radiator and shields". This resulted in a prediction of a higher heat rejection rate and a faster cooldown. This condition was simulated in the thermal/vacuum tests by cooling the chamber walls with liquid nitrogen to eliminate parasitic input from the chamber. The results were exactly as predicted with the original thermal model and substantiate where the modeling error occurred. The authors also state that if pre-flight thermal vacuum testing had been performed with HEPP integrated on LDEF (lack of time and resources made this impossible), the problem might have been discovered and the flight program sequence adjusted to accomplish all objectives.

5.2 REFERENCES (FOR SECTIONS 1 THROUGH 5)

1. Dursch, H. W., Spear, W. S., Miller, E. A., Bohnhoff-Hlavacek, G. L., and Edelman, J., "Analysis Of Systems Hardware Flown On LDEF - Results Of The Systems Special Investigation Group," NASA CR-189628, Contract No. NAS1-19247, April 1992.

2. Dursch, H. W., and Spear, S., "On-Orbit Coldwelding - Fact or Friction?", *LDEF 69 Months in Space; First LDEF Post-Retrieval Conference*, NASA CP-3134, January 1992.

3. Hickey, J. R.,Brinker, D.J., and Jenkins, P., "Studies of Effects on Optical Components and Sensors: LDEF Experiments A0-147 (ERB Components) and S-0014 (APEX)", *LDEF 69 Months in Space; Second LDEF Post-Retrieval Conference*, NASA CP-3194, April 1993.

4. Durin, C., Berthoud, L., and Mandeville, J.C., "System Results from FRECOPA", *LDEF 69 Months in Space; Third LDEF Post-Retrieval Conference,* NASA CP-3275, February 1995.

5. Gruenbaum, Peter, and Dursch, H.W., "Space Environmental Effects on Solar Cells: LDEF and Other Flight Tests", *LDEF 69 Months in Space; Third LDEF Post-Retrieval Conference*, NASA CP-3275, February 1995.

6. Hill, David C., and Rose, M.F., "Summary of Solar Cell Data from LDEF", NASA Contract NAS8-39131-DO#17, October 1994.

7. Whiteside, J. B., et. al, "Effects of 69 Months in Low Earth Orbit on Kapton Antenna Structures", Journal of Spacecraft and Rockets, Vol. 35, No. 5, September 1994.

8. Feinberg, L., et al, "HST Returned Hardware Evaluation Symposium Proceedings", NASA GSFC, December 15, 1994.

9. Dursch, H. W., "LDEF Systems Special Investigation Group Investigation Plan", Boeing Defense & Space Group, February 1990.

10. Wilson, Brenda, "LDEF Archive System", *LDEF 69 Months in Space; Third LDEF Post-Retrieval Conference,* NASA CP-3275, February 1995.

11. Morelli, M.D., and Forman, S.E., "Prevention of Particulate Contamination from Fasteners on the Space-Based Visible Telescope", SPIE Vol. 1754, Optical System Contamination, 1992.

12. Dursch, H. W., Keough, B., and Pippin, H.G., "Evaluation of Seals and Lubricants Used on the Long Duration Exposure Facility", NASA CR-4604, June 1994.

13. Barnard, R. W. and Pasternak, J.P.; "Stable Low Resistance Contacts to Aluminum Conductors" & "Effects of Interdiffusion on the Properties of Indium Plated Contacts", Bell Telephone Laboratories, 1974.

14. Bable, H.W., David, K.E., and Jones, C.A, "Material Considerations for Space Station Freedom", 41st Congress of the International Astronautical Federation, October 1990.

15. Yaung, J.Y., Wong, W.C., and Blakkolb, B.A, "LDEF SP-HVDE Post-Flight Results: Leakage Current and Discharge, *LDEF 69 Months in Space; First LDEF Post-Retrieval Conference*, NASA CP-3134, January 1992.

16. Brinker, D.J., Hickey, J.R., and Scheiman, D., "The Effects of the Low Earth Orbit Environment on Space Solar Cells: Results of the Advanced Photovoltaic Experiment (S0014)", *LDEF 69 Months in Space; Second LDEF Post-Retrieval Conference*, NASA CP-3194, April 1993.

17. Stella, P.M., "LEO Effects on Candidate Solar Cell Cover Materials", *LDEF 69 Months in Space; Second LDEF Post-Retrieval Conference*, NASA CP-3194, April 1993.

18. Young, L.E., "Impact of LDEF Photovoltaic Experiment Findings Upon Spacecraft Solar Array Design and Development Requirements", *LDEF Materials Results for Spacecraft Applications*, NASA CP-3257, December 1993.

19. Christie, Robert J., Lu, C.Y., and Aronoff, I., "Applicability of LDEF Environmental Effects Data to the Design of Space Station Freedom Electrical Power System", AIAA Journal (AIAA-92-0848), January, 1992.

20. McIntosh, R., McCreight, C., and Brennan, P., "LDEF Low Temperature Heat Pipe Experiment Package (HEPP) Flight Results", *LDEF 69 Months in Space; Second LDEF Post-Retrieval Conference*, NASA-CP 3194, April 1993.

6.0 OPTICAL HARDWARE - DEGRADATION OF OPTICAL MATERIALS IN SPACE

The following report was authored by Dr. Donald Blue, GTRI, under contract to the Systems SIG. This report summarizes optical related findings that have occurred during the 5 years of testing and analysis of LDEF optical systems and hardware. The report is a continuation of Dr. Blue's ongoing documentation of the effects of the LEO environment on LDEF optical hardware. Results from other retrieved spacecraft hardware including HST and various Shuttle experiments are also discussed.

6.1 FILTERS / MIRRORS / WINDOWS

Several issues are of concern regarding the effects of space exposure on optical filters, mirrors, and windows. These issues include radiation effects, the effects of temperature and temperature cycling, atomic oxygen effects, micrometeoroid and orbital debris impacts, contamination including locally generated condensates, exposure-induced optical scatter, and material choices for substrates, dielectric layers, and coatings. In particular, the LEO environment places great stress on materials and components.

In Section 6.1 effects of radiation on these optical components and effects related to temperature and temperature cycling are discussed. The remaining issues will be discussed in later sections.

6.1.1 Radiation Effects

High-energy radiation effects should not be significant for the majority of space applications involving optical hardware. Earth orbits which require that the satellite spend extensive time in the Van Allen radiation belts will be exceptions. Interplanetary spacecraft will receive much lower radiation doses during passage through the radiation belts. Nicoletta and Eubanks (ref. 1) measured the effects of a flux of 2.7×10^{13} electron/cm^2 on two different optical filters. The electron energies ranged from 0.3 MeV to 1.5 MeV. The effects were minor compared to damage from subsequent ultraviolet radiation. No effects of high-energy radiation from the space environment were reported as altering properties of optical components on the LDEF (charge coupled devices are the exception), and none were reported in a review of optical materials and experiments in the LDEF Space Optics Handbook (ref. 2). A report by Blue and Roberts (ref. 3) reviewed previous reports on the effects of radiation on optical filters. While UV irradiation may damage organic-based cements and materials resulting in decreased transmission, damage to nonorganic optical materials has not been reported.

There are three broad classes of high-energy particles which are of concern: galactic and solar cosmic rays, particles trapped in the Earth's magnetosphere, and energetic electrons. Energetic particles can also produce Cerenkov radiation in optical elements, stimulating optical sensors with intensities rivaling signals produced from other sources such as stars.

Extremely energetic cosmic rays, though rare compared to other forms of high-energy radiation for orbiting spacecraft, cause "single-event upsets," a disturbance to which digital electronics are particularly susceptible. Protons trapped in the Earth's radiation belts have produced similar effects.

The principal mechanisms of radiation damage in solids are ionization and atomic (lattice) displacement. Charged particles such as protons, deuterons, and helium ions mainly interact with the atomic electrons in the solid. Because atoms are much bigger than nuclei, interaction with the atomic nucleus is much less probable. For charged particles much heavier

than the electron, little change in direction and little change in energy are suffered by the particle. The struck electron may well be knocked out of the atom, producing an ion and a free electron. Chemical bonds may be broken. Free radicals or new chemical species may be produced. Cosmic rays, though uncharged, cause similar effects in solids.

High-energy electrons also induce excitation and ionization in stopping media in the same way, although up to half the energy of the incoming electron may be lost in each encounter and a considerable deflection may result. In contrast, neutrons, being uncharged, behave in a quite different manner. Neutrons interact only weakly with electrons (the magnetic moments of the particles causing the interaction), and the slowing down of fast neutrons in matter is caused almost entirely by collisions with the atomic nuclei. While the neutrons produce little ionization while slowing down, the struck nuclei may be knocked out of their position in a lattice or molecule and will produce some ionization as they slow down.

Electrons and ions produced by these events can be trapped at lattice flaws or other local low-energy positions where they may change the absorption spectra from the infrared to the ultraviolet region in the material. Browning or other discoloration may result, and an optical element may become severely degraded as a result of irradiation.

The general unit of radiation used to express an absorbed or delivered dose is the rad. The rad may be defined as a radiation dose equal to the absorption of 100 ergs/gram at the point of interest. The rad applies to any material and to any radiation. The unit is sometimes referenced to silicon equivalent dosage using the term rad(Si). However, for most materials rad and rad(Si) do not differ by significant amounts, and the term rad will be used almost exclusively in the following reviews.

High levels of radiation (10^{13} neutron/cm^2, 10^5 rad gamma) have reduced relative transmission in glasses and epoxies (refs. 4 & 5). Use of plastic injection-molded domes, optics, and windows is common in many different electro-optical systems. Radiation-induced breakage of molecular bonds is an issue of concern for these materials. The review of radiation effects by Blue, McMillan, and Liu (ref. 4) cites unpublished work at Harry Diamond Laboratories indicating no change in transmission of Lexan after irradiation of 10^4 rad gamma. As will be discussed, studies of radiation effects in laser diodes and LEDs do not indicate damage to the encapsulating plastic domes or windows, but rather show the effects of radiation damage to the semiconductor device itself. Typical levels of radiation for these studies are 10^7 rad gamma and 10^{12} neutrons/cm^2. Again, levels of radiation this high should not be encountered for the majority of space-based sensors. Radiation damage effects should not begin to appear until a radiation dose of at least 1/3 Mrad or greater has been accumulated.

Materials such as quartz, calcite, and glasses suffer a loss in transmission when subjected to sufficiently high radiation doses. Transmission losses occur first in the UV region, and are similar to the effects of contamination on these materials as will be discussed for the LDEF satellite results. Figure 6-1 shows a typical example. This figure shows the transmittance of a 1-mm thick fuzed quartz window irradiated in a continuous output nuclear reactor as reported by Suzuki et al (ref. 6). The authors state that transmission was measured to a wavelength of 2.5 microns, but transmittance was unaffected at wavelengths longer than 800 nm. A recent publication by Liepmann (ref. 7) reviews the effects of Co^{60} gamma radiation on the transmission and index of refraction of several optical glasses. For the UV spectral region, fluorophosphate glasses with low impurity content are of interest. Radiation effects in these glasses have been reported (ref. 8). Fogdall and others at Boeing Defense & Space have reported studies of irradiation of optical coatings and mirrors (ref. 9), multilayer coated mirrors (ref. 10),

and a general literature search (ref. 11). The results of these simulations were in good agreement with the experimental results obtained from the LDEF and other satellites.

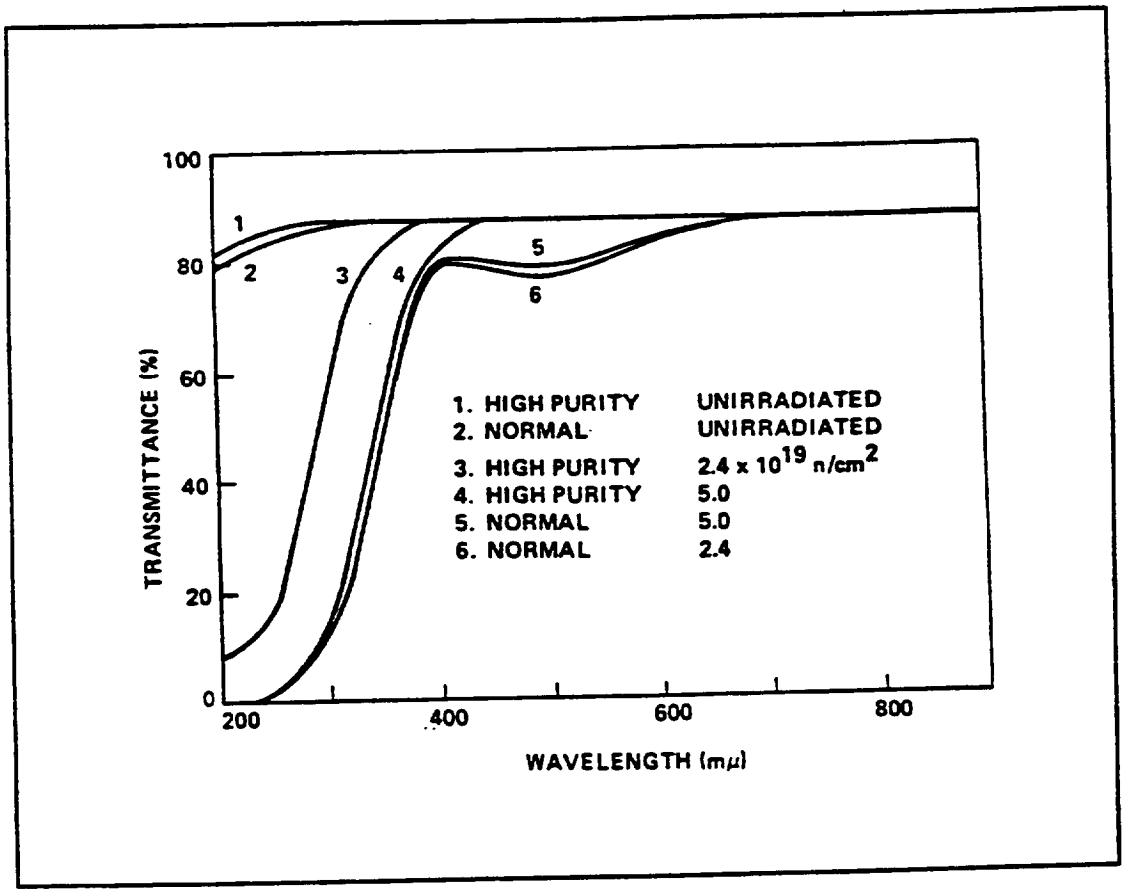

Figure 6-1. Optical Transmission of Fused Quartz (ref. 6) Irradiated by Neutrons at a Temperature of Approximately 500°C.

6.1.2 Temperature Cycling

Temperature cycling of optical components is similar to repeated high-temperature anneals. If the component properties are sensitive to such temperature cycling, performance changes will occur. Filters and mirrors composed of multilayer dielectric stacks exhibited such effects on the LDEF.

Narrow-band interference filters and mirrors aboard LDEF showed evidence of reduced transmittance, small shift of center wavelength, and bandpass broadening (refs. 4, 12 - 14). The magnitude of this shift, often only a few nanometers of wavelength, is unimportant in many cases, but can be significant in narrow-band systems. Multilayer dielectric stacks are quite sensitive to changes in layer thickness, layer index of refraction changes, or alteration of the index step at layer interfaces.

Figure 6-2 shows the spectral transmission for a visible-spectrum narrow-band interference filter both before and after exposure to the space environment, and illustrates these effects (ref. 3). Figure 6-3 shows prelaunch and postrecovery transmission of a narrow-band filter designed for the long-wave infrared region, which shows the same shift of peak transmission toward shorter wavelengths (ref. 12). These effects also have been observed for filters designed for the UV region. Figure 6-4 shows transmission of a narrow-band filter from the FRECOPA experiment (ref. 13) This experiment contained 20 filters, mirrors, antireflection coatings, and beam splitters for use in the visible, infrared, and UV regions. Results for two filters are presented in figure 6-4, one looking into the LDEF interior (dashed lines), and the other exposed directly to the surrounding space environment (solid lines).

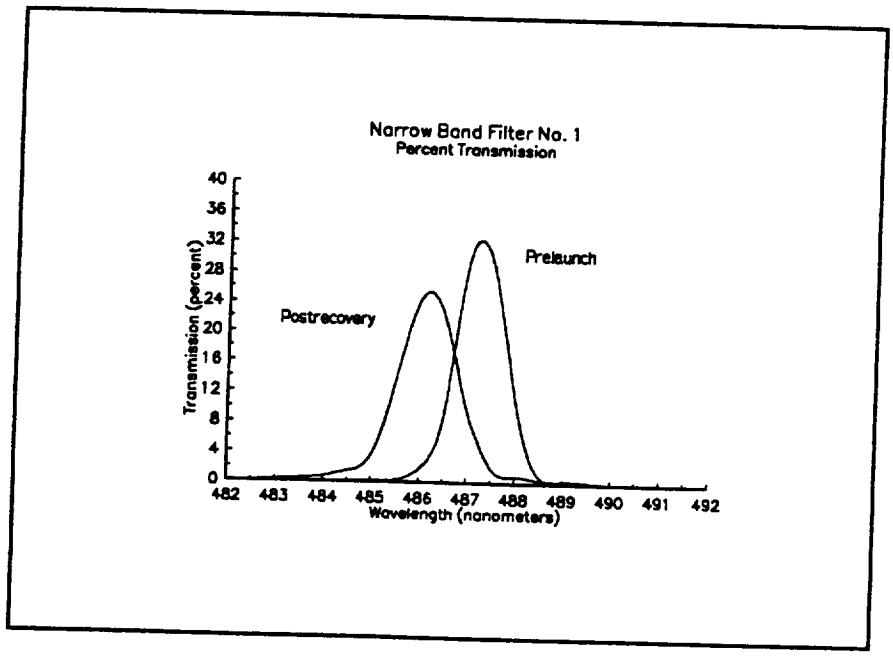

Figure 6-2. Prelaunch and Postrecovery Spectral Transmission of a Narrow-Band Filter (from Blue and Roberts (ref. 3)).

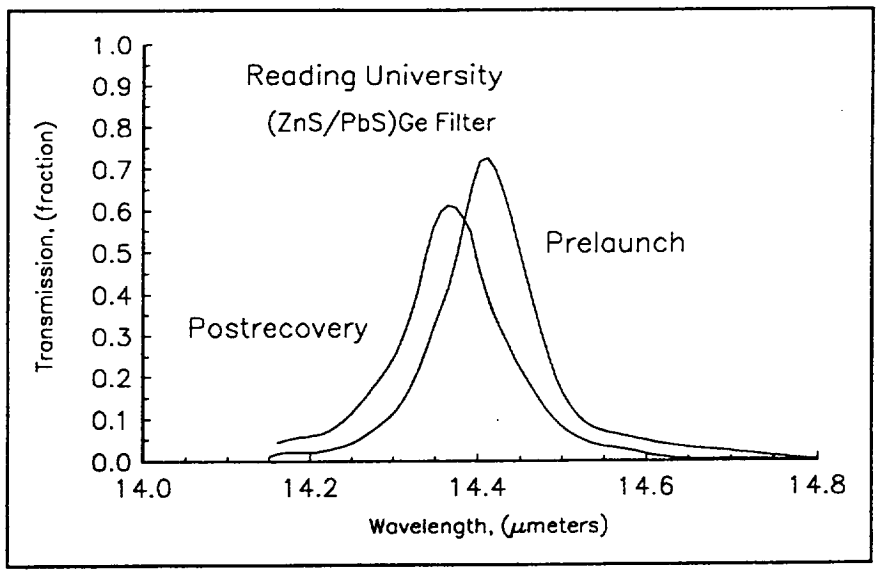

Figure 6-3. Prelaunch and Postrecovery Transmittance for one of the Filters from the Reading University set. (ref. 12).

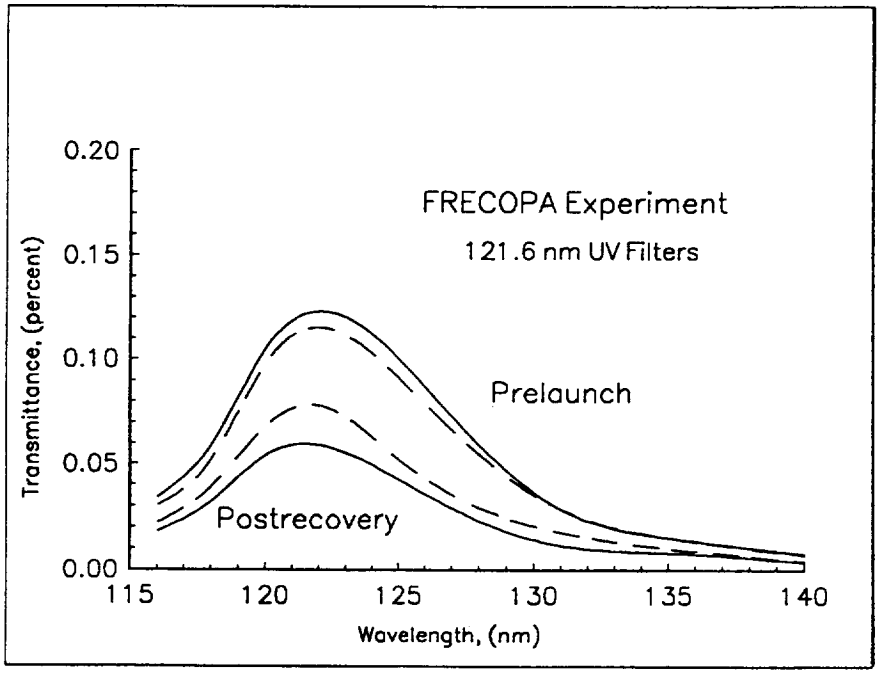

Figure 6-4. Spectral Transmittance of a Narrow-Band Filter from the FRECOPA Set (ref.13).

Realignment or compaction of the deposited layers resulting in layer thickness decreases of less than 1/10 Angstrom per layer are sufficient to explain the observed wavelength shift for some LDEF filters (ref. 15). The associated small reductions in filter throughput and increased bandpass correspond to a change in the internal reflectance of the layers in the stack of about 3 parts per thousand. This change in internal reflection is likely the result of interdiffusion between layers or contamination at the interface. An example of such contamination is water suspected of being incorporated in ZnS layers during fabrication. The water molecules are believed to ionize in the space environment, and move to the energetically favorable dielectric-layer interfaces (ref. 16). Other sources of water molecules are water vented by the shuttle or evaporation from other sources on the satellite, while additional contaminants which have the capability to diffuse into the surface could also affect filter performance.

Table 6-1. summarizes conclusions from several recent studies regarding multilayer dielectric stack mirror and filter degradation.

SPACE-ENVIRONMENT INDUCED DEGRADATION
OF FILTERS AND MIRRORS

For high-energy irradiations under 1/3 Mrad, degradation effects are minimal.

Radiation-induced absorption and contamination-induced absorption in optical materials is strongest in the UV spectral region, decreasing for longer wavelengths.

Temperature cycling in orbit extends and continues previous annealing producing additional changes where possible.

Narrow-band filters exhibit a *"Blue"* shift as a result of compaction/densification.

Loss of transmission and bandpass broadening result from component interdiffusion and other sources of disruption at the interfaces between the high- and low-index materials making up the stack.

Contamination (and in some cases erosion) causes an increase in off-axis scattering from as-manufactured values.

Table 6-1. Conclusions Regarding Multilayer Filters and Mirrors

6.2 THIN FILM OPTICAL COATINGS

Thin film coatings on substrates are common optical elements with applications as mirrors and filters. Degradation of these coatings by contamination, discoloration, erosion or pitting from dust and debris, or delamination are of concern to the systems designer. The spectral transmission or reflectance properties of the surface can be altered by a contamination layer. Several experiments on the effects of the space environment on such coatings have been reported and are reviewed here.

Herzig et al (ref. 17) have reported results of space exposure of coatings on LDEF and previous space shuttle flights. Materials included SiC, Al, Au, Os, Ir, Pt, Al/MgF_2, and Al+SiO_x, all deposited on polished fused silica substrates. The results for the different materials tend to be complementary but difficult to summarize because of the variety of effects found on the various materials. The reflectance of Pt and Ir films was slightly reduced, with indications from different experiments that the effect (whatever the cause) on the Ir layer occurred within a short time of its initial exposure with little change in reflectance thereafter. The Au film showed degradation effects apparently resulting from contamination around the periphery which reduced sputtering of the Au atoms near the edges of the film. As a result, the edges showed greater surface roughness and greater reflection loss. The Os film disappeared from its substrate, apparently by oxidation. The Al film apparently added an oxide layer, but the reflectance decreased only in the UV where the oxide absorbs. Again, the experiments indicate that changes to the Al film occurred within the first few days in orbit, with little change thereafter.

The coated Al films survived with little change in reflectance except for the effects of contamination or possible changes in the material used as the coating. The Al+SiO_x mirror showed enhanced reflectance in the UV region which the authors considered to indicate a possible change in the oxidation state of the SiO_x coating. For the SiC coating, a specimen on the LDEF trailing-edge exhibited less than half the drastic reflectance loss in the VUV (50 nm to 180 nm) of its leading-edge counterpart. Contamination and oxidation are suspected as possible sources for the observed degradation in performance of the SiC coating.

Bonnemason has reported results of measurements in the VUV and visible spectral regions for mirrors and diffraction gratings using Al and Pt coatings on glass (ref. 18). In the VUV region (58 nm-220 nm), these coatings suffered greater degradation in reflectance for the inward-facing set than the space-facing set where losses of 30 percent (Al coating) and 35% (Pt coating) were measured. Other effects of the space environment on coatings are discussed in Section 6.7.

6.3 OPTICAL FIBERS

The major effect of space exposure on optical fibers is radiation-induced attenuation. Studies of attenuation in optical fibers lead to the general result that the intrinsic attenuation of the fiber, the radiation-induced permanent attenuation, and the radiation-induced transient attenuation all tend to decrease as the operating wavelength increases. These results suggest that the longest convenient wavelength within the useable spectral window of the fiber should be used if possible. Radiation-induced damage effects tend to anneal and vanish if the fibers are maintained at room temperature or above for periods of minutes.

The effects of high-energy radiation on optical fibers have been studied for several decades. Both permanent and transient damage effects from radiation have been reported. Radiation effects have been a major concern for several potential application of fiber optics (ref. 19). For consideration of radiation effects, the fibers may be divided into two general groups: glass fibers and plastic fibers.

Effects caused by neutron and gamma radiation on glass optical waveguides were reported by Maurer, Schiel, Kronenberg, and Lux (ref. 20) in 1973. Accumulated doses reached 1.4×10^{12} neutrons/cm^2 and 4300-rad gamma producing increased attenuation of several hundred dB/km at 0.5 microns, but the attenuation decreased with wavelength to only a few dB/km at 1 micron. Absorption increased linearly with radiation dose over the wavelength region covered by these measurements.

All silica fibers with low OH-ion concentrations are reported to have high radiation resistance (ref. 21). This study found that absorption around 650 nanometers in silicon-based fibers is caused both by Si-O defects and by fabrication-induced defects. The study also found that factors other than material composition can alter the response of optical fibers to ionizing radiation. These results are typical for glass fibers, and suggest that these fibers will have sufficient radiation hardness for the majority of their applications in space.

Similar results have been obtained for the effects of high-energy radiation on plastic fibers. Radiation induced absorption is also wavelength dependent for plastic fibers, decreasing monotonically toward longer wavelengths for both neutron and gamma radiation. Radiation resistance of plastic fibers is as high or higher than many commercial glass fibers, but not as high as high-purity vitreous silica which has been found to be one of the most radiation resistant materials available. Watkins and Barsis at Sandia (ref. 22) have measured absorption in six glass and plastic fibers resulting from neutron fluences as high as 4×10^{14} neutrons/cm^2. Earlier work at Sandia has examined the effects of dose rate, some effects of impurities, and transient effects (refs. 23 -25). The values of the radiation-induced absorption were found to be independent of dose rate over the range from 5×10^2 to 6×10^6 rad/day.

A pulse of radiation impinging on a fiber can cause both luminescence and absorption effects. Luminescence can cause interference with information transmission. Absorption centers created by the radiation pulse attenuate the transmitted energy. During the radiation pulse, transient absorption can be many orders of magnitude greater than any resulting residual absorption. Following the radiation burst, the transient absorption decreases with time. The recovery of the transient absorption, for a given material, was found to be independent of dose, irradiation type, and wavelength (refs. 3 & 4). The luminescence effects observed were of sufficient strength to interfere with signal transmission in typical data-link applications, necessitating consideration of these effects during system design.

During the last decade, optical fibers have been developed with a substantial increase in radiation hardness. Values of radiation-induced loss as low as 10^{-8} dB/km-krad have been reported (ref. 26). The fiber optic technology represented on the LDEF is characteristic of the early 1970s, and does not incorporate these advances.

The LDEF satellite contained six experiments related entirely or in part to fiber-optic systems and/or fiber optic system components. Johnson and Taylor (ref. 27) have summarized the results of these experiments in a report which also includes copies of the original investigators' publications and reports. This report also includes a discussion of three planned space experiments which will use or test fiber optic systems or fiber optic technology. The original reports contain many references to recent work relating to radiation effects in fiber optic materials. The reader interested in further details of the LDEF fiber optic experiments will find the Johnson and Taylor report and its included references a convenient source of information. The fiber optic materials carried aboard the LDEF included plastic, quartz, glasses of various types, and various types of silica.

In general, the effects of space exposure on the LDEF optical fiber components were minor. Color changes to the polymer jackets around the fibers were observed, and stains similar to the discolorations found throughout the LDEF noted, but fiber optic cable performance was rarely compromised. One externally mounted optical fiber was severed by a micrometeoroid impact, while many other external fibers showed evidence of impacts, but survived and were operational after recovery. The experiments were mounted on both leading-edge and trailing edge positions. The expected effects on the optical fibers caused by the accumulated radiation dose of several hundred rads or less would be difficult to detect in the worst case dose, and below measurement accuracy in most of the experiments. Additional shielding could add additional radiation resistance where necessary.

The literature on radiation effects in fiber optic cables provides information necessary for estimating the additional attenuation to be expected from the radiation dose accumulated during the LDEF exposure. Calculated values will be on the order of 100 dB/km or less depending upon shielding, material, and cladding. In general, while observed losses were typically smaller than calculated, measurement uncertainty made it difficult to determine conclusively that a radiation-induced increase in attenuation occurred for the experiments.

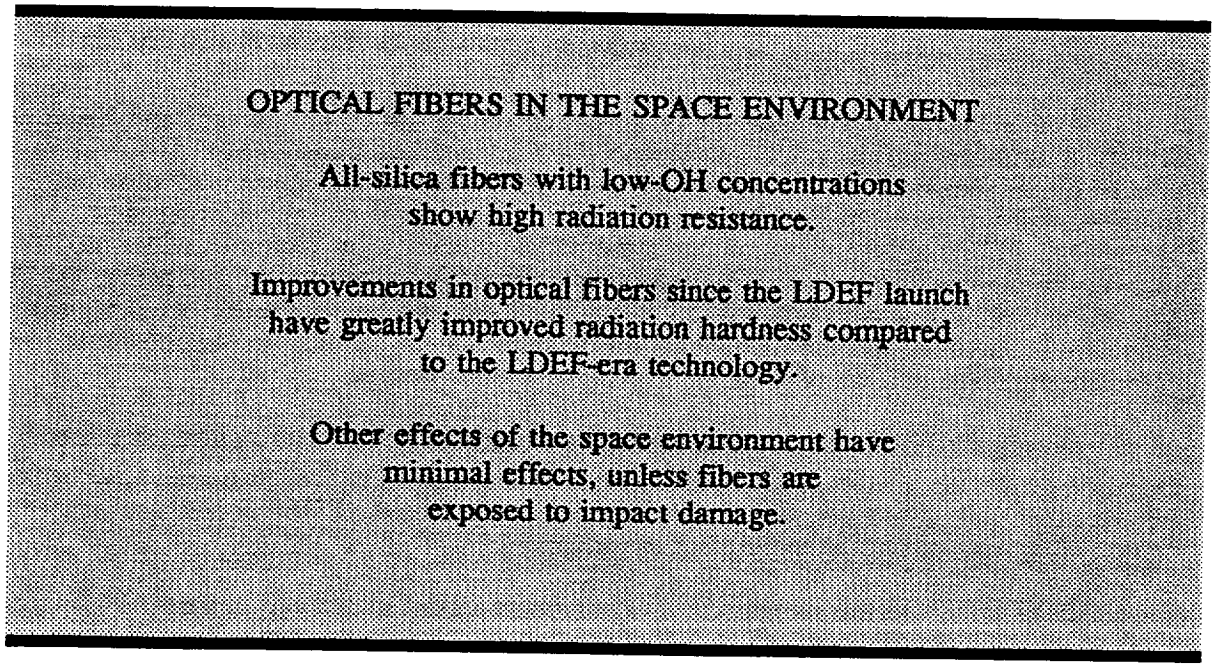

Table 6-2. Considerations Regarding Use of Optical Fibers in the LEO Space Environment

The results of the LDEF fiber optic experiments, summarized in table 6-2, indicate that modern fiber optic system performance in a space environment should be satisfactory, with the possibility of employing additional thermal and radiation protection where extreme situations may be encountered.

6.4 LIGHT SOURCES AND DETECTORS

Several LDEF experiments included light sources and detectors of various types. The optical system designer will be concerned with possible changes in spectral response, responsivity, and noise spectral-distribution. Results reported by LDEF experimenters suggest that the effects of age and general workmanship and process control are more important than the effects of the space environment. No reports of space-environment-related degradation mechanisms have been reported. Failures of the detector window, lead attachment problems, and workmanship problems have been noted. The basic detection mechanisms are unaffected by direct exposure to the space environment.

Postrecovery performance of large-area silicon photovoltaic detectors (800 cm^2) was reported by Blue (ref. 28). Measurements of junction leakage, junction capacitance, noise spectral density, and responsivity did not indicate any significant effects of 69 months in LEO in spite of a noticeable scar on one detector from an impact. Diode leakage current more than doubled in one case, but decreased in other devices. These changes were not significant. Responsivity remained near 0.44 A/Watt in agreement with the nominal value when originally manufactured. Figure 6-5 shows the results for typical prelaunch and postrecovery junction capacitance measurements for one of these diodes.

Noise remained within the manufactures specifications. Figure 6-6 shows current noise for one of the diodes. Current noise at 70 Hz and above was below 0.1 $pA/Hz^{1/2}$, and well below the manufacturers specification of 4 $pA/Hz^{1/2}$.

Radiation effects on silicon avalanche photodiodes have been reported by Walters and Hall (ref. 29). No significant changes to the detector properties were observed after irradiation to a fluence of $5x10^{12}$ neutrons/cm^2 except for an order of magnitude increase in detector leakage current. The smaller radiation dose received by the LDEF would not be expected to produce observable effects based upon this result. Hodgson, Holsen, and Derup (ref. 30) have reported postrecovery measurements on avalanche photodiodes mounted under a silver-coated Teflon foil cover located on the leading edge of the LDEF. Measurements included breakdown voltage at set values of reverse current, responsivity vs bias, noise equivalent power, and photoresponse uniformity. Minor changes were observed, but no significant changes in noise or responsivity.

Charged couple devices (CCD) imaging arrays based on silicon were becoming available at the time the LDEF experiments were being prepared. Silicon CCD devices are among the most sensitive semiconductor devices to radiation. Williams and Nelson (ref. 31) found that irradiation levels as low as 1 rad(Si) will cause loss of stored information in a CCD at an exposure rate of $3x10^7$ rad/sec. Killiany et al (ref. 32) have measured the dark current induced by ionizing radiation in a 256-stage linear CCD imager. Dark current increased by more than an order of magnitude at a dose level of $4x10^4$ rad (Si). The increase in dark current degrades image quality by increasing the background level and decreasing image resolution. The higher dark current also reduces allowable integration time because the potential wells are filled with dark current in a shorter time. Irradiation of a CCD with $5x10^{13}$ neutrons/cm^2 increased the dark-current by an order of magnitude (ref. 24).

A decrease of transfer efficiency of charge under the gate electrodes and radiation-induced bias charges are additional examples of radiation effects which degrade image quality. The radiation dose received by the LDEF was sufficient to permit these effects to be observed, and the reported results for a PdSi CCD imaging array are in reasonable agreement with degradation expected from previous studies of radiation effects (ref. 33).

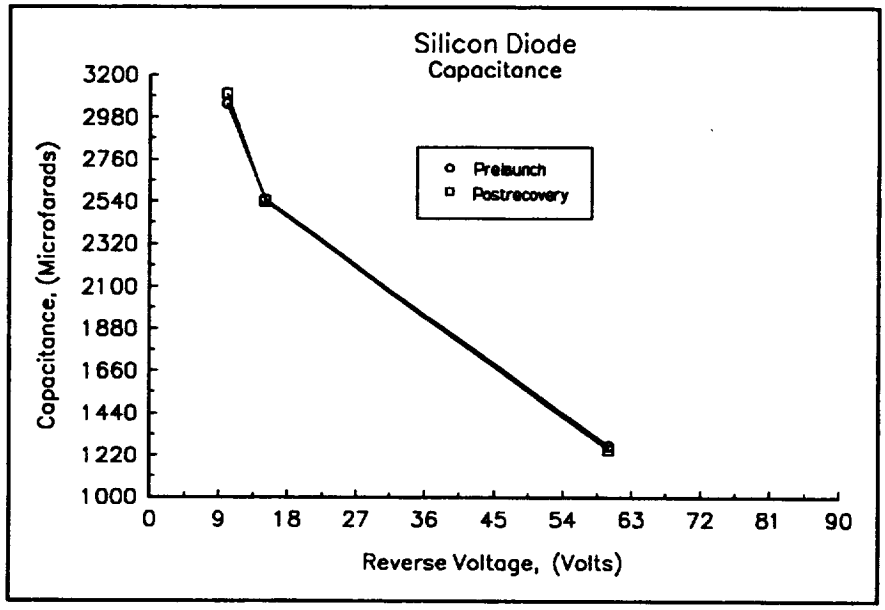

Figure 6-5. Prelaunch & Postrecovery Capacitance Measurements for a Silicon Pn-Junction Diode.

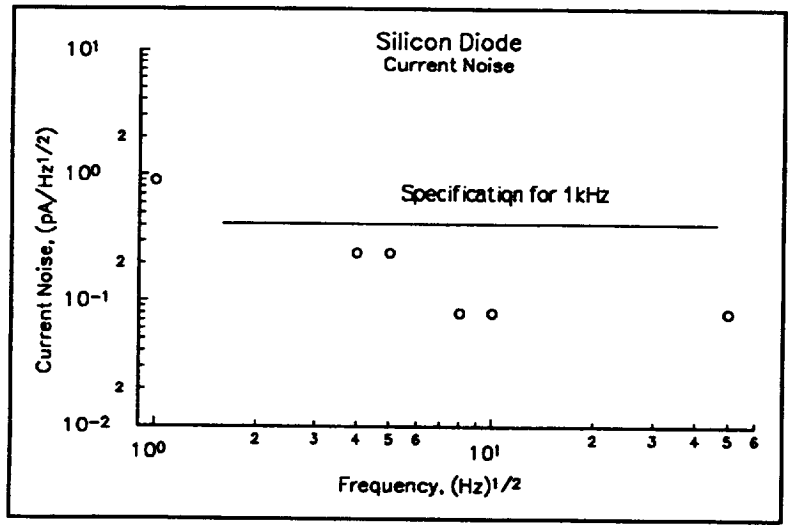

Figure 6-6. Noise Spectral Density for a Silicon Pn-Junction Diode. The Noise is well within the Manufacturer's Specification.

The calculated total received dose for the device was 68 krads, larger than anticipated because of the extended time in orbit and a greater than expected radiation flux. An increase in dark current, threshold potential shifts, and degradation in CCD transfer efficiency were observed. The changes in operating voltage and threshold potential shifts were of a magnitude that could be accommodated by periodic recalibration of the chip and self-adjustment of the drive electronics. The degradation of the transfer efficiency was the most serious. Adding additional charge to fill the traps created by the radiation dose (fat zero) improved operation. The magnitude of this charge provided an estimate of the trap density. The calculated trap density expected from the radiation dose and the trap density determined from the transfer efficiency measurements were in reasonable agreement, providing support for the assertion that the loss in transfer efficiency was the result of the radiation dose received while in orbit. Degradation of the CCD imaging chip represents the only direct ionizing-radiation-induced effect on optical components that has been reported.

Included in the same set of radiation detectors (ref. 15) on the LDEF were InGaAsP photodiodes, PbS, PbSe, InSb, and HgCdTe (photoconductive and photovoltaic) devices. For these detectors, the radiation dose received while in orbit was well below the dose required to observe the onset of radiation induced degradation (ref. 15). The basic physical photodetection mechanism for these devices was not degraded as a result of their exposure to the space environment. Their space exposure did leave some scars from micrometeoroid impacts. Also, failures of electrical contacts and metallization failures were found in both the control devices and the space-exposed devices. Moreover, some drift in device parameters was noted for both the space-exposed and control detectors. Reported improvements in fabrication technology, lead attach procedures, and process technology have taken place since the 1970s when these detectors were manufactured.

The only detector material found to be unsatisfactory in the LDEF collection was Triglycine Sulphate (TGS) which was used for pyroelectric detectors. Robertson (ref. 34) reported that all the control and flight TGS detectors were not functional at the time of postrecovery remeasurement. Moreover, the collection of various pyroelectric infrared detectors provided examples of processing or fabrication problems. These problems, which included contact failure or intermittent contact to the pyroelectric material, should be of more concern than the effects of the LEO space environment.

6.5 ELECTRO-OPTICAL SYSTEM COMPONENTS

6.5.1 Semiconductor Diode Lasers (LEDs)

The GaAlAs semiconductor diode lasers in the LDEF component set were of the single-heterostructure close-confinement structure which typified devices of this type manufactured in the early 1970s (ref. 20). Rapid progress has been taking place in laser diode technology over the past decades, and these diodes rapidly became obsolete as improved technology supplanted the 1970s fabrication techniques.

The diodes were tested using a silicon controlled rectifier circuit which provided low-voltage high-current pulses at a rate controlled by an external pulse generator. Diode radiation was monitored by a silicon photodiode instrument manufactured by UDT. Remeasurement indicated greater light output from all devices, a result believed caused by better collection efficiency of the post-recovery experimental arrangement rather than improved diode properties. Actual absolute diode power output is difficult to measure and was not attempted. The original equipment and geometry of the prelaunch measurements could not be duplicated exactly. The performance of the diodes relative to one another had no significant change. As a result, it was concluded that the space exposure and the years in storage did not degrade laser diode performance.

6.5.2 Light-Emitting Diodes

Monsanto MV10B GaAsP light emitting diodes (LED) were aboard the LDEF. The voltage-current characteristic and the current-light output characteristic of the device and its stored control were reported (ref. 4). Micrometeoroid impacts were observed on the top of the plastic dome, and around the edges of the dome of the space-exposed device. Particles striking the tray surface were moving roughly normal to the flight direction, with some particles having a velocity component in the flight direction.

The results of the current-light output measurements are shown in figure 6-7. As the figure shows, both the stored diode and the diode exposed to space reproduced their original characteristics quite well. It can be seen from the figure that the stored diode has somewhat greater light output for a given drive current, indicating greater quantum efficiency. At low currents, hysteresis occurs which makes exact reproducibility difficult.

The electrical and emission properties of the devices were essentially unchanged as a result of the passage of nearly 13 years since their acquisition, including the nearly 6 years in space. The results indicate that the space environment, with its associated temperature cycling, ionizing radiation, and direct UV and solar radiation exposure, did not degrade the light emission properties of the LED's.

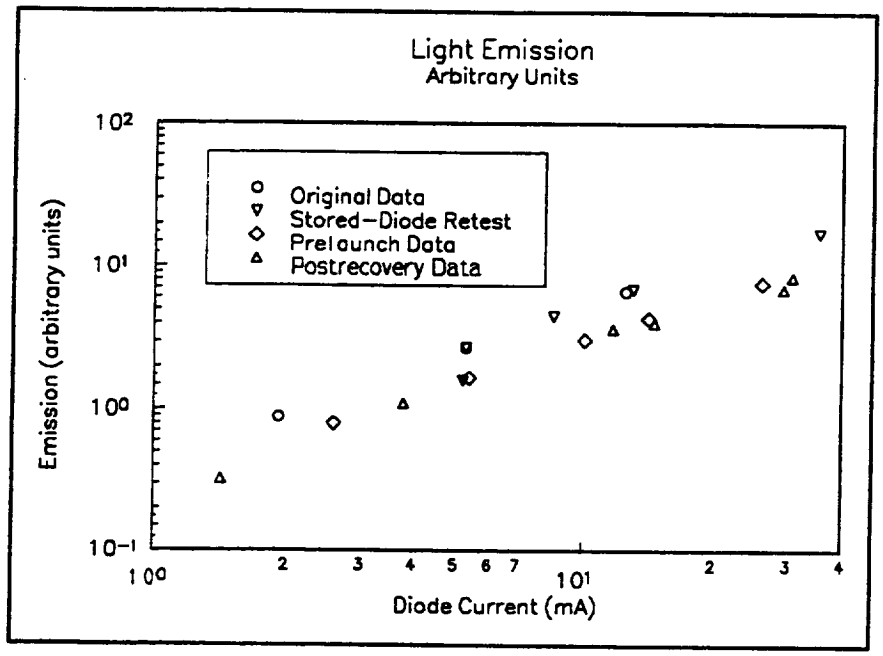

Figure 6-7. Light-emitting Diode Output vs Drive Current. Note that the Control Diode has Slightly Greater Output than the Flight Unit.

6.5.3 Gas Lasers

HeNe and CO_2 gas lasers were included among the components selected for inclusion on LDEF in the late 1970s (ref. 15). During the nearly 20 years since that time, the applications for these lasers in space-based systems have largely been supplanted by semiconductor lasers which are better suited in several ways for many space system applications (small size, robust construction, low-voltage requirements). The potential degradation of other types of lasers similar to gas lasers, such as excimer and dye lasers, was expected to be comparable to the degradation of the HeNe and CO_2 gas lasers.

When the laser tubes were retested in May 1990, no laser action could be obtained. The characteristics of the tubes suggested that the mixture of fill gas had changed during the period between initial and post-flight tests (about seven years). While the extended period in orbit was unplanned, this result is consistent with changes expected from gas diffusion through the glass envelope. The tubes were in otherwise good physical condition, having survived the launch and recovery phases without apparent degradation. The inability to achieve lasing action because of fill-gas composition changes was anticipated long before the recovery mission was launched. Gas lasers must be refilled every 2 years or so. For space-system applications, solid-state lasers should be used where possible.

6.5.4 Nd:YAG Laser Rods

Because of their importance to electro-optic systems, Nd:YAG lasers were included in the list of components included on the LDEF (ref. 15). However, the size and weight of a typical YAG laser suggested that only the items considered potentially sensitive to space exposure be included. Thus, the power supply, the optical bench and cavity, and the mirrors were not included. Only the Nd:YAG laser rods and an example of a flash lamp were placed on the tray. Potential degradation effects on laser mirrors were represented by the many multilayer-dielectric laser mirrors carried on the LDEF.

Three Nd:YAG rods were measured before launch. Two were mounted on the LDEF beneath an aluminum cover (simulating the protection expected for a typical satellite installation) while the third was stored as a control. During the 13 years between prelaunch and postrecovery measurements, the laser cavity tarnished, and the entire laser system needed refurbishment. The power supply was found to be unrepairable, and a substitute was used during the postrecovery measurements. Also, the pump lamps were replaced, as their output was below specifications. At the time of remeasurement, the YAG laser system was over 20 years old (such experimental problems were not uncommon for the many LDEF experimenters).

The renovated cavity was more efficient than the cavity in its 1970's condition, and the performance of all rods exceeded their originally measured parameters. However, the relationships between the parameters of the remeasured rod characteristics remained the same as the relationships in the original measurements, and the relative improvement in coefficients was the same for both the space-exposed rods and the stored YAG rod. On the basis of these results, it was concluded that space exposure did not change the rod properties. It should be noted that the protected 1/4 wavelength coatings on the ends of each rod were also in good condition for all rods at the time of remeasurement.

6.5.5 Laser Flashlamp

A laser flashlamp for the tray and a second stored control lamp were characterized by the supplier both before launch and after recovery (ref. 15). One lamp was mounted under an aluminum cover to better simulate the minimum protection offered by a typical laser installation.

The postrecovery characteristics of the flight lamp as well as those of the control lamp were found to be unchanged after exposure to the space environment. Similar lamps are used for laser rod pumping, and as position indicators for satellites.

6.5.6 Electro-Optic Modulator

An electro-optic light modulator was included among the components aboard the LDEF (ref. 15). The modulator makes use of the electro-optic effect in ADP (ammonium-dihydrogen phosphate crystal) to shift the phase of portions of a light beam passing through the modulator and change the intensity of the beam by means of the resulting interference effect. An identical modulator was stored while the LDEF was in orbit. The modulator on the LDEF was mounted with an aluminum fixture that covered the apertures while the stored unit had plastic caps covering the apertures.

The modulator parameters measured were optical transmission, half-wave voltage, and roll-off frequency. Both the stored unit and the unit on the LDEF tray showed no changes in properties within experimental error upon remeasurement (ref. 15). No measurable changes in optical transmission were found. The half-wave voltage and roll-off frequency were unchanged.

6.6 OPTICAL BAFFLE COATINGS

Measurements of normal reflectance of several optical-black surface finishes, characterizing their suitability as optical-baffle coatings for sensors operating from near-infrared to near-millimeter wavelengths, were published in the late 1970s (refs. 35 & 36). Samples of several of these black coatings were then exposed to the space environment aboard the LDEF satellite in order to determine the effect of space exposure on their performance.

During the nearly 12 years between this initial study of the coatings and the remeasurement of the LDEF samples, several other reports on infrared reflectance of optical-black surface finishes were published (refs. 37-39). A recent set of publications provides an updated resource base for the selection of black baffle surfaces (refs. 40-42). Smith (refs. 43 & 44), derived a reflecting-layer model for a dielectric film which includes both reflection and scattering. The model was fitted to reflectance spectra for seven optical-black coatings (including some optical coatings on the LDEF) for wavelengths extending to 300 microns. The Smith model provides an indication of the parameters which change as a result of the effects of space exposure, although the model cannot easily explain all results at far-infrared wavelengths beyond about 250 microns.

Normal-incidence reflectance of optical-black coatings depends upon coating thickness and surface smoothness, as well as the optical constants of the coating. The data from the LDEF samples indicate that space exposure reduces normal reflectance in general, and significantly reduced reflectance at extreme infrared wavelengths. The results have important implications for the use of these materials for optical baffle applications in space-based optical systems which are discussed the following paragraphs.

Figure 6-8 shows normal reflectance for the polyurethane-based coating, Chemglaze Z306, one of the many coatings exposed aboard the LDEF (ref. 45). Measurements at cryogenic temperatures (near the temperature of liquid helium) indicate increased reflectance of five to ten percent where the coatings become partially transparent (wavelengths beyond one hundred mm) and negligible differences at shorter wavelengths where the films are strongly absorbing. Specimens exposed on the LDEF leading edge also showed reduced reflectance in the near-infrared and increased scattering as a result of increased surface roughness (ref. 46). A coating protected by a quartz window did not show these effects.

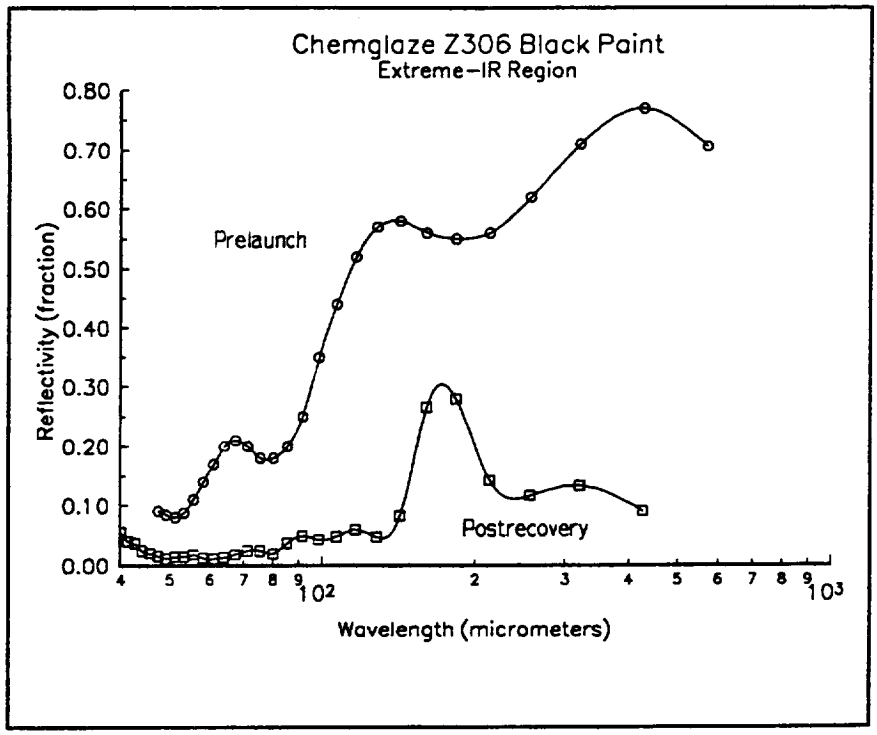

Figure 6-8. Prelaunch and Postrecovery Normal Reflectance of Z-306 Flat Black Paint. Reduced Reflectance after Recovery was Typical of all Measurements of Black Paint Samples.

In another experiment, a graphite epoxy composite panel coated with Z306 was eroded by atomic oxygen, reducing solar absorptivity from 0.95 to 0.93 (ref. 47). The black coating was sufficiently eroded as to allow the underlying red primer to be visible. The atomic oxygen fluence at the tray location was 8.7×10^{21} oxygen atoms/cm^2.

The most noticeable effects on the space-exposed samples 12 years after sample preparation (including nearly 6 years in space) are the reduction in reflectance at all wavelengths and the trend to decreasing reflectance with wavelength beyond about 150 microns. These changes suggest that the coatings will exhibit improved performance as optical baffles after aging and exposure in the space environment compared to their characteristics when freshly prepared.

The oscillations in the reflectance of Z306 at the longer wavelengths were typical of all black coatings measured. They are the result of interference effects between the black coating and the aluminum substrate. The reflecting-layer model of Smith (refs. 43 & 44) was used to analyze the reflectance spectra. A fit to the spectra at the longest wavelengths of the measurements was not possible with the model. An example of an approximate fit to the spectra for sample Z306 is shown in figure 6-9. The postrecovery reflectance data could not be fitted with a change in surface roughness or coating thickness, indicating that surface roughening or loss of material from erosion or other effects of space dust and debris did not cause the decreased reflectance. The approximate fit to the postrecovery spectra in figure 6-9 was obtained by increasing the value of the imaginary component of the index of refraction from 0.066 to 0.22 while leaving the real component unchanged. The implication is that space exposure increases the imaginary component of the complex index of refraction for all samples resulting in increased absorption at all wavelengths.

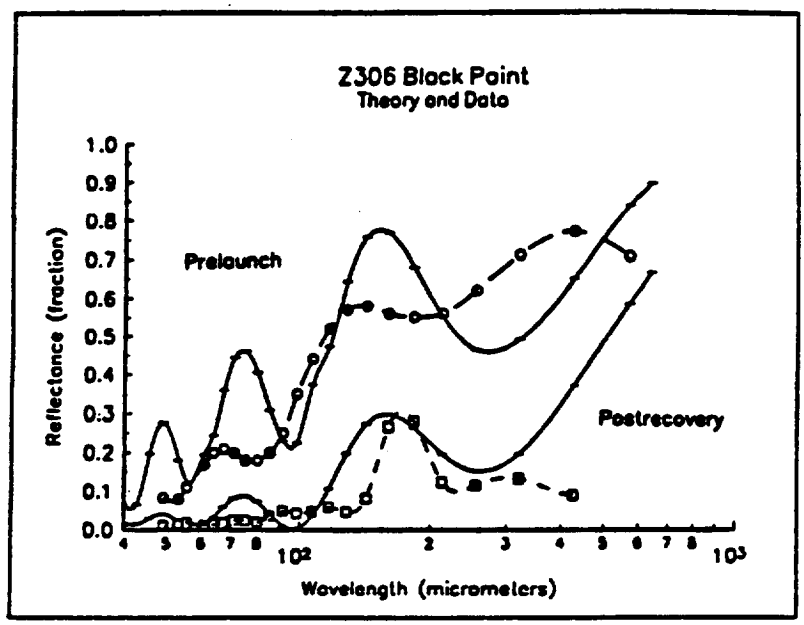

Figure 6-9. Comparison Between Measured (dashed lines) and Calculated Reflectance using the Smith Model (Solid Lines). Postrecovery Calculations Assume Increased Absorption in the Black Coating.

The typical coating consists of absorbing particles (pigment) with a binder (ref. 48) The authors speculate that the increased absorption may be related to the loss of volatile components in the binder, and the degradation of the pigment and binder by UV radiation resulting in an increased density of absorption sites in the paint films. While these effects could occur during natural ageing, space exposure may accelerate them. Postrecovery analysis of the LDEF satellite indicated that considerable outgassing of the black paint in the interior of the structure was a major source of contamination. Protection for exposed optical surfaces may be essential in many cases in order to avoid contamination from the various painted surfaces and other sources during the initial period of outgassing, redistribution, and fixing in place of material during a period of several days following launch.

6.7 ATOMIC OXYGEN/MICROMETEOROID IMPACTS/DEBRIS

6.7.1 Overview

Meteoroids originate from both asteroidal and cometary sources. Along with man-made debris, they can cause damage to spaceborne sensors. The scars left by impacting particles on optical components were observed by many LDEF experimenters. Location of an optical system on an orbiting spacecraft can make a difference. For the LDEF satellite, the Earth-viewing end experienced fewer micrometeoroid impacts than the space-viewing end, as predicted. The flux of small particles can have a sand-blasting effect on optical coatings, and erode metal surfaces.

6.7.2 Atomic Oxygen Effects And Micrometeoriod Impacts

Atomic oxygen exists in the highest layers of the Earth's atmosphere where the solar flux can separate the O_2 molecule, and its density varies with altitude, solar intensity, and other factors. Atomic oxygen is extremely reactive. Its effects on materials have been the subject of many publications in recent years. Physical damage to an optical surface by impactors depends most strongly on the density and velocity of the impinging object and the material properties of the impacted system. Also of interest to the system designer is the possibility of further degradation from the secondary debris resulting from an impact. While not mentioned in the various experimenters' reports from recent studies of space phenomena, the possibility of energetic particle impacts producing bursts of radiation similar to those produced by high-energy radiation may be a consideration for some sensitive optical systems.

The loss of the Os thin-film metal layer from a mirror reported by Herzig et al (ref. 17) is typical of the effects expected from atomic oxygen. Other experimenters have reported similar findings.

Experimenters at NASA MSFC and Southern University exposed a collection of thermal-control coatings to the space environment at the LDEF trailing edge as well as at the leading edge (ref. 49). The darkening of UV-grade quartz windows mounted over some of these coatings was caused by contamination on the inner window surface arising from degradation of the thermal control coating as well as some contribution from other sources on the LDEF. Contamination was greater on the leading edge window samples than on the trailing edge samples. It was suggested that this contamination difference may have arisen because the inner surfaces of the leading-edge windows were not exposed to atomic oxygen (which could reduce contamination buildup), but could have been subjected to more rapid cooling during sun/shadow transitions than samples located at the trailing edge.

Figure 6-10 shows some examples of transmission measurements for the windows contaminated by material from various thermal control coatings. Each of the 25 thermal control coatings in this experiment had a mirror mounted at right angles to the coating for the collection of outgassed products. The mirrors included Al + SiO_x, Al + MgF_2, Au, Ag, and Os on pyrex and glass substrates. Postrecovery analysis indicated that contamination and degradation effects were limited to the wavelength region at 300 nm or shorter. Complete oxidation of the Ag film and removal of the Os film on the leading edge mirrors along with substantial oxidation of the corresponding mirrors on the trailing edge samples is taken as an indication of the magnitude of the atomic oxygen fluence, and an indication of a reduced fluence on the trailing edge components.

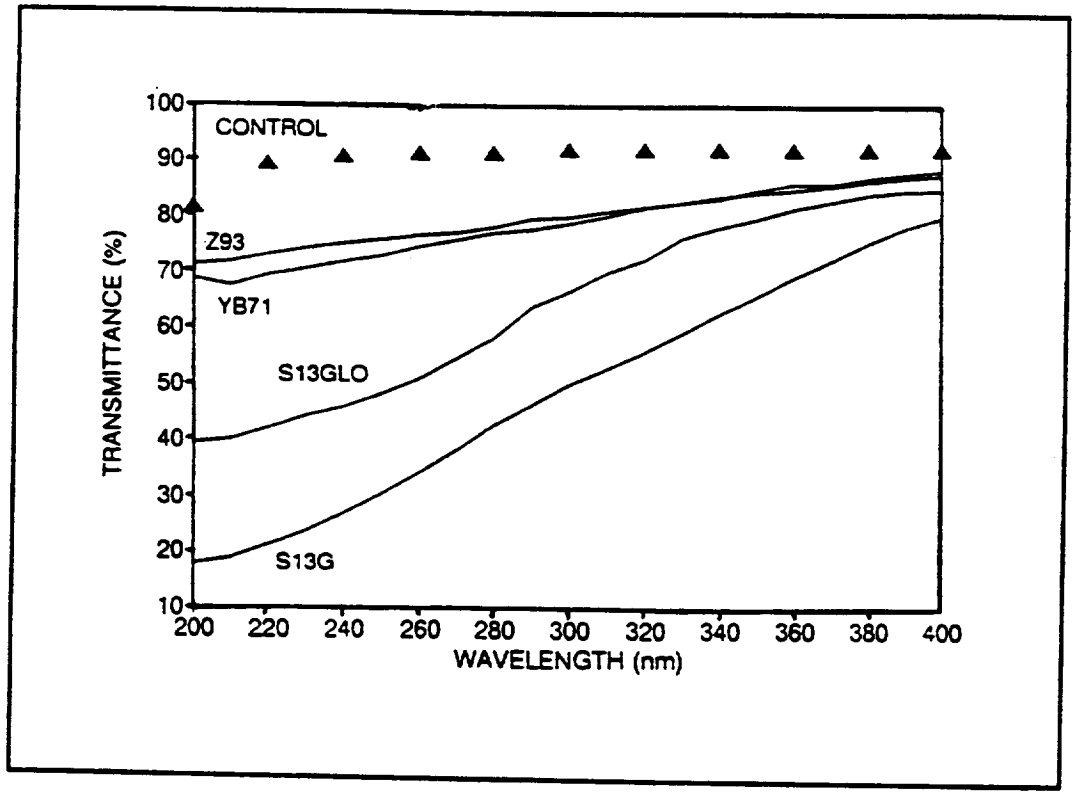

Figure 6-10. Transmittance of Quartz Windows from the Trailing Edge of the LDEF after Contamination from Decomposition of Various Thermal Control Coatings.

The LDEF contained a group of pyroelectric radiation detectors which included units with three different window materials, Ge, Irtran II (ZnS), and KRS-5 (TlBrI). The Ge and Irtran II windows were undamaged. However, the KRS-5 windows contained nonuniform regions on the front surface which were slightly cloudy (white) or metallic in appearance (ref. 34). Transmission losses through the windows reached 50 percent, with larger losses corresponding to regions with greater damage. Surface analysis showed the presence of Si in the form of silicates on the surface of the exposed windows but not on an undamaged control detector window. The Si concentration was higher in the less damaged regions, lower in the more damaged regions. Further, the ratio of thallium to bromine, 1:1 in the undamaged control sample, ranged from 4.6:1 in regions of low damage to values higher than 26:1 in regions of high damage.

These results suggested that space exposure, perhaps the direct effects of solar UV or other energetic radiation sources, caused the loss of bromine, but that the Si-containing contamination layer provided protection, inhibiting the loss of the halide. This supposition is supported by the work of Mendenhall and Weller who reported the results of MgF_2 coatings on clean substrates irradiated with alpha particles in high vacuum (ref. 50). The films were degraded as a result of loss of the fluorine. The conversion of the MgF_2 from a dielectric film toward a film of Mg metal parallels the result observed for the iodide-containing pyroelectric-detector windows. Here, the contamination layer provided a beneficial effect, reducing the halide loss where the layer was present.

One of the most extensive recent experiments to determine performance and stability of materials under atomic oxygen exposure was Energetic Oxygen Interactions with Materials - III (EOIM-III) in which an extensive set of materials were exposed to the AO environment in space while a parallel set of materials were evaluated on the ground in an AO simulation facility (refs.

51 & 52). Both sets of materials were exposed to a fluence of approximately 2.4×10^{20} atoms/cm^3.

Optical baffle materials included boron carbide on graphite, magnesium oxide on beryllium, beryllium (black etched) on beryllium and beryllium foam, Martin Black, and textured aluminum. These materials experienced little or no degradation in reflectance and scattering for the ground-tested and space-exposed samples. Chemical changes were noted: loss of carbon on the Martin Black and boron carbide materials, a slight increase in oxygen content for the magnesium oxide coatings on beryllium. Some optical-baffle materials showed a loss of reflectivity, in agreement with the extreme-infrared measurements on LDEF. In general, the exposure to atomic oxygen produced some changes, but did not degrade the optical performance of this group of baffle materials.

Many types of optical materials and coatings were included. Both bare metal and dielectric-coated mirrors were included. Reflectance of a boron-nitride (BN) coated mirror dropped by 4.6 percent (but 2.7 percent for the ground-test sample), the surface receded nearly 100 Angstroms, but the surface roughness remained unchanged for both samples. The results are interpreted as indicating that the AO-degradation mechanism for BN is associated with chemical-oxidation rather than a mechanical-roughening mechanism. This experiment did not confirm the problems with ZnS that were reported by several LDEF investigators. It is speculated that heavy contamination on the EOIM-III surfaces may have protected both the ZnS and ZnSe surfaces from attack by atomic oxygen. Such contamination also protected deposited diamond surfaces from recession, although recession was measured on ground test samples. In another experiment, an antireflection coating of AlN/SiH protected the underlying diamond layer from atomic oxygen attack.

No significant reflectance losses were found for a bare Be mirror, an $\approx$ 2000 Angstrom-thick Al coating on Si, and Al_2O_3/Al/B-SiC. Comparisons of total-integrated-scatter yielded results dominated by particulate scatter for the post-recovery mirror samples, but it was suggested that the scatter would otherwise be unchanged. The interested reader is referred to the original report (ref. 15) for the many qualifications and details regarding these experiments.

The authors of the EOIM-III report (ref. 51) recommend a mirror of $(Si_3N_4/Al_2O_3)^n$/Al design for operation in space because of its superior thermal-shock resistance and resistance to atomic oxygen.

Pyroelectric detectors (polyvinylidene fluoride film) with various protective coatings showed some visual changes, but no functional changes; for coatings such as Si with an oxide layer and coatings containing layers of ZnS, PbTe, and PbF2, degradation was reported to minimal or nonexistent.

Other materials which would be of interest to optical system designers included structural materials which would find application in the larger optical systems and solar-cell support structures. The general results are that unprotected organic materials will erode in the LEO environment, whereas inorganic materials and fluorinated polymers suffer significantly less erosion.

Erosion sustained in the space environment aboard LDEF was believed to be the cause of an increase in transmittance for a metal neutral-density filter (refs. 3 & 15). The small increase in transmittance (0.5 percent) was found only for a sample exposed to the space environment. An identical covered and protected filter was found to be unchanged after recovery. At the location on the LDEF for these filters, the atomic oxygen fluence was insufficient to produce the observed effects.

A set of filters provided by Barr Associates suffered alterations in properties similar to changes noted by others (ref. 53). This experiment was located in a leading edge position, which provided a maximum in debris and micrometeoroid impacts, as well as a maximum in atomic oxygen fluence. One filter using the optical cement (APCO R113) survived without significant change, while a second filter using a different cement (EPON 828 with Versamid 140 hardener) showed considerable loss in transmittance. An air-spaced version of this second filter without EPON cement did not show the major loss in throughput. These results suggest that the degradation of the EPON cement was the major contributor to the transmission loss.

Transmittance of some metal-dielectric multi-layer filters in the Barr set increased due to pinholes in the coatings. Materials in this filter set which performed well were thallium fluoride, cryolite (sodium aluminum fluoride), and zirconium oxide. Filters containing lead fluoride and lead sulfide layers showed significant transmission losses.

Satisfactory performance of thallium fluoride in a space environment is not consistent with the experience of other investigators (as reviewed in Section 6.1) where filters containing this compound were found to deteriorate. Because fluorides and halides may not be stable in the harsh environment of near-Earth orbit, their use in optical components is discouraged.

The postrecovery optical transmission properties of the lead-containing filters can be reproduced rather well by an assumed increase in absorption, presumably arising from free atoms of lead in the filters. It is possible that some reduction of the lead compounds by atomic oxygen occurred, or that some reduction occurred as a result of dissociation at high temperature. Problems with lead compounds have been noted in other LDEF experiments (refs. 14 & 16). The authors report that the lead compounds are no longer being used in space-borne filters.

Results of recent experiments, described in the next section, offer some ideas for protection of sensitive optical surfaces against atomic oxygen attack. Oxides such as SiO_2 offer a protective and resistive coating which is not degraded. The required layer thickness is several tens of Angstroms. In many cases, the layer can be thin enough as to have no significant optical effect. In other cases, the thickness and index of the layer would be included in the optical design.

6.8 CONTAMINATION

6.8.1 LDEF Results Overview

The contamination environment of the LDEF was reviewed by Carruth et al (ref. 54). Deposition of contamination from sources on the LDEF structure (self-contamination) and the shuttle, combined with the interaction of this contamination with atomic oxygen and solar UV were the major factors leading to contamination-induced effects during the mission. Contamination on the ram surfaces is dominated by direct flux (incident molecules with kinetic energy equivalent to the LDEF orbital velocity), while contamination in the wake region is dominated by outgassed products. The effects of contamination on optical components were observed on several LDEF experiments. For a sufficient atomic oxygen flux, oxidation could remove contaminants on a surface leaving a relatively clean surface, while surfaces with low atomic oxygen fluence can accumulate contamination throughout the life of the orbiting spacecraft. On ram oriented surfaces, an invisible contaminant film remained which was invariably found to be a silicate when investigated by surface analysis. The silicate layer represents the oxidized remnant of the molecular film found elsewhere on the LDEF (ref. 55).

Pippen and Crutcher (ref. 56) discussed some of the contamination issues of concern to the spacecraft designer. The complex and dynamic nature of spacecraft contamination and related effects defy detailed prediction, but are clearly of concern to the systems designer. The discussion in this section and the associated references will illustrate these issues. In space-based optical systems of the future, micromachining and other microfabrication technologies can be expected to play a more prominent role, reducing both the weight and size of components. Contamination control may become increasingly important for the smaller optical assemblies.

Deposition of contaminants has been observed in the interior of LDEF. This contamination was heaviest at locations near vents and apertures where atomic oxygen could flow into the interior with ease. Modeling of the atomic oxygen flow indicated that the contamination patterns were consistent with the thermally distributed flux of ambient atomic oxygen. The result (ref. 54) indicates that the contamination deposits were fixed in position as the result of the reaction of the atomic oxygen flux with the outgassed contaminants in the satellite interior.

Carbon-based film contamination originated from paint solvents, polymeric thin films, and composite materials. The silicon/silica-based film contamination had its origin in adhesives, coatings on specimens and support hardware, and from paints. Particulate contamination included fibers, pollen, dust, and remains of degraded materials (ref. 57)

Vallimont (ref. 58) has reported a reduction in transmission of an uncoated ULE-glass substrate in the short wavelength region. The transmission loss was caused by contamination, and will be discussed in the following pages.

Despite the amount of contamination found on the LDEF, experienced observers consider the LDEF to be among the cleaner spacecraft launched in recent years (refs. 59 & 60). Systems designed for future satellites should anticipate higher levels of contamination, although (it goes without saying) a major effort should be made to thoroughly bake all satellite elements capable of outgassing, and thoroughly clean all parts before launch. The launch vehicle should also be clean and present a low contamination environment to the satellite.

6.8.2 Results of LDEF Experiments

LDEF optical components open to the environment received the same light brown coating or deposit found throughout the spacecraft. The composition of this layer, as determined by several LDEF investigators, consisted typically of silicates and hydrocarbon compounds, along with particles of contaminants.

When a set of windows, filters, and other components selected by Harvey (ref. 61) for use in the UV region were retrieved from the returned LDEF, the components were found to be coated with the typical light-brown contamination layer. Again, no measurable absorption in the visible region was found, but measurements in the 100 nm to 300 nm region indicated substantial absorption. Figure 6-11 shows transmission for one of the windows. For other windows, the loss in transmission in the UV region was even more catastrophic.

Optical filters for the visible region, mounted in a tray on the starboard side of the LDEF, received a light coating of the contamination layer. Cleaning with alcohol removed the stain layer but did not change the optical transmission in the visible region (ref. 3). These results indicate that the LDEF self-contamination layer reduces transmission in the UV region, but produces little or no loss in the visible region. In the infrared region, absorption from vibrational modes of the condensed organic films can be observed (ref. 6), and component performance can be compromised.

Guillaumon and Paillous have compared the effects of space exposure of materials flown on the FRECOPA tray located on LDEF's trailing edge with a similar experiment on the MIR space station (ref. 62). FRECOPA was exposed to UV only, whereas the MIR provided about 13 months exposure to both AO and UV radiation simultaneously. The total atomic oxygen fluence on MIR was estimated to be between 3.6 to 5.9 x 10^{20} atoms/cm^2 (the AO fluence was estimated by measurement of Kapton erosion). The MIR sample experienced a higher level of contamination, the origin of which has not been defined. The authors conclude that the contamination level of the LDEF is much lower and less varied than the levels to be expected on a larger manned space station with extravehicle and internal activity. Further, the reflectance of aluminum paints deteriorated badly on both LDEF and MIR, and measurable increases in weight of several materials were considered to be the result of oxidation as well as contamination.

While the effects of contamination are observable initially in the UV spectral region, their effects extend to increasing wavelengths as the thickness of the contamination layer increases. As discussed in Section 6.1.1, these effects are similar to the effects of radiation on transparent materials. Table 6-3 summarizes the major effects of contamination on optical surfaces. The impact of contamination on system performance will depend on the operating spectral band as well as the density of the contamination layer.

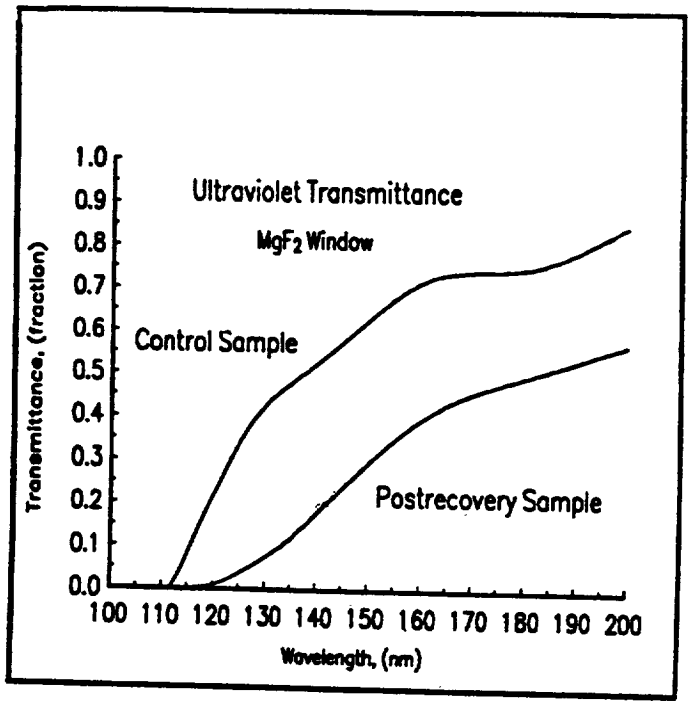

Figure 6-11. Ultraviolet Transmission of a MgF_2 Window Showing Reduction of Transmission as a Result of Contamination of the Front Surface (ref. 61).

CONTAMINATION EFFECTS ON OPTICAL SURFACES

The effects of contamination on optical surfaces include:

Reduction Of Transmittance

Spectral Variation Of Transmittance

Reduced Reflectance

Time-Varying System Sensitivity

Table 6-3. Effects of Contamination on Optical Surfaces

6.9 STRUCTURAL MATERIALS

Structural materials are of concern to the optical system designer. Degradation of the optical bench or main support structure for typical optical systems will compromise system performance. Temperature cycling, as experienced by any orbiting system, must be controlled or compensated to maintain optical alignment. Careful materials choices can insure satisfactory performance over the design life of the system.

Extensive analysis of the postrecovery condition of the various materials carried aboard the LDEF satellite, supported by lessons learned from previous spacecraft, provides the current basis for selection of structural materials for optical systems. Several NASA publications are of value to the systems designer. The reports on the LDEF Materials Workshop (ref. 63), the Huntsville Materials Conference (ref. 64), and the report of the LDEF Systems Special Investigation Group (ref. 65), contain reports and summaries regarding electrical, optical, mechanical, and thermal systems, polymer erosion, composites and structural materials, and several miscellaneous topics including lubricants, adhesives, and seals. Some of the highlights from NASA conferences on materials are listed in table 6-4.

6.10 RELATED TOPICS

Spacecraft charging refers to the phenomenon of varying electric potential or charge buildup on an entire spacecraft, or portions of a spacecraft, from interaction with charged particles and plasmas in space. The result of the charging may be noise pulses (ref. 66), electrostatic discharges, or accelerated degradation of exposed surfaces. Arcing, in addition to the noise pulses generated, also generates local heating and physical damage to materials which is another potential source of effluents for redeposition onto optical element surfaces.

Shuttle glow is the phenomenon of light generated catalytically by the surfaces of the spacecraft moving through the upper atmosphere. Glow phenomena are a potential source of error for sensitive optical measurements in this near-space region. In addition to damage and discoloration in materials, high-energy radiation is a source of visible and near-visible radiation which also can be a problem for optical sensors.

GENERAL OBSERVATIONS ON MATERIALS FOR USE IN SPACE

Metals

Aluminum structures survived space exposure with minimal changes.
Chromic-acid-anodized Al optical properties change little for long-term exposure.
Copper and Silver were heavily oxidized.
Fiber-reinforced aluminum-matrix composites were stable.

Polymers and Polymer Films

Uncoated polymers, composites, and films on the leading edge were eroded/oxidized.
Silvered Teflon (Ag/FEP) has limited life in LEO.
Siloxane-containing films are more resistant to atomic oxygen than FEP.
Atomic oxygen erosion rates do not change significantly with temperature for a 20°C change.

Polymer-Matrix Composites

Dimensional stability of graphite fiber reinforced composites is controlled by outgassing behavior, thermal expansion changes are small.

Ceramics And Glasses

Several of these materials demonstrated generally excellent stability with no surface protection, although cracks and craters from impacts occurred.
Optical properties of glasses are affected by the spacecraft contamination.

Table 6-4. Material Considerations as Reported by LDEF Investigations.

6.11 DESIGN GUIDELINES

The following tables provide some general conclusions, supported by the experimental results from the LDEF program and other space-related studies, for materials and components exposed to the LEO environment. Table 6-5 presents some general guidelines regarding material selection for LEO applications, mainly determined by the LDEF experience.

Most metals will oxidize in this environment, and an oxide or other protection is desirable. Inorganic silicates have proven to be an effective barrier against atomic oxygen erosion. Exposed surfaces of optical windows, filters, and mirrors can be expected to accumulate a layer of condensed outgassed material from the spacecraft itself as well as from the launch vehicle. Such contamination can be avoided through use of a shutter to protect such surfaces until the system has been in space for several weeks.

Table 6-6 lists the two general types of optical system components which appear to be the most vulnerable in the LEO environment. Systems and sensors making use of silicon CCD's require radiation protection. The difficulty of providing sufficient protection will depend upon the application. Multilayer dielectric-stack filters and mirrors are common elements in optical systems. Several modes of performance degradation for these components have been noted. Windows with dielectric coatings can also be affected. Careful material choice (to reduce interdiffusion between layers and to inhibit dendritic growth) and special manufacturing procedures (to reduce layer-thickness reduction over time and aid stability) are desired.

As mentioned above, a coating of several tens of angstroms of silicates can offer protection from atomic oxygen attack for susceptible materials. Material selection for dielectric layers should emphasize covalently-bonded materials and oxides. Materials such as Si and SiOx performed well. Halides did not perform well. Traditional materials such as MgF_2, CaF_2, and Cryolite, and $ThBr_2$ are suspect, and PbS was unsatisfactory in several experiments. Table 6-7 lists several recommended materials as well as some which are undesirable or suspect.

The performance of polymer films and polymer-matrix composites aboard LDEF have been analyzed, but the results are difficult to summarize in a few sentences. Silvered Teflon suffers AO erosion and would not be useful for 30-year missions, but could be useful for missions of no more than a few years. Cracks develop in the surface of the material; solar UV radiation embrittles, roughens, and crosslinks the FEP surface layer. Adhesive from below the surface can then reach the surface and cause discoloration, affecting thermal properties. Another problem in generalizing results for plastic materials is that every manufacturer uses somewhat different plasticizer, dyes, and other additives. Thus, similar materials from different manufacturers may well behave somewhat differently in the harsh environment of near-Earth-orbit.

Siloxane-containing films have been found to be more resistant to AO than FEP. Silicone coatings tend to develop surface crazing under AO exposure. While the thermal coefficient of expansion shows little change in composites, dimensional changes are dictated by the outgassing behavior of the material. AO effects in composites are seen in the ram direction.

The harsh environment of LEO includes not only atomic oxygen erosion, but also solar ultraviolet radiation, temperature cycling in orbit, vacuum, condensates containing volatile materials from surface coatings, grease, and oils, micrometeoroid and man-made debris impacts, and high-energy radiation. The relative amounts of these environmental hazards sustained by an optical system will vary with orbital altitude and inclination, and viewing direction on the satellite. Some general conclusions regarding material and component selection and testing are given in table 6-8.

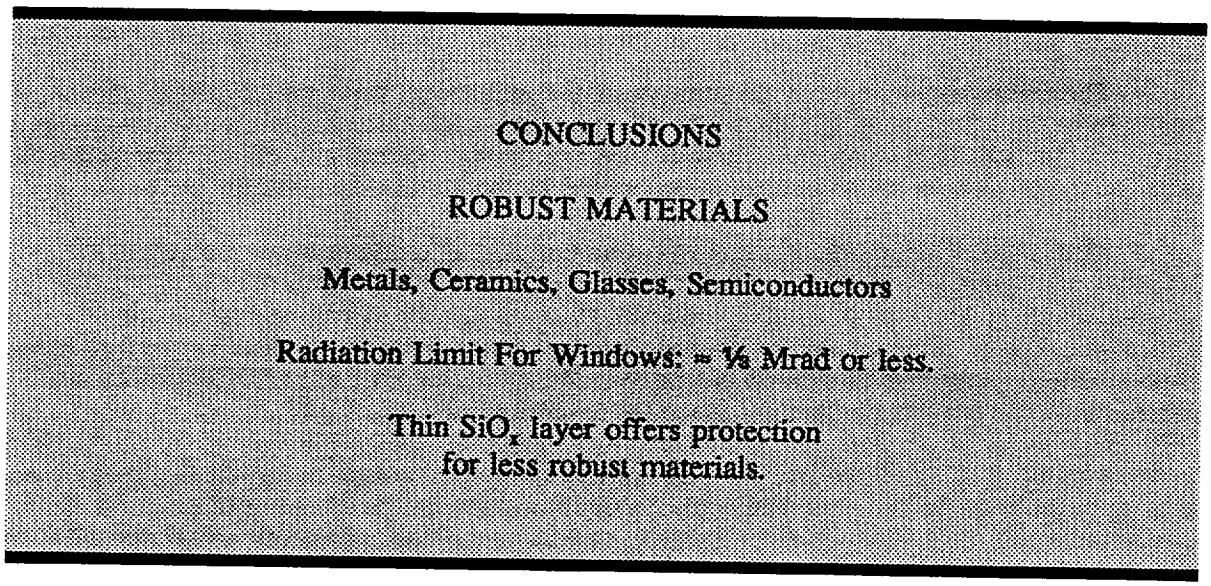

Table 6-5. Conclusions Regarding Materials for LEO Applications

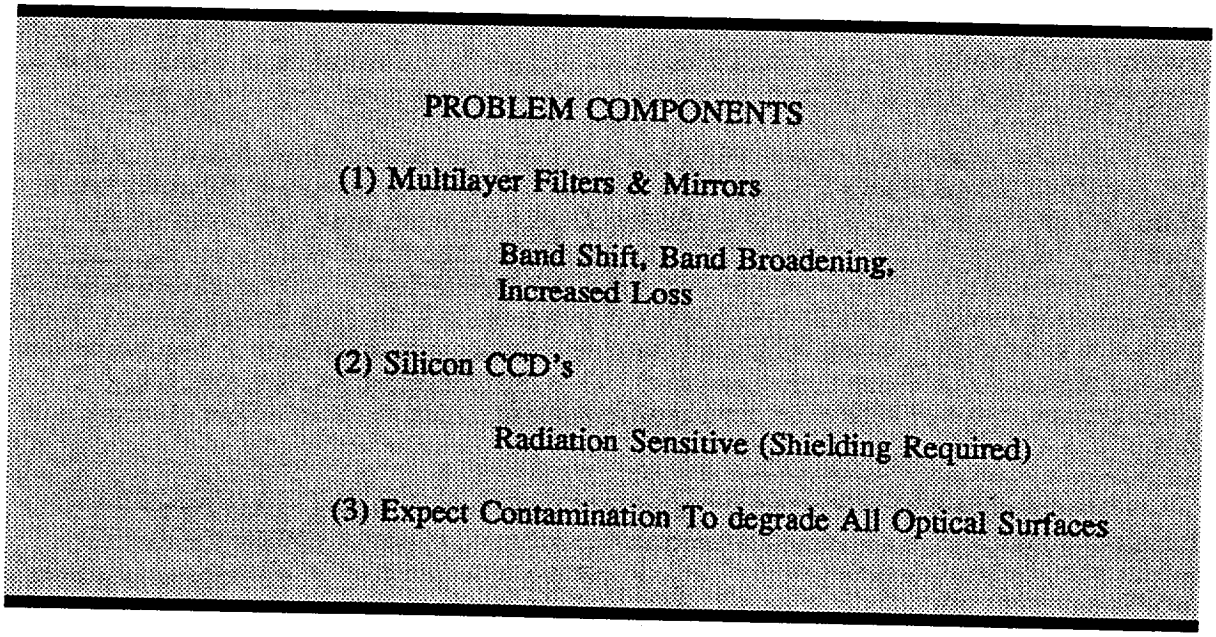

Table 6-6. These Optical Components have been Found to Present Potential Problems in a Space Environment.

GENERAL CONCLUSIONS REGARDING OPTICAL MATERIALS

RECOMMENDED MATERIALS

Si, SiO_2, Al_2O_3, Quartz, ULE Glass

POORLY PERFORMING MATERIALS

KRS-5, KRS-6, PbS
All Halides

SUSPECT SUBSTRATE MATERIALS

Fluorides Such As MgF_2, CaF_2

Table 6-7. Material Choices for LEO Applications

GENERAL CONCLUSIONS

(1) Radiation Effects Do Not Differ From Ground Testing Results

(2) Radiation In Space Gives Rise To Additional Absorption Sites, Increasing Attenuation From The UV To The Far-IR In Paints And Compounds.

(3) Covalently-Bonded Materials Do Not Degrade As Much As Ionically-Bonded Materials. However, Carbon-Carbon Bonds Are Attacked By Atomic Oxygen.

(4) Interface Between Materials Can Be Degraded, Affecting Device Performance.

Table 6.8. Conclusions Regarding Optical Materials in Space.

6.12 REFERENCES (FOR SECTION 6)

1. Nicoletta, C. A., and Eubanks, A. G.,"Effects of Simulated Space Radiation in Selected Optical Materials," Appl. Opt., 11, 1364-70 (1974).

2. Kemp, W. T., Taylor, E., Bloemker, C., White, F., Renser, G., and Watts, A., "Long Duration Exposure Facility Space Optics Handbook," Phillips Laboratory, Kirtland, NM, Report No. PL-TN-93-1067, September (1993).

3. Blue, M. D., and Roberts, D. W., "Effects of Space Exposure on Optical Filters," Appl. Opt. 25, 5299-304 (1992).

4. Blue, M. D., McMillan, R. W., and Liu, Y., "Radiation Effects In Electro-Optical Components And Systems," Technical Report No. TE-77-20, MRDC, DRDMI-TI, Redstone Arsenal, AL, August (1977).

5. Yang, L. C. and Varsi, G., "Nuclear Radiation Effects on Laser Explosive Initiation Systems," Fifth Symposium on Nuclear Survivability and Vulnerability of Ordinance and Propulsion Systems, Menlo Park, CA, October (1975).

6. Suzuki, H., Iseki, T., and Yamamoto, A., "Effect of Reactor Irradiation on the Physical Properties of Fused Quartz," Bull. Tokyo Inst. of Tech., No. 121, 83-88 (1974).

7. Liepmann, M. J., "Gamma Radiation Effects On Some Optical Glasses," Proc. SPIE Int. Soc.Opt. Engr. (USA), 1761, 284-95 (1992).

8. Ehrt, D., "Structure And Properties Of Phosphate Glasses," Proc. SPIE Int. Soc. Opt. Engr. (USA), 1761, 213-22 (1992).

9. Fogdall, L. B., Cannady, S. S., Gellert, R. I., Polky, J. N., and Davies, F. W., "Natural And Induced Space Radiation Effects On Optical Coatings And Materials," Final Report, Contracts N00123-78-C-0989 and N60530-79-C-0263, NWC, China Lake, CA, December (1979) (Part I), and April (1981) (Part II).

10. Fogdall, L. B., and Cannady, S. S., "Irradiation Of Multilayer Coated Mirrors In a UV-Proton-Electron Radiation Environment," Final Report, Contract No. N60530-82-0245, NWC, China Lake, CA, July (1983).

11. Fogdall, L. B., "Space Radiation Effects On Optical Coatings And Materials- Literature Search," Final Report, Contract No. N00123-78-C-0989, NWC, China Lake, CA, February (1979).

12. Seeley, J. S., Hunneman, R., and Hawkens, G. J., "Exposure to Space Radiation of High-Performance Infrared Multilayer Films and Materials Technology Experiment (A0056)," Final Report, Reading University, April (1991).

13. Charlier, J., "Vacuum Deposited Optical Coatings Experiment," presented at the First Post-Retrieval Symposium, LDEF-69-Months In Space, NASA CP-3134, 1343-60, January (1992).

14. Donovan, T. M., Bennett, J. M., Dalbey, R. Z., Barge, D. K., and Gyetvay, S., "Space Environmental Effects on Coated Optics," presented at the First Post-Retrieval Symposium, LDEF-69 Months In Space, NASA CP-3134, 1361-76, January (1992).

15. Blue, M. D., " Investigation Of The Effects Of Long Duration Space Exposure On Active Optical System Components," NASA CR-4632, Contract No. NAS1-14654, NASA Langley Research Center, October (1994).

16. Donovan, T., Johnson, L., Klemm, K., Scheri, R., Bennett, J., Erickson, J., and di Brozolo, F., "Effects Of Low Earth Orbit On the Optical Performance Of Multilayer Enhanced High Reflectance Mirrors," presented at the Third LDEF Post-Retrieval Symposium, LDEF-69 Months In Space, Williamsburg, VA, 8-12 November (1993).

17. Herzig, H., Toft, A. R., and Fleetwood, C. M., "Long-Duration Orbital Effects On Optical Coating Materials," Appl. Opt., 32, 1798-1804 (1993).

18. Bonnemason, F., "Ruled and Holographic Diffraction Gratings Experiment (AO 138-5)," Presented at the First Post-Retrieval Symposium, LDEF-69 Months In Space, NASA CP-3134, 1301-14, January (1992).

19. Friebele, J. E., Long, K. J., Askins, C. G., and Gringerich, M. E., "Overview of Radiation Effects in Fiber Optics." SPIE Proceedings, 541, 70 (1985); Friebele, J. E., Atkins, C. G., and Gringerich, M. E., Effect of Low Dose Rate Irradiation on Doped Silica Core Optical Fibers, Appl. Opt., 23, 4202 (1984).

20. Maurer, R. D., Schiel, E. J., Kronenberg, S., and Lux, R. A., "Effect of Neutron and Gamma Radiation on Glass Optical Waveguides," Appl. Opt., 12, 2024 (1973).

21. Ediriweera, S. R., and Kvasmik, F., "Optical Fiber Radiation Damage Measurements," Optical Systems Advanced Engineering, Siu-Chung Tam, Donald E. Silva, M. H. Kvok, Editors., Proc. SPIE 1399, 64-75 (1991).

22. Watkins, L. M., and Barsis, E. H., "Absorption Induced in Glass and Plastic Fibers by 14-MeV Neutrons," Report Number SAND 75-8714, Sandia Laboratories, Albuquerque, New Mexico, (1976).

23. Watkins, L. M., "Absorption Induced in Fiber Waveguides by Low Dose-Rate Electron and Gamma-Ray Radiation," Report Number SAND 75-8222, Sandia Laboratories, Albuquerque, New Mexico, (1975).

24. Mattern, P. L., Watkins, L. M., Skoog, C. D., and Barsis, E. H., "Absorption Induced in Optical Waveguides by Pulsed Electrons as a Function of Temperature, Low Dose-Rate Gamma and Beta Rays, and 14-MeV Neutrons," Report Number SAND 75-8640 Sandia Laboratories, Albuquerque, New Mexico, (1975).

25. Mattern, P. L., Watkins, L. M., Skoog, C. D., Brandon, J. R., and Barsis, E. H., "The Effects of Radiation on the Absorption and Luminescence of Fiber Optic Waveguides and Materials," Report Number SAND 74-8622, Sandia Laboratories, Albuquerque, New Mexico, (1974).

26. Campbell, A. B., et. al., NRL Memorandum report, p. 6982 (1992), cited by Johnston, A. R., Hartmayer, R., and Bergman, L. A., "Radiation And Temperature Effects On LDEF Fiber Optic Samples," presented at the First Post-Retrieval Symposium, LDEF-69 Months In Space, NASA CP-3134, 1439-1453, January (1992).

27. Johnson, A. R., and Taylor, E. F., "A Survey of the LDEF Fiber Optic Experiments," Jet Propulsion Laboratory, California Institute of Technology, Pasadena, CA, Report Number JPL D-10069, (1992).

28. Blue, M. D., "Degradation Of Electro-Optic Components Aboard LDEF," presented at the Second Post-Retrieval Symposium, LDEF-69 Months In Space, NASA CP-3194, NASA LaRC, VA, 1333-42, April (1993).

29. Walters, R. A., and Hall, E. C., "Operation and Survival of Silicon Avalanche Detectors in an Nuclear Weapon Environment," IEEE Southeastcon Proceedings, 24-27 (1974).

30. Hodgson, R. R., Holsen, J. N., and Drerup, R. A., "Post-Flight Characterization of Optical System Samples, Thermal Control Samples, and Detectors from LDEF Experiment M0003, Sub-Experiments 6 and 13," presented at the First Post-Recovery Symposium, LDEF-69 Months In Space, NASA CP-3134, NASA LaRC, VA , 1315, January (1992).

31. Williams, R. A., and Nelson, R. D., "Radiation Effects in Charge Coupled Devices," IEEE Trans. Nuc. Sci., NS-22, No. 6, 2639-44 (1975).

32. Killiany, J. M., Saks, N. S., and Baker, W. D., "Effects of Ionizing Radiation On a 256-Stage Linear CCD Imager," IEEE Trans. Nuc. Sci., NS-22, No. 6, 2456-61 (1975).

33. Blue, M. D., "Degradation Of Optical Components In Space," presented at LDEF Materials Results for Spacecraft Applications, NASA CP-3257, 217-26, December (1993).

34. Robertson, J. B., "Effect Of Space Exposure On Pyroelectric Infrared Detectors," presented at the LDEF Materials Workshop '91, NASA CP-3162, 501-06, September (1992).

35. J. R. Grammer. W. H. Alff, M. D. Blue, and S. Perkowitz, "Far-Infrared Reflectance Of Optical Baffle Coating Materials," in Thermophysics and Thermal Control, Vol. 66 of Progress in Astronautics and Aeronautics, New York, 39-46 (1978).

36. W. H. Alff, M. D. Blue, and S. Perkowitz, "Reflectivity Of Radiation Absorbing Coatings," in Proceedings of the Third International Conference of Submillimeter Waves and Their Applications, The Physical Society, Univ. of Surrey, Guildford, U. K., 276-277 (1978).

37. D. W. Bergener, S. M. Pompea, D. F. Shepard, and R. P. Breault, "Stray Light Rejection Performance Of SIRTF: A Comparison," Proc. SPIE Int. Soc. Opt. Engr. (USA), 511, 65-72 (1984).

38. D. B. Betts, F. J. J. Clarke, L. J. Cox, and J. A. Larkin, "Infrared Reflection Properties Of Five Types Of Black Coatings for Radiometric Detectors," J. Phys. E (GB), 18, 689-96 (1985).

39. S. Ungar, J. Mangin, M. Lutz, G. Jeandel, and B. Wyncke, "Infrared Black Paints for Room And Cryogenic Temperatures," Proc. SPIE Int. Soc. Opt. Engr. (USA), 1157, 369-376 (1989).

40. McCall, M. H. C. P., Sinclair, R. L., Pompea, S. M., and Breault, R. P., "Spectrally Selective Surfaces For Ground And Space-Based Instrumentation: Support For A Resource Base," Proc. SPIE Int. Soc. Opt. Engr. (USA), 1945, 497-504 (1994).

41. Pompea, S. M., and McCall, S. H. C. P., "Outline Of Selection Processes For Black Baffle Surfaces In Optical Systems," Proc. SPIE Int. Soc. Opt. Engr. (USA), 1753, 92-104 (1992).

42. McCall. S. H. C. P., Pompea, S. M., Breault, R. P., and Regens, N. L., "Reviews of Black Surfaces For Space And Ground-Based Optical Systems," Proc. SPIE Int. Soc. Opt. Engr. (USA), 1753, 158-170 (1992).

43. S. M. Smith, "Specular Reflectance of Optical Black Coatings in the Far Infrared," Appl. Opt., 23, 2311-26 (1984).

44. S. M. Smith, "The Specular Reflectance of IR-Opaque Coatings," Int. J. Infrared Millimeter Waves, 5, 1589-95 (1984).

45. Blue, M. D., and Perkowitz, S., "Space Exposure Effects on Optical-Baffle Coatings at Far-Infrared Wavelengths," Appl. Opt., 31, No. 21, 4305-09, 1992.

46. Linton. R. C., and Kamenetzky, R. R., "Interim Results Of Experiment A0034," presented at the Second Post-Retrieval Symposium, LDEF-69 Months In Space, NASA CP-3194, 1151-69, April (1993).

47. Golden, J. L., "Selected Results For LDEF Thermal Control Coatings," presented at the Second Post-Retrieval Symposium, LDEF-69 Months In Space, NASA CP-3194, 1099-1110, April (1993).

48. S. M. Smith, "Specular Reflectance of Optical-Black Coatings on the Far Infrared," Appl. Opt. 23, 2311-26 (1984).

49. Linton, R. C., Kamenatzky, R. R., Reynolds, J. M., and Burris, C. L., "LDEF Experiment A0034: Atomic Oxygen Stimulated Outgassing," presented at the First Post-Retrieval Symposium, LDEF-69 Months In Space, NASA CP-3134, 763-79, January (1992).

50. Mendenhall, D. E., and Weller, R. A., "Destruction of a MgF_2 Optical Coating by 250 kev α-Particle Radiation," Appl. Phys. Lett., 57, 1712-14 (1990).

51. Chung, S. Y., Brinza, D. E., Minton, T. K., Stiegman, A. E., and Liang, R., H., "Flight- and Ground-Test Correlation Study of BMDO SDS Materials: Phase I Report," JPL Pub. 93-31, December (1993).

52. Johnson, L., Klemm, K., Moran, M., "Accelerated Atomic Oxygen Test Results for Developmental Optics," presented at the Topical Meeting on High Power Laser Optical Components, Boulder, CO, 26-27 September (1993). (NAWCWPNS TP 8151).

53. Mooney, T. A., and Smajkiewicz, A., "Transmittance Measurements of Ultraviolet and Visible Wavelength Filters Flown Aboard LDEF," presented at the First LDEF Post-Retrieval Symposium, LDEF-69 Months In Space, NASA CP-3134, 1511-21 (1992).

54. Carruth, M. R. Jr., Rantanen, R., and Gordon, T., "Modeling of the LDEF Contamination Environment," presented at the LDEF Materials Results For Spacecraft Applications, NASA CP-3257, 87-95 (1993).

55. Stuckey, W., and Koontz, S., "LDEF Contamination: Panel Discussion Summary," presented at the LDEF Materials Workshop '91, NASA CP-3162, 689-98, September (1992).

56. Pippen, G., and Crutcher, R., "Spacecraft Contamination Issues From LDEF: Issues for Design," presented at the LDEF Materials Results for Spacecraft Applications, NASA CP-3257, 97-102, December (1993).

57. Stein, B. A., "LDEF Materials Overview," presented at the Second Post-Retrieval Symposium, LDEF-69 Months In Space, NASA CP-3194, 741-89, April (1993).

58. Vallimont, J., and Havey, K., "Effects of Long-Term Exposure on Optical Substrates And Coatings," presented at the First Post-Retrieval Symposium, LDEF-69 Months In Space, NASA CP-3134, 1341-42, January (1992).

59. Stein, B. A., "LDEF Materials Overview," presented at the Second Post-Retrieval Symposium, LDEF-69 Months In Space, NASA CP-3194, 1099-1110, April (1993).

60. Lehn, W. H., and Hurley, C. J., "Skylab D024 Thermal Control Coatings and Polymeric Films Experiment," presented at the LDEF Materials Workshop '91, NASA CP-3162, 293-308, September (1992).

61. Harvey, G. A., "Effects Of Long-Duration Exposure on Optical System Components," presented at the First Post-Retrieval Symposium, LDEF-69 Months In Space, NASA CP-3134, 1327-40, January (1992).

62. Guillaumon, J-C., and Paillous, A., "Spacecraft Materials: A Comparison Between Flight Results Obtained on LDEF and MIR," presented at the LDEF Materials Results for Spacecraft Applications, NASA CP-3257, 485-98, (1993).

63. LDEF Materials Workshop '91, NASA CP-3162, Compiled by B. A. Stein, and P. R. Young, Proceedings of a workshop sponsored by NASA Langley Research Center, (1992).

64. LDEF Materials Results For Spacecraft Applications, NASA CP-3257, Proceedings of a conference held in Huntsville, Alabama, (1993).

65. Dursch, H. W., Spear, W. S., Miller, E. A., Bohnhoff-Hlavacek, G. L., and Edelman, J., "Analysis of Systems Hardware Flown on LDEF - Results Of The Systems Special Investigation Group," NASA CR-189628, Contract No. NAS1-19247, April (1992).

66. Nanevicz, J. E., and Adamo, R. C., "Occurrence of Arcing and Its Effects on Space Systems." Space Systems And Their Interaction With The Earth's Space Environment, ed. by H. B. Garrett and C. P. Pike, Prog. Astronaut, Aeronaut., 71, 252-75 (1980).

7.0 EFFECT OF LONG DURATION SPACE EXPOSURE ON OPTICAL SCATTER: LDEF AND LATER MISSIONS

The effects of induced optical scatter, caused by micrometeoroid and debris impacts, atomic oxygen, ultraviolet radiation, and contamination are discussed in this section. This report includes results from LDEF, other recent missions such as HST, and ground based testing. The goal of this review paper is to provide designers of optical systems with recent published information on optical scatter due to space environmental effects; thus providing a knowledge base to investigate their own mission-specific optical scatter requirements.

7.1 INTRODUCTION

The measurement of optical scatter has received increased attention in the last decade. In addition to being a serious source of degradation of signal to background noise, optical scatter reduces light throughput, limits resolution, and is a source of practical difficulties in design of many optical systems. It is the major factor in determining whether optical systems are capable of differentiating a weak target source in the vicinity of a much stronger one (ref. 1). Scattered light is particularly troublesome in optical systems, especially systems to be used in the infrared spectral region (ref. 2). On the other hand, the measurement of optical scatter has been a useful inspection tool to evaluate surface quality, characterize surface roughness, and locate surface defects. As a result, Bi-directional Reflectance Distribution Function (BRDF) measurements and scatter analysis have proven useful in a variety of optical design problems and play an important role in the early stages of sophisticated spacecraft optical system design (ref. 2).

Depending on the amount of and type of space environmental exposure to a spacecraft optical surface, scattering sites can be created by a combination of meteoroid and debris impacts, contamination, AO erosion, thermal cycling effects, and solar UV radiation degradation. One spacecraft, the LDEF, provided significant insight into optical scatter effects on optical materials due to long duration space environmental effects at LEO.

LDEF had a total of 57 experiments mounted in 86 trays facing outward from the LDEF structure as shown in figure 7-1. The satellite was gravity-gradient stabilized and mass loaded so that one end of the LDEF was always pointed at Earth and one side (the leading edge) was always oriented in the orbit path. The orientation remained constant throughout the entire mission, which lasted nearly six years, providing an excellent platform for long duration space exposure of a wide assortment of materials, including optical materials.

This report reviews studies done on induced optical scatter due to space environmental effects from LDEF and other recent missions. It is organized into five sections related to the space environment: 1) micrometeoroid and debris impacts, 2) contamination, 3) atomic oxygen erosion and UV irradiation, 4) scatter modeling codes, and, 5) surface morphological features measurement and photodocumentation on LDEF.

The BRDF is defined in radiometric terms as the scatter surface radiance divided by the incident surface irradiance, as originally derived and credited to F.E. Nicodemus (ref. 3). The scattered surface radiance is the light flux scattered per unit surface area per unit projected solid angle. The incident surface irradiance is the light flux on the surface per unit of illuminated surface area (ref. 4). A drawing of the BRDF geometry is shown in figure 7-2. The BRDF is commonly used to describe scattered light patterns, and is a function of incident angle, and wavelength, as well as sample parameters (orientation, transmittance, absorptance, surface finish, index of refraction, bulk homogeneity, contamination, etc) (ref. 5). To some, the BRDF is equivalent in importance to the index of refraction (ref. 6), in that it gives a fundamental representation of how light interacts with surfaces, and how it is distributed in angle space.

Figure 7-1. LDEF on-orbit.

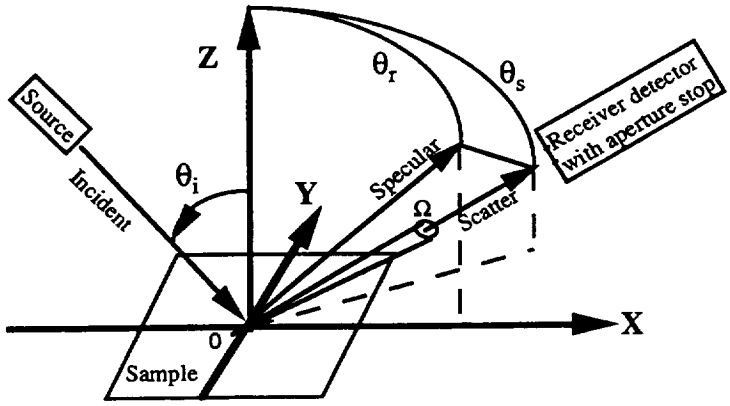

Figure 7-2. Geometry for Definition of BRDF. Plane of incidence is the XZ plane. Z axis is normal to sample surface. Scatter plane is arbitrary, here it is shown out of the plane of incidence. The θ_i is the angle of incidence, $\theta_i = \theta_r$, Ω is the receiver solid angle, and θ_S is the diffuse scatter angle. [Adapted from ASTM E-1392-90 Standard Practice for Angle Resolved Optical Scatter Measurements on Specular Diffuse Surfaces.]

For example, the parameter used to characterize the sensitivity of an optical system to off-axis radiation is the Normalized Detector Irradiance (NDI). The NDI is usually computed using measured scatter data from each optical or baffle component in a sensor. The measured scatter data used is the BRDF for mirrors and baffles and the Bidirectional Transmittance Distribution Function (BTDF) for refracting elements (ref. 7).

7.2 METEOROID AND DEBRIS (M/D) IMPACTS

Many satellite surfaces, especially the leading edge, will be subjected to significant bombardment by small particles in the 1 to 100 micron size domain. These particles are both micrometeoroids and man-made debris (ref. 8). While it is unlikely that micrometeroids could cause catastrophic structural damage to the spacecraft, they can cause extensive damage to the windows, solar cells, protective coatings, and other more delicate components (ref. 9). Earlier experiments by Mirtich et.al. showed that spaceflown metallic mirrors impacted by small particles, with missions up to 20 years (e.g. the OSOIII and SERTII satellites that were launched in 1967 and 1970 respectively) indicate very small reductions in reflectivity (less than one percent) in agreement with the predictions (ref. 10). However scatter predictions have indicated that scattered light in optical systems is a problem, and must be accounted for as it propagates through an optical system (ref. 11). Until LDEF and other recent missions, impact-caused scatter has not been studied significantly since most LEO-orbiting imaging optics in the past have looked directly toward Earth and thus had little threat of being impacted (ref. 12).

The LDEF underscored the realization that space is not a pristine environment. In the course of its flight, lasting almost six years at altitudes from 350 km to 500 km, in a fixed orientation, the spacecraft's impacts were detected and collected by a variety of sensors and collection devices. For example, a 1 square meter detector on the LDEF Interplanetary Dust Experiment (IDE), encountered over 15,000 collisions with zodiacal dust, meteor stream grains, orbital debris, and possibly beta-meteroids and interstellar matter (ref. 13). The particles encountered ranged in size from submicron to 100 microns in diameters (ref. 14). Recent missions like LDEF have contributed greatly to the understanding about the effects of meteroid debris impacts on optical scatter as described in the following paragraphs. One striking example on LDEF of meteoroid and debris (M/D) impacts and optical scatter was in the M0003-2 experiment. Researchers found that BRDF measurements taken at M/D impact sites had increased in optical scatter three orders of magnitude (10^{-5} to 10^{-2} inverse steradians) over a non-impacted area on the same sample (ref. 15).

LDEF Meteoroid and Debris Special Investigation Group (M/D SIG) Study (ref. 16 and 17)

The magnitude of impact effects on various exterior LDEF materials, including optics and power system components, was evaluated by the LDEF M/D SIG. The optics and power system component impact features documented on LDEF were described as typical of the damage experienced by brittle materials as shown in figure 7-3. The impacts show a central crater, usually filled with finely crushed material, and exhibiting little or no crater lips. These craters are usually surrounded by conchoidal fracture areas, which act as spallation zones. There are typically 2 to 4 (occasionally more) cracks which run outward from the impact site for 10 or more crater diameters.

The researchers found only minor changes in the transmissivity and reflectivity, but that the scatter dramatically increases. Additional studies with reflective optics having dielectric coatings, showed they may be affected by M/D impacts as well because the coatings which provide the reflectivity are removed in the vicinity of the impacts. Further, the amount of coating material removed by an impact may be much larger than in ductile materials due to delamination of the coatings from the substrate and from each other. Figures 7-4 to 7-6 are

examples of the damage experienced by the brittle optics and power systems components on LDEF.

In summary, the researchers found that the scatter is dominated by crater formation rather than by crack generation. Soft targets (e.g. metals and plastic) will produce the largest craters. Hard targets (glasses and ceramics) produce smaller craters; however, these craters are frequently surrounded by larger surface spalls giving the effect of large shallow craters. Multilayer coated optics can suffer from delamination effects around the impact sites, which produce large local changes in reflectivity or transmission and scatter.

Overall LDEF Meteoroid and Debris (M/D) Flux Assessment (ref. 18)

An assessment of the M/D impact flux around the entire LDEF was made, with a section on assessing the magnitude of impacts on optical surfaces. In this study, Zweiner and Finkenor reported for leading edge surfaces that up to 140 impacts/year/meter square, for non-penetrating small (high probability) impacts causing craters in the 0.1 to 3 mm range, can be expected on spacecraft surfaces and must be planned for and considered in spacecraft designs requiring long periods of exposure in the LEO environment. By always exposing optical systems in the trailing direction the flux can be reduced by a factor of 10. The type of impacts evaluated in this report will not normally cause penetration of an optical surface, but they will create scatter sites for light. The impact crater size distribution versus individual sizes was approximated by an equation. This approximation permitted an estimation of the actual number of impacts below 0.5 mm where incomplete manual counting on LDEF occurred. Then a summation was made using this relation for all diameters between 0.1 and 3.0 mm. The total sum was used to normalize the size distribution data into a fractional distribution. No associated optical scatter measurements were done in this study.

LDEF Experiment #AO172 (ref. 19)

This study provided additional morphological information on impacts, and is correlated to ground studies. Experimental results revealed that six of the seven impacts on glass and glass ceramic samples exposed to the trailing edge of LDEF contained central melt zones surrounded by a halo of fragmented material, similar to those produced by laboratory impacts at velocities above 10 km/s. Numerous radial cracks extended from the point of impact to a certain radius. Bubbles trapped in the melt region of the BK-7 glass indicate temperatures and pressures at impact reached those necessary for vaporization of the micrometeoroid and glass. No impacts were observed on samples located on the Earth-facing side. The depth of the damage field associated with the seven impact events is approximately one-fifth the crater diameter. Glass fiber produced in the ejecta of the fused silica impact were observed to have lengths up to 100 mm. These impacts were thought to be due to a projectile with a large component of velocity in the direction of the debris field. Optical transmission measurements of all samples, except the commercial purity SiO_2 glass, revealed no detectable change in optical transmission. The optical degradation of the SiO_2 was a consequence of deposition of layers of carbon-containing contamination on the interior surfaces of the fused silica.

Space Power Hypervelocity Facility (ref. 20)

A LDEF-related ground based simulation used dust-sized olivine particles fired at a copper plate using the Space Power Institute Hypervelocity Facility, to simulate micrometeoroid damage from natural debris to spacecraft in LEO. Techniques were developed in this study for measuring crater volume, particle volume, and particle velocity, with the particle velocities ranging from 5.6 to 8.7 km/s. A roughly linear correlation was found between the crater volume and particle energy which suggested that micrometeoroids follow standard hypervelocity relationships. The residual debris analysis showed that for olivine impacts of up to 8.7 km/s, particle residue is found in the crater. The researchers concluded that the micrometeoroid damage to satellites can be accurately modeled using the hypervelocity facility.

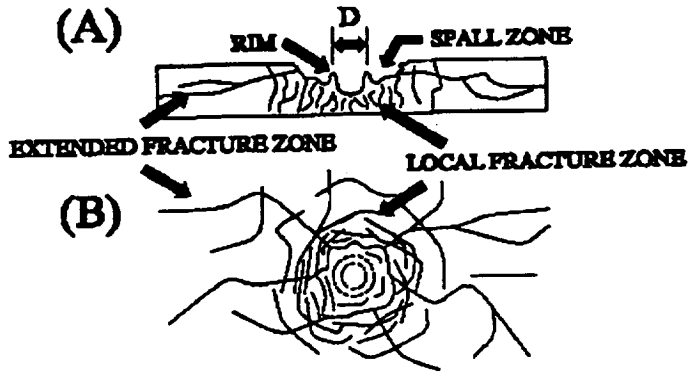

Figure 7-3. Illustration of the general morphology and associated feature diameter, D, for impact features into optics and brittle materials. (A) Cross-sectional view and (B) top view.

Figure 7-4. Photograph of an impact in metal-oxide-silica. The impact feature shown in this example is ~2.2 mm across the center (a depression in the glass) with the total damage area extending to several centimeters. This large amount of fracturing (i.e., the cracking in the surface as well as the conchoidal fractures and spallation of the substrate) is typical of impacts into brittle materials.

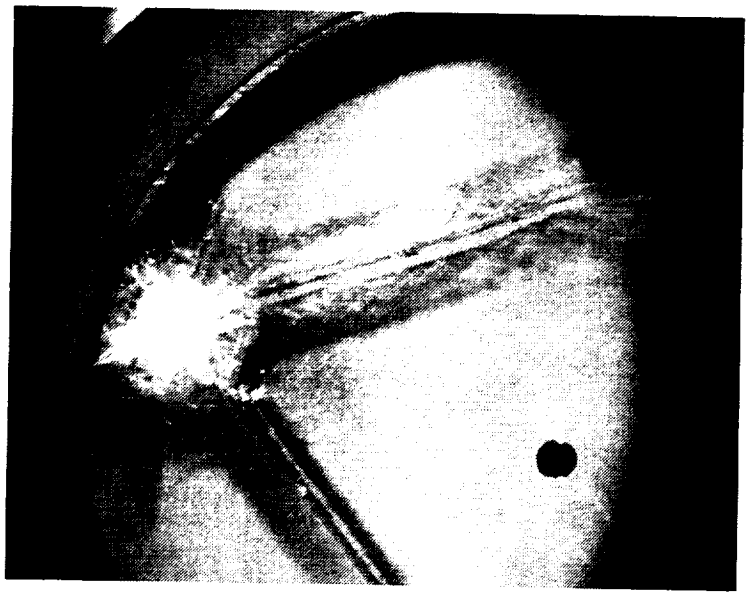

Figure 7-5 Photograph of an impact feature in a glass sample from tray B8. This picture shows an ~5mm diameter spallation zone and associated conchoidal fracture zone. The entire sample is cracked with two large wide cracks going all the way through the substrate, effectively breaking the sample in three pieces.

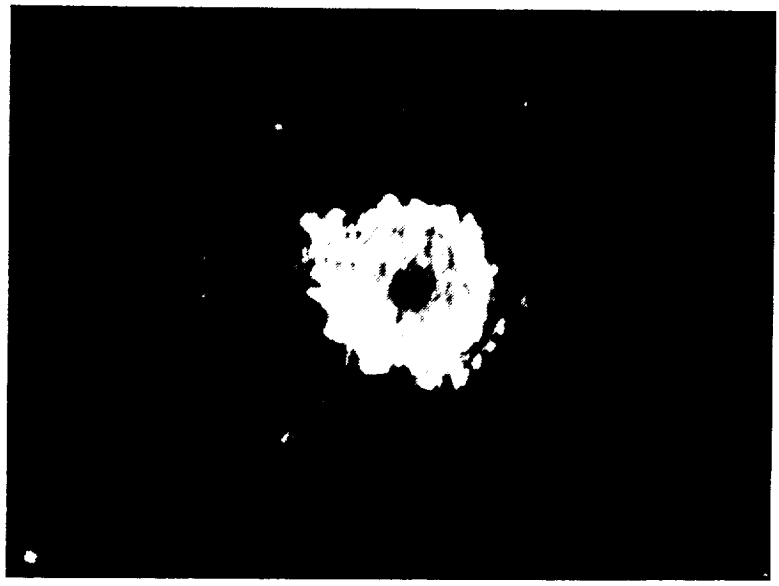

Figure 7-6 Photograph of an impact feature in a germanium substrate from experiment A0187-2. Note the large amount of surface cracking associated with the crater, and the surrounding conchoidal fracture and spallation damage.

7.3 CONTAMINATION

Contamination is a critical issue for spaceborne optical systems. Contaminants can arise from a variety of sources, including outgassing, debris shaken loose by launch or maneuver vibrations, and particulates created by collisions of space debris with baffle or sunshade materials. Upon return of LDEF, investigators analyzed the contaminant deposition on many samples and structure surfaces with a battery of tests. In addition, the contaminant distribution was mapped, contaminant sources identified, and transport mechanisms described. From this large library of information, this section will highlight those results which described optical scatter effects due to contamination. The section will be divided into two sections: 1) contaminating molecular films, and 2) particulate contamination. For other topics concerning contamination on the LDEF, readers are encouraged to review Section 8.0 of this Final Report summarizing the overall effects of contamination and browse the previous LDEF Conference Proceedings.

7.3.1 Contaminating Molecular Films

For space applications, the amount and composition of outgassed materials is of concern to the optical designer. One of the primary dangers is that the outgassed products can form a film with absorptive properties on optical components (ref. 21), as shown in figure 7-7. This can alter the transmissivity and reflectivity of the optical component, as well as introduce optical scatter. LDEF for example was estimated to have had nearly a pound of contaminating molecular film deposited on the surface while it was in flight (ref. 22). Two specific LDEF experiments illustrate this point in terms of contamination as a contributor to scatter on optical components.

LDEF Experiment #M0003-2 (ref. 23)

BRDF measurements on bare fused silica samples were reported from both leading and trailing locations in this study. The BRDF values recorded averaged about 10^{-5} inverse steradians for the post-flight samples, and a high resolution scatter mapping instrument provided scatter maps of the fused silica sample. Upon cleaning the surface of the uncoated fused silica with solvents, the scatter was significantly reduced, indicating considerable contamination on the sample surface, as shown in figure 7-8.

LDEF Experiment #S0050-2 (ref. 24)

Eastman Kodak Company included twelve substrate and coating samples on the LDEF structure. There were three fused silica and three Ultra Low Expansion (ULE) uncoated glass samples, two ULE samples with high reflectance silver coatings, and two fused silica samples with a solar rejection coating. A set of duplicate control samples was also manufactured and stored in a controlled environment for comparison purposes. BRDF measurements were performed post-flight on the high reflectance silver-coated flight samples (with contaminants), in addition to spectral reflectance and stress measurements. An increase in scattered light was measured on the contaminated flight sample versus that of the control sample. Figure 7-9 shows the BRDF curve from this study.

The following paragraphs describe related ground experiments on film contaminants. Though they are not from the LDEF mission, and were not necessarily done for low Earth orbits, they add further insight into the problem of outgassing residue, film deposition, and optical scatter.

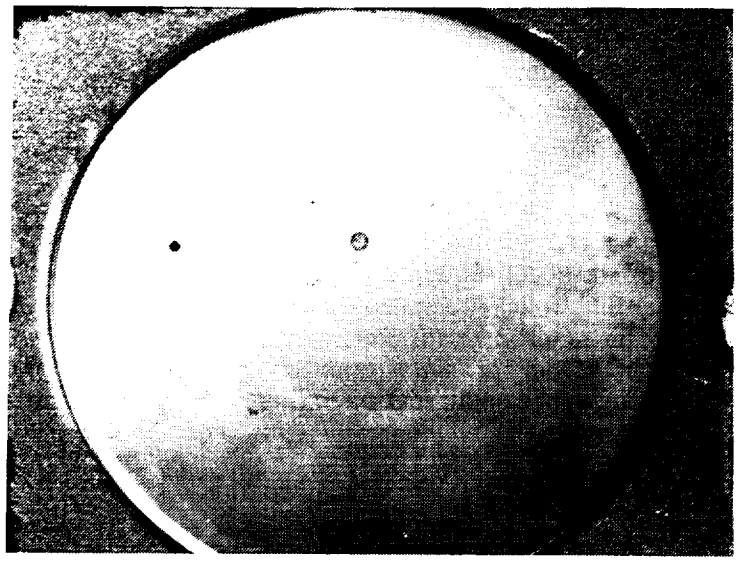

Figure 7-7. Contaminants on the surface of a MgF_2 optical window from Experiment S0050-1.

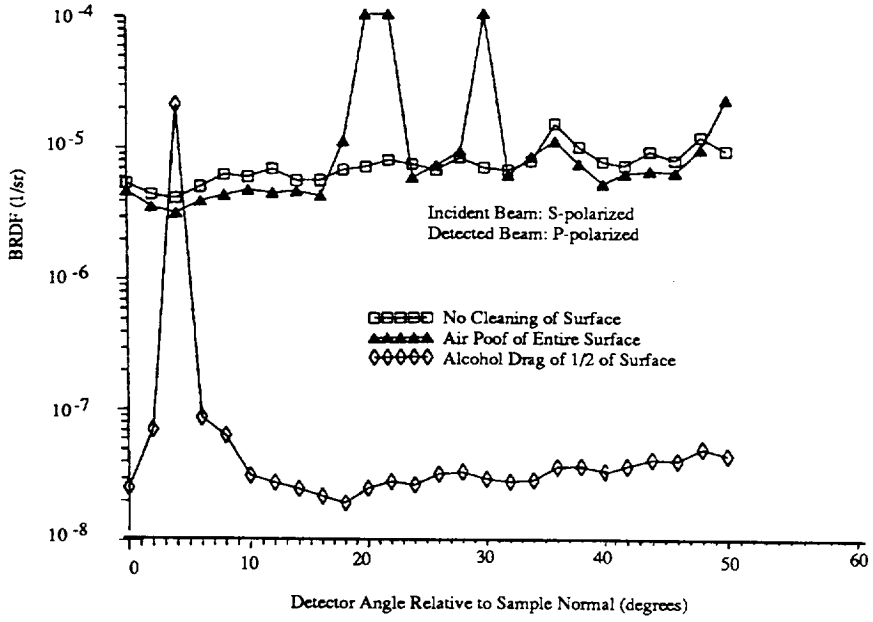

Figure 7-8. Scatter data showing effects of surface cleaning on fused silica sample.

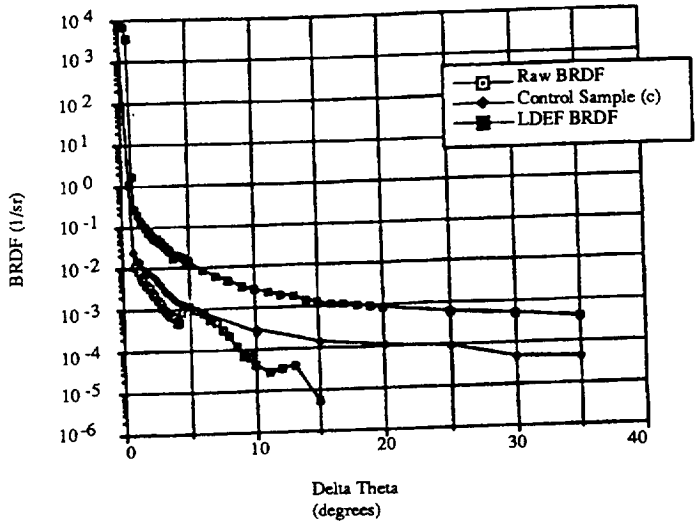

Figure 7-9. BRDF measurement of LDEF flight and control samples on high reflectance silver-coated ULE.

Hughes Aircraft Ground Study (ref. 25)

Exhaust from bi-propellent rocket boosters is a potential source of contamination for cooled sensor optics. The effect of monomethyl hydrazine nitrate (MMH-nitrate) on scatter at 3.39 micron wavelength was investigated as a function of temperature in the range of 200-350 Kelvin and as a function of thickness. The space simulation deposition of MMH-nitrate took place under high vacuum onto a bare beryllium mirror. This task determined that scatter from MMH-nitrate contamination is highly dependent on many factors including: 1) the substrate temperature during deposition, 2) the temperature history of the substrate after film deposition; 3) the temperature and pressure of the environment during and after deposition; 4) the rate of deposition, and 5) the length of time the contaminant is allowed to remain on a surface.

Midcourse Space Experiment Program (ref. 26)

Experiments have been performed under vacuum to measure the degradation of the 0.6328 um BRDF of a superpolished mirror and a superpolished quartz crystal microbalance (SPQCM) with condensed contaminant films for the Midcourse Space Experiment (MSX). The contaminant films studied were nitrogen, oxygen, carbon dioxide and carbon dioxide over nitrogen, and a mixed gas of equal parts nitrogen, oxygen, and carbon dioxide. In addition, the density of many of the films on the SPQCM was measured. Increases in BRDF were dependent on the condensed film thickness, temperature ranges used (15K-300K), and morphological changes in the film (e.g. shattering, fracturing). The following conclusions were drawn by the researchers:

1) Nitrogen films had minimal effects on the BRDF for the temperature (15K) and thicknesses (up to 8.25 μm) studied.
2) Oxygen on the 15K surface had the most effect on BRDF. A film as thin as 0.25 μm acted like a diffuse surface with a flat BRDF profile and increased the BRDF two orders of magnitude.
3) Carbon dioxide increased the BRDF. At 15K, it was observed to fracture with a 1.5 μm thick film, increasing its BRDF orders of magnitude. At 40-50K, no fracture was observed, and the BRDF change was small.

4) Water contaminant films were observed to shatter at both 25 and 40K for film thicknesses varying between 0.5 and 1.0 μm. After shatter, water films had the highest BRDF observed.
5) Layered nitrogen and carbon dioxide films at 15K behaved much like the carbon dioxide component alone.
6) A condensed mixture of nitrogen, oxygen, and carbon dioxide gases on a 16K surface was not observed to shatter and had little effect on the BRDF (less than a factor of two) for thicknesses up to 3.5 μm.

Hubble Space Telescope (HST) Returned Hardware Evaluation (ref. 27)

Reflectance degradation was investigated on optical elements from the returned Hubble Space Telescope system components. The Wide Field Planetary Camera flight pickoff mirror and the aperture window; as well as several filters from the High Speed Photometer instrument, were found to be contaminated with the same contamination layer (hydrocarbons, esters, silicones), but the thickness varied. Photoelectron spectroscopy was used to identify the surface chemical elements of the contaminant, and also to form a "square well" to measure the thickness of the film with atomic force microscopy. The contamination layer on the HSP filter was found to be 160 Angstroms-thick. The thickness of the aperture window and the pickoff mirror contaminant layer was deduced by using the ratio of sputter times and found to be 150 Angstroms, and 450 Angstroms, respectively. The investigators suggest that the contamination happened during normal on-orbit HST mission operations; outgassed molecules from electronics and other components that impinged on optical surfaces and were partially polymerized there by exposure to Earth-albedo UV. The suggested explanation is consistent with the results of the LDEF experiments.

No optical scatter measurement results were available for review at this time.

CIRRIS 1A Program (ref. 28)

This paper presents the activities that were pursued to reduce or eliminate contamination and off-axis light leakage for the Cryogenic InfraRed Radiance Instrument for the Shuttle (CIRRIS) 1A program flown on STS-39. The data showed how telescope light leakage and or contamination effects can dominate signal floor and place a limit on the weakest signal that can be measured when these undesired elements are present. BRDF measurements were made of the super-polished primary and secondary mirrors. The BRDF measurements indicate the quality of the mirror in terms of its scatter properties, and how contaminants will affect the type and quality of data. One unobvious result the authors reported was that a visibly clean mirror does not always correlate with what the BRDF measurements would indicate for cleanliness. They described how a visibly dirty mirror can give good BRDF values in the infrared, while a visibly clean mirror can give a poor BRDF measurement in the infrared. One explanation for this difference, according to the researchers, is how light interacts with contaminants at different wavelengths (visible versus IR). Finally, the investigators emphasized how the utilization of BRDF measurement is critical to learning whether the telescope mirror has been contaminated, and whether the scatter will cause the data to be degraded beyond the point of acceptance.

Summarized here are several methods available for minimizing molecular thin film contamination on optical surfaces. Where outgassing is a problem, much of the detrimental contamination deposited on spacecraft can be avoided with proper choice of materials and pre-flight bake-out procedures. Further, for an accessible ground-based optical system, normal cleaning procedures are appropriate for collecting optics and other optical-related hardware. For systems already in space, the procedures developed for insitu cleaning of optics may apply. These techniques include laser cleaning, plasma or ion cleaning, and jet snow cleaning (ref. 29). BRDF is one tool for detecting film residue on optical components, and verifying the effectiveness of cleaning techniques.

7.3.2 Particulate Contamination

The following LDEF examples, and other mission studies, deal with particulate contamination and the impact on induced optical scatter. Readers are encouraged to consult a paper by R.P. Young on low scatter mirror degradation by particulate contamination from orbit for background information on this general topic (ref. 30).

LDEF Materials Special Investigation Group (LDEF MSIG) Contamination Study (refs. 31 and 32)

Because of the large number of different materials types on board LDEF, and the long duration of space exposure, principal investigators found themselves faced with a daunting task of understanding the contamination history of the LDEF. They were challenged by the possibilities of migration of particles on the surface of the satellite in orbit, cross contamination from the Shuttle Bay, and the identification of contaminant sources not only from the LDEF itself, but the shuttle and ground-based activities. To further exacerbate the problem, the LEO environment affected the contaminant particles, and the surfaces of LDEF, contributing to the problem of determining the particle's source and the time of arrival on the LDEF surface. Investigators in these studies warn of the possible danger to contamination-sensitive hardware such as optics. Details from the contamination studies can be found in the references listed here, as well as from the other LDEF Materials SIG papers and LDEF Proceedings.

LDEF Meteoroid and Debris Special Investigation Group (M/D SIG) Study (ref. 33)

In this study, researchers found that M/D impacts on the LDEF surface often had an associated spray pattern "ejecta" from the projectile's impact that sprayed contaminants to nearby samples as shown in figure 7-10. They described the M/D impact related contamination to be more localized then other contamination types, and often generated from impactors and targets which are non-volatile and normally considered "safe", such as the aluminum experiment tray lip. These spray patterns and their sizes are directly related to the separation distance from the crater and geometrical orientation of the material surfaces with respect to the crater. The localized, heavy contamination is of particular concern to imaging optics due to the increased scatter. For solar power systems and thermal control materials, the concern is for reduced reflectivity and transmissivity, as well as, absorptivity and emissivity variations.

The LDEF and later missions, both stimulated and provided new work in the field of optical scatter due to particle contaminants. The following is a sampling of some of the work done for other missions.

Martin Marietta Energy Systems Ground Based Study (ref. 34)

In this study, the scatter and contamination of a low-scatter beryllium mirror with particles similar in size, shape, and composition to particles that could be released from a typical baffle material such as Martin Black was examined. The approach was to measure the optical scatter from the mirror at 10.6 micron wavelength with the mirror in the "cleaned" state. Then carefully controlled contamination was applied in a clean room with aluminum oxide powder. Calculations of expected optical scatter based on Mie scattering theory were made using the measured particle densities and assuming spherical particles. Their results showed reasonably good agreement between the Mie theory calculations and the BRDF measurements at the 10.6 micron wavelengths for particles comparable in size with the scattering wavelength. However, the authors demonstrated that the Mie theory calculations underestimated the scattering for real super-wavelength size particle distributions on the mirror surface and overestimated the scattering for a sub-wavelength size particle distribution. For the sub-wavelength size particle distribution, the increase in scatter in this experiment was negligible at the 10.6 micron wavelength.

Figure 7-10. Photograph showing an impact into the side of an aluminum structure which then sprayed material over 40 impact crater diameters across the germanium surface adjacent to it. This is the type of contamination that would be expected from an impact on the inside of a telescope shroud.

Space Based Visible Sensor Package Study (ref. 35)

This report describes a test program undertaken at Lincoln Laboratory to minimize the creation and spread of metallic particulates generated from the hundreds of fasteners used in the Space Based Visible (SBV) telescope packaging. The scattering performance of these mirrors is a function of the level of particulate contamination inside the telescope housing during ground processing, launch, and flight. The SBV sensor is a high straylight rejection telescope whose performance is driven by the low scattering surfaces of its primary mirrors. The SBV package is one of a suite of optical sensors to be launched on the MSX spacecraft. The prime function of the SBV is to view targets in deep space or near the Earth's limb. Researchers described the mission requirements for an off-axis telescope with high stray light rejection and low BRDF optics, a type of design extremely sensitive to particulate contamination. Early in the SBV program, instrument manufacturers and users noted one level of mirror performance in ground testing and a lower level on-orbit. Often this drop in performance could be tied to a suspected increase in BRDF suggesting increased scatter from contamination. Issues such as fastener material, insert material, lubrication, locking methodology, and insert types are described.

Midcourse Space Experiment (ref. 36)

Spacecraft-produced contamination in the optical viewing path of the sensor will obscure or degrade the farfield observation. Other problems related by the author are that radiometers will exhibit enhanced background intensities and temporal variability, and imagers will exhibit structured backgrounds and bright streaks caused by particle tracks. These optical effects will be wavelength dependent. Particles reaching the optical components will cause increased scatter and decreased system rejection performance. Their modeling of the orbital particle radiant

intensity signatures in the near field surrounding spacecraft indicated that substantial differences will exist between the spectra and intensities of different particle compositions. The authors made predictions for silver, aluminum, alumina, carbon, carbon dioxide and water ice, silicon dioxide, and titanium dioxide. The MSX provided simultaneous spectral coverage from 0.1 to 26 microns. These differences are exploited to determine particle composition and potentially their source. Thus, optical instrumentation will permit assessment of the success of contamination prevention through careful ground handling procedures. These sensors also will permit continuous measurement of the orbital production mechanisms (such as ageing, impacts, abrasion, and erosion) during long term spacecraft missions. Identification of generation rates and sources will guide future space system designers.

7.4 ATOMIC OXYGEN / ULTRAVIOLET (UV) EXPOSURE

Experiments on the LDEF have indicated how the properties of materials changed after nearly six years of exposure to atomic oxygen (AO). When atomic oxygen collides with a spacecraft surface, atomic oxygen may initiate a number of chemical and physical reactions with the materials of the surface with which it collides. These interactions contribute to material degradation, surface erosion, and contamination (ref. 37). Of concern is not only the possible erosion of optical elements themselves, but the possibility that the degradation residue from neighboring eroding structures will redeposit on optical elements and cause significant optical scatter problems. Following are some LDEF studies of interest that discuss results of atomic oxygen and UV exposures.

LDEF Materials Special Investigation Study (ref. 38)

For Chemglaze (now Aeroglaze) Z306 thermal control paint, the LDEF exposure led to a loss of the binder material and to loss of pigment to a depth of at least 10 microns into the coating. This study, and others heightened the concern for optical components because of the degradation of Z306 and other AO-eroded materials on LDEF, and possible redeposition of residue on optical components.

LDEF Experiment #S0069 (ref. 39)

AO erosion of the exposed silverized Teflon (Ag/FEP) surface in this experiment was typical of that observed on other flights. Erosion created a non-uniform etching pattern with peaks about 1.5 μm apart which were highly light scattering. In addition, where Ag/FEP was struck by meteroid and debris impacts, the morphology was described as craters with blow-back areas at the crater rim, or layers of silver/Inconel and adhesive missing altogether. These results are an issue for nearby optical surfaces, in situations where it is essential that the stray light background be minimized.

LDEF Experiment #S0050 (ref. 40)

Space environmental effects were shown to improve the scattering properties of black paints used for baffling optical systems in this study. The researcher hypothesized that the increased absorption of the black paint may be related to loss of volatile components in the coating binder, and degradation of the pigment and binder by UV radiation providing an increased density of absorption sites in the paint films. Though the effects could occur during natural ageing, the author speculated the space exposure may accelerate them. A reflecting-layer model was then used to analyze the reflectance spectra. The author reported the post-recovery reflectance data could not be fitted with a change in surface roughness or coating thickness, indicating that surface roughening or loss of material from erosion of other effects of space dust and debris did not cause the decreased reflectance.

Whether a material (such as the black coating described above) has degraded by ageing or space environmental effect and how its optical properties are altered is only one concern. If

contaminants are generated from degrading black surface, and deposited onto mirror surfaces, the result may be increased scattered light in an actual optical system. The optical system degradation may be even more pronounced and detrimental than alteration of the black coating (refs. 41, 42, and 43).

Following is another study examining the effects of AO on materials. This is a non-LDEF mission.

Surface Effects Sample Monitor (SESAM) Experiment (ref. 44, 45)

This experiment was mounted (amongst many others) on the ASTRO-SPAS satellite. The system serves in general as a vehicle for a cooperative German/US science program with four missions; of which only the first mission has been flown and results published. The German part of the program is being managed by Deutsche Argentur fur Raumfahrtangelegenheiten, and the satellite is being developed and manufactured by Messerschmitt-Bolkow-Blohm (MBB). The system consists of a reusable Space Shuttle dedicated satellite for operation in the vicinity of the Shuttle Orbiter. The satellite is deployed and later retrieved by the orbiter, and serves as a platform for well characterized samples undergoing space exposure. At the end of the mission the samples are investigated with respect to surface roughening and scattering. Three sets of samples are exposed to different mission conditions: Phase 1 samples are exposed during shuttle launching, Phase 2 samples are exposed to space atomic oxygen, and Phase 3 samples are exposed during the landing phase, to collect information on the contaminants entering the cargo bay after venting. Sample investigations are carried out using a total integrated scatter apparatus, and a Nomarski microscope system. The 1993 space mission determined that conditions in space increased the scattered light from mirrors. The agencies expect to return SESAM to space in 1996 and 1997.

7.5 SCATTER ANALYSIS TOOLS

Two computer programs that are useful for evaluating the effect of space exposure on optical scattering are examined in this section. The first has the acronym SPENV, and was used on LDEF to evaluate the nature of M/D impacts on induced optical scatter. The second is called PEARLSS which evaluates the effect of particulates in the optical train. These are only two of a large number of scatter analysis programs available. Readers are encouraged to review the list in J. Stover's book (ref. 46).

POD Associates LDEF Study (SPENV Computer Program) (ref. 47, 48)

The SPENV computer program addresses the issue of surface erosion of optical components, and considers the nature of the M/D impact damage and the first-order estimates of induced optical scatter. The authors suggest the studies are of interest to the hypervelocity impact community since they involve the problems of fragmentation, cratering and cracking logic, in addition to the estimates of optical scatter. In order to assess impact damage, POD Associates have incorporated the existing micrometeoroid and debris models into a computer program called SPENV. This code allows predictions of expected impact fluences as a function of satellite parameters.

POD Associates performed first-order estimates of the probable modes of particle impact damage and consequential increases in optical scatter for satellite optics in LEO. The methodology requires use of the existing near-Earth particle environment. Both simple ductile metal cratering and brittle material cracking have been addressed. The analyses include estimates of fractional area affected. For an orbit of 1000 km, inclination of 60° and period of 6 years, even the leading edge surface suffers from less than 1 percent areal damage due to simple ductile cratering. However, if star cracking in brittle materials occurs the affected areas rapidly

increase. Note that the orbit chosen is one of the worst cases, involving a local peak in the man-made debris population.

Many optics are not simple metal mirrors, for which the major response is near hemispherical cratering, but frequently are comprised of brittle dielectrics (including multilayer coatings). These suffer conchoidal cratering, star cracking and interlayer delamination. The modeling between the induced mechanical damage and the resulting increased optical scatter becomes more complex.

To assess the optical scatter for these conditions, the cracks were treated as cylinders with all dimensions large compared to the operating wavelength to determine the scatter. Further the researchers calculated the crack pattern if it becomes dense. They found that cracks are less efficient scatterers than are craters. Since it was shown that the usual associated damage area of the cracks is also less than that of the craters, the result is that the craters are expected to dominate the overall scattering.

If the cracks are narrow compared to the operating wavelength, they behave as dielectric "needles". The effective refractive index is based on the mismatch between the crack region and the surrounding medium. For scatter measurements done at wavelengths which are different from the tuned wavelength of the quarter wave stack, the value of this index is similar to that for the individual layer materials. However, at the tuned wavelength the effective index may be much higher, since the optical stack behaves as a single dielectric with high refractive index (giving high reflectivity).

In summary, the researchers demonstrated the correlation between crater morphology and scatter to be quite complex because of dependencies on the details of crater sizes and crack lengths. The models used presently give reasonable agreement with the LDEF experimental data in terms of impact fluences and directionality on the spacecraft body. The analyses of increased optical scatter (BRDF) demonstrate strong dependencies on the details of crater sizes and crack lengths. Presently, their analyses indicate the potential for large increases in optical scatter for unshielded optics on the leading edge, but only small increases for Earth-looking cases. Additional work has been performed to estimate the change in optical scatter with this model at POD Associates (ref. 49). However, this report was not available for review at this time, since it is in the process of being published, and has not yet been released.

According to D. Atkinson of POD Associates, the new report will describe how the SPENV code is used to model the impact effects on optics. These models have been validated for small (1"-2" dia) sample surfaces. Models are available for larger surface areas as well, but no test data are yet available to validate the models. Further, this code is now capable of examining the effect of environmental effects over time, looking at the entire period of time an optic is exposed, and different times along the period (ref. 50). This suggests another role for BRDF, as a design tool for optical system performance degradation.

Nichols Research Corporation Study (PEARLSS code) (refs. 51 & 52)

A computer model was developed by the Nichols researchers to determine the degradation of sensor performance due to particulate contamination. The Particulate Effects Analysis on Response Levels of Spaceborne Sensors (PEARLSS) code, is designed to simulate the key aspects of the contamination problem. Particulate contamination can degrade the ability of the sensor to perform its acquisition, detection, imaging, and/or track correlation functions. These authors report that to accurately predict the effects of particles in sensors, the particles must be tracked through time as they are created, moved around, bounce from surfaces, and either adhere to a surface or leave the system. Creation of noise across the focal plane is one problem, but of greater long-term significance is the degradation caused by the deposition of this contamination onto the optics, thus changing the BRDF. This can lead to significant off-axis

rejection problems, especially in modern superpolished mirror systems which are built to very tight tolerances and with detectors so sensitive that even a small amount of scattered radiation can cause serious noise problems. The authors explain how the contaminants that collect on the surfaces of the sensor during manufacture and storage can easily be shaken loose by vibration. Further, collisions with space debris can result in hypervelocity impacts.

The PEARLSS code is subdivided into several functional blocks, each of which performs part of the overall task of determining sensor degradation due to particulates. Key functional areas are the inputs: contaminant generation, particle tracking, particle deposition and BRDF, light scattering, thermal heating and emissions, radiation sources (Earth, Sun, others) imaging of scattered radiation, and noise map outputs. Inputs and substructures are designed to increase the flexibility of the simulations. Light from various sources is scattered off of the particulates. This radiation is mapped as a noise scene at the front mirror and the focal plane. The code is intended for performing parametric studies on design parameters such as sunshade geometry, system materials, temperatures, pre-launch cleanliness levels, and pointing directions. Sources of radiation currently modeled are the Sun and Earth, as well as user-defined sources. An overview of the simulation's approach to tracking contamination and scattered radiation is given. To provide a systematic method for treating the scattering properties of randomly oriented, nonspherical particles, Mie theory is utilized. The spherical particle approximation from the simple Mie theory provides a good fit to measurements at all scattering angles, and is used in PEARLSS for all scattering calculations. This simulation deals with contamination generation, migration, and deposition, as well as the resulting optical degradation, in a single end-to-end code. The PEARLSS simulation can provide detailed noise maps at the focal plane due to off-axis scattering from particulates in the field of view. These noise maps can be used with signal processing simulations to determine the system's overall response to contamination. This simulation provides a useful engineering tool for studying particulate effects in a wide range of systems.

Their conclusions are, that impacts will produce a shower of smaller particles, which can imbed in system materials, bounce about in the system, or cause cascades of other particle showers through the system. The amount of time particles linger in the field of view affects the sensor's ability to recover from contamination effects, and the spatial and temporal structure of the noise. Studies show that the most critical factor which affects particle lifetimes is the energy loss per impact. The energy lost upon impact is a quantity which depends on the materials involved. Knowledge of particles dynamics with respect to the materials used in a typical system is critical to successful simulation.

7.6 MORPHOLOGICAL FEATURES MEASUREMENT AND PHOTO DOCUMENTATION

The previous paragraphs have described how space environmental effects degraded the surface. In this section we are concerned primarily with characterizing and documenting the physically altered surfaces on LDEF and how those structures scatter light. Following are two studies that were responsible for characterizing, quantifying, and photodocumenting the change in surface topography on LDEF. The third paragraph describes the LDEF Archive which will eventually house all LDEF-related data, including the morphological and feature measurement material.

Meteoroid and Debris Special Investigation Group (M/D SIG) Photo Survey Study (ref. 53)

During a three month period (February through April 1990) members of the M/D SIG, as well as other individuals, examined and photodocumented thousands of impact-related features from all exposed surfaces of the LDEF spacecraft. The impact craters were visually identified and given location coordinates. Crater sizes and impact penetration hole diameters were quantified, then all impacts were photodocumented and stored on laser disk drives. Details on material type, crater morphology, number of impacts, sizes, etc., are available in this valuable resource if needed for scatter modeling and validation studies.

Aerospace Corp LDEF M0003 Experiment Deintegration Study (ref. 54)

The M0003 experiment hardware consisted of four trays, two on the leading edge and two on the trailing edge. Over 1270 materials samples of more than 200 material types (of which a significant number were optical materials and components) were mounted on the trays. As each test sample was removed from the four LDEF M0003 trays, they were individually examined and photographed through high resolution optical microscopes using brightfield, dark-field, and Nomarski techniques. The samples experienced various space induced damage such as crazing, surface roughening, discoloration, erosion, and contamination, as well as other damage mechanisms. Observations of the effects were recorded by a single examiner to maintain a consistent criteria for the qualitative description of all M0003 samples and hardware. This set of photomicrographs is an excellent resource for examining morphological features caused by meteroid and debris impacts, as well as other space environmental effects on optical materials.

LDEF Archive System (ref. 55)

To ensure the long-term accessibility of the LDEF-related data, photographs, publications and hardware, Boeing Aerospace Operations, under contract to NASA Langley Research Center, established the LDEF Archive System. The archive is available through a single point of contact via computer network, phone, mail or personal visit, and it provides the foundation for a broader Space Environmental and Effects Archive System. It is designed as a comprehensive resource that will include existing LDEF special investigation group and other LDEF-related data bases. The data being assembled for each experiment include hardware drawings, material lists, design review documentation, photographs, publications, correspondence and research data.

7.7 CONCLUSIONS

While reviewing the various published LDEF papers, several observations became apparent. The first is that early LDEF results appeared to stimulate work on induced optical scatter due to space environmental effects, directing not only later LDEF investigation into scatter effects, but also ground experiments for upcoming missions.

Secondly, because of the wide range of scientific disciplines and materials on-board LDEF there was a natural and beneficial cross-application of results which added significant information on the formation of optical scatter sites on exposed space materials. For instance, the meteroid and debris scientists have contributed critical information on the deterioration of optical components from impacts, and the materials specialists have identified materials degradation mechanisms. The authors referenced here are acknowledged for their important contributions to the study of optical scatter.

Third, there was a large amount of technical information on optical scatter from LDEF, but it had never been reviewed in its entirety. Similarly, other missions have investigated optical scatter, but often their investigations have focused on one type of scatter source, e.g. contamination, while leaving unmentioned the combined contributions of the other scatter sources resulting from space environmental effects including micrometeoroid and debris impacts, AO erosion, UV degradation, thermal effects, and the synergistic effects of these environmental effects combined. This report has attempted to collect the optical scatter information from LDEF and later missions for the reader, and summarize the findings here in hopes of beginning this process.

The results from the LDEF experimenters and other recent mission suggest the following conclusions concerning optical scatter effects on optical systems:

- *Micrometeoroid/debris impacts on high resolution optics may result in small reductions in reflectivity, and/or transmission; but can increase scattered light significantly. Modeling the scatter effects can be quite complex because of dependencies on impact morphologies.*
- *Contamination on surfaces can increase the optical scatter. Whether deposited on surfaces as a film residue from outgassing; or particles shaken loose by launch vibrations; or created by M/D impacts on systems materials, contamination is a major concern to optical designers. The designer must evaluate the required image quality and evaluate the proximity to contamination generators, and guarantee that materials on the spacecraft surfaces do not degrade the more sensitive optical components on board over the design life of the system.*
- *Atomic oxygen erodes unprotected materials such as certain metallized coatings and carbon-based materials, resulting in roughened surfaces and the generation of contaminants. Both the change in topography and contaminants contribute to increases in optical scatter on or near critical optical surfaces.*
- *BRDF is now recognized as a sensitive parameter to judge the effects of space environmental effects on optical scatter. Its role continues to expand to include evaluation of space optical system performance degradation over time.*
- *Modeling, ground-based, and space flight optical scatter studies have provided useful optical scatter data and performance predictions, especially for contamination and M/D impacts parameters. However, additional studies concerning the <u>combined</u> effects of outgassing residue, particle deposition, AO erosion and M/D impacts on critical low scatter space optical components should also be considered.*

7.8 REFERENCES (FOR SECTION 7)

1. Bennett, J. M. and L. Mattson, Surface Roughness and Scattering, Optical Society of America, Washington, DC, pg. 30, (1989).

2. Stover, J. C. Optical Scattering: Measurement & Analysis, McGraw-Hill, Inc. N.Y. pg. 161, (1990).

3. Nicodemus, F. E., J. C. Richmond, J. J. Hsia, I. W. Ginsberg, and T. Limperis, "Geometric Considerations and Nomenclature for Reflectance", U.S. Dept. Of Commerce, Washington, DC, NBS Monograph 160, (1977).

4. Bennett, J.M. and L. Mattson, Surface Roughness and Scattering, Optical Society of America, Washington, DC, pg. 30, (1989).

5. Stover, J.C., Optical Scattering: Measurement & Analysis, McGraw-Hill, Inc. N.Y. pg. 161, (1990).

6. Pompea, S. M. and S. H. C. McCall, "Outline of Selection Processes for Black Baffle Surfaces in Optical Systems", SPIE Int. Soc. Opt. Engr. (USA) 1753, pg.92- 104, (1992).

7. Krone-Schmidt, W. and R. C. Loveridge, "Cryo-vacuum BRDF Measurements of MMH-Nitrate", SPIE Int. Soc. Opt. Engr. (USA) 1754 , pg. 58-71, (1992).

8. Watts, A. D. Atkinson, C. Coombs, and L. Crowell, " Optical Scatter Due to Impact Effects", SPIE Int. Soc. Opt. Engr. (USA) 1761, pg. 72-81, (1992).

9. Crawford, G., M. F. Rose, R. H. Zee, "Morphology Correlation of Craters Formed by Hypervelocity Impacts", LDEF Materials Results for Spacecraft Applications, NASA CP-3257, pg. 245-258, (1993).

10. Mirtich, M.J. et.al. "Effect of Eleven Years in Earth Orbit on a Mirror Surface", Journal of Spacecraft and Rockets, 27, number 3, May-June (1990).

11. Stover, J.C. Optical Scattering: Measurement & Analysis, McGraw-Hill, Inc. N.Y. pg. 161, (1990).

12. Allbrooks, M. and D. Atkinson, "The Magnitude of Impact Damage on LDEF Materials", LDEF M&D SIG Support, NAS9-17900, SC-02N0165768, Project No. 960-12-171, (1992).

13. Singer, S.F., et.al. "First Spatio-Temporal Results from the LDEF Interplanetary Dust Experiment", Adv. Space Res, 11, No. 12, 115-122, (1991).

14. Mulholland, J. D., et.al., "LDEF Interplanetary Dust Experiment: A Time Resolution Snapshot of the Near-Earth Particulate Environment", Workshop on Hypervelocity Impacts in Space, Univ. of Kent at Canterbury, July (1991).

15. DeHainaut, L. L., Kenemuth, J. R., et. al., "Degradation of Optical Components in a Space Environment", presented at the 2nd LDEF Symposium, San Diego, CA. NASA CP-3194, (1993).

16. Allbrooks, M. and D. Atkinson, "The Magnitude of Impact Damage on LDEF Materials", LDEF M&D SIG Support, NAS9-17900, SC-02N0165768, Project No. 960-12-171, (1992).

17. Kemp, W.L. ,Watts, A., et.al. Long Duration Exposure Facility Optics Handbook, Phillips Laboratory Report PL-TN-93-1067, (1993).

18. Zweiner, J. M. and M. Finkenor, "Micrometeoroid / Space Debris Effects on Materials", LDEF Materials Results for Spacecraft Applications, NASA CP-3257, pg. 259-279, (1993).

19. Weidlocher, D. E., D. Kinser, R. A. Weller, "LDEF Materials Results for Spacecraft Applications, NASA CP-3257, pg. 227-243, (1993).

20. Crawford, G., M. F. Rose, R. H. Zee, "Morphology Correlation of Craters Formed by Hypervelocity Impacts", LDEF Materials Results for Spacecraft Applications, NASA CP-3257, pg. 245-258, (1993).

21. Pompea, S. M. and S. H. C. McCall, "Outline of Selection Processes for Black Baffle Surfaces in Optical Systems", SPIE Int. Soc. Opt. Engr. (USA) 1753, pg. 101, (1992).

22. Crutcher, E. R., L. S. Nishimura, K. J. Warner and W. W. Wascher, "Migration and Generation of Contaminants from Launch Through Recovery: LDEF Case History", First LDEF Post-Retrieval Symposium, NASA CP-3134, pg. 121-140, (1992).

23. DeHainaut, L. L., Kenemuth, J. R., et.al., "Degradation of Optical Components in a Space Environment", presented at the 2nd LDEF Symposium, San Diego, CA. NASA CP-3194, (1993).

24. Havey, K. A. Mustico and J. Vallimont, "Effects of Long Term Space Environment on Optical Substrate and Coatings", SPIE Int. Soc. Opt. Engr. (USA) 1761, pg. 2-13, (1992).

25. Krone-Schmidt, W. and R.C. Loveridge, "Cryo-vacuum BRDF Measurements of MMH-nitrate", SPIE Int. Soc. Opt. Engr. (USA) 1754, , pg. 58, (1992).

26. Seiber, B. L., R. J. Bryson, R. P. Young Sr., B. E. Wood, and D. Dykeman, " Effect of Cryocontaminants on Cryogenic Super-Polished Mirror and Super-Polished Quartz Crystal Microbalance, SPIE Int. Soc. Opt. Engr. (USA) 1754, , pg. 215-225, (1992).

27. Tveekrem, J.L. "Optical Component Degradation Assessment, Part II--Surface Chemistry, HST Returned Hardware Evaluation Symposium, December 15, 1994.

28. Wheeler, N. B, D. Smith, D. Dean, H. Gardiner, et.al., "An Assessment of the Near-Field Contamination and Off-Axis Leakage Effects on Earthlimb Background Measurements from CIRRIS 1A", SPIE Int. Soc. Opt. Engr. (USA), 1754, pg. 156-168 (1992).

29. Glassford, A.P. Editor, SPIE Int. Soc. Opt. Engr. (USA), 1754 , (1992).

30. Young, R.P. "Low Scatter Mirror Degradation by Particle Contamination", Optical Engineering, 15, no. 6, pp. 516, (1976).

31. Crutcher, E. R. W.W. Wascher, "Particle Types and Sources Identified With LDEF", First LDEF Symposium, CP-3134, (1992).

32. Crutcher, E. R. , "The Characterization of Particles on Spacecraft Returned From Orbit", Particles on Surfaces: Detection, Adhesion, Removal, ed. K.L. Mattal, Marcel Dekker, Inc. pg. 219-252, (1995).

33. Allbrooks, M. and D. Atkinson, "The Magnitude of Impact Damage on LDEF Materials", LDEF M&D SIG Support, NAS9-17900, SC-02N0165768, Project No. 960-12-171, (1992).

34. McNeely, J. R., M. B. McIntosh, and M. A. Akerman, "Scatter and Contamination of a Low-Scatter Mirror", SPIE Int. Soc. Opt. Engr. (USA) 1530, 288-298, (1991).

35. Morelli, M. D. and S. E. Forman, "Prevention of Particulate Contamination from Fasteners on the Space-Based Visible Telescope, SPIE Int. Soc. Opt. Engr. (USA) 1754, pg. 249-260, (1992).

36. Green, B.D., "Optical Signatures of Particles in Space", "SPIE Int. Soc. Opt. Engr. (USA), 1754, pg. 1103-1113 (1992).

37. Bourassa, R., J. R. Gillis, K.W. Rousslang, "Atomic Oxygen and Ultraviolet Radiation Mission Total Exposures for LDEF Experiments", LDEF-69 Months in Space, 1st LDEF Post Retrieval Conference, NASA CP-3134, Part 2, pg. 643-661, (1992).

38. Golden, J. L. "Results of An Examination of the A-276 White and Z306 Black Thermal Control Paint Disks Flown on LDEF", NASA CP-3134, First LDEF Post-Retrieval Symposium, (1992).

39. Zweiner, J. M. et.al., "Unusual Material Effects Observed on the Thermal Control Surfaces Experiment (S0069), First LDEF Post-Retrieval Symposium, NASA CP-3134, pg. 919-933, (1992).

40. Blue, M. D. A Final Look at LDEF Electro-Optic Systems Components, Third LDEF Conference Proceedings, NASA CP-3275, Part 3, pg. 1179-1188 (1995).

41. Bass, M. ed., "Black Surfaces for Optical Systems", Handbook of Optics, Optical Society of America, McGraw-Hill, Inc., pg. 37.1-37.70, (1995).

42. Dyer, J. , R. Benson, J. Guregian, "Outgassing Analyses Performed During Vacuum Bakeout of Components Painted with Chemglaze Z306/9922, SPIE Int. Soc. Opt. Engr. (USA), 1754, 177-194, (1992).

43. Pompea, S. M. and S. H. C. McCall, "Outline of Selection Processes for Black Baffle Surfaces in Optical Systems, SPIE Int. Soc. Opt. Engr. (USA) 1753, pg. 92-104, (1992).

44. Schmitt, Dirk-Roger and H. Swoboda, "Scatter and Roughness Measurements on Optical Surfaces Exposed to Space", SPIE Int. Soc. Opt. Engr. (USA) 1530, pg. 104-110, (1991).

45. Weiss, S. "Germans Study How Space Degrades Photonic Materials, Photonics Spectra, December (1994).

46. Stover, J. S., Optical Scattering: Measurement and Analysis, McGraw-Hill, Inc. pg. 161, (1990).

47. Atkinson, D. and A. Watts, "Impact Damage and Optical Scatter", Int. J. Impact Engng., 14, pp.49-60, (1993).

48. Watts, A. D. Atkinson, C. Combs, and L. Crowell, " Optical Scatter Due to Impact Effects", SPIE Int. Soc. Opt. Engr. (USA), 1761 (1992).

49. Atkinson, D. and A. Watts, "Impact Effects on Optics Survivability", Phillips Laboratory Technical Report #94-1046, Defense Technical Information Center, (1994).

50. Atkinson, D. Personal telephone conversation with author on 01-19-95.

51. Jackson, J. L. and L. A. Whitlock, "Simulation of Effects on Sensor Performance from Particulate in the Near-Field of View, SPIE Int. Soc. Opt. Engr. (USA), 1687, pg. 158-168, (1992).

52. Whitlock, L. L. Glasgow, and J. Jackson, "Contamination Dynamics Modeling Studies for PEARLSS, NRC Technical Report, NRC-TR-92-024, (1992).

53. See, T., M. Allbrooks, D. Atkinson, C. Simon, M. Zolensky, "Meteoroid and Debris Impact Features Documented on the Long Duration Exposure Facility: A Preliminary Report", NASA JSC # 24608, Publication #84, August 1990.

54. Gyetvay, S., H. Kan, M. Meshishnek, and J. Coggi, "M0003 Data Base Guide Book", The Aerospace Corp., Second LDEF Post Retrieval Symposium, June 1992.

55. Wilson, Brenda, "LDEF Archive System", LDEF 69 Months in Space; Third LDEF Post-Retrieval Conference, NASA CP-3275, February 1995

8.0 A CONTAMINATION SUMMARY OF LDEF

This report summarizes the contamination observed on the LDEF experiment trays, the LDEF structure, electronics, and support hardware (tray clamps, etc). The prelaunch contamination levels will be discussed first, followed by summaries of visual observations from the post-mission survey. These general descriptions will be followed by more detailed discussions of specific components of the LDEF, and an in-depth summary of materials degradation and contamination effects. It should be noted that LDEF was not designed or handled as a contamination sensitive payload during ground operation activities. As such, the post-mission results may reflect various qualities of workmanship, improper handling, etc. An attempt to differentiate between true contamination effects and workmanship (e.g., improperly applied coatings) has been made.

8.1 OBSERVED LDEF CONTAMINATION

This section will focus primarily on contamination deposition and effects. Other environmental effects such as atomic oxygen degradation, and solar illumination will be discussed in so far as they influence or contribute to the contamination environment and effects.

A time line of contamination generation and accumulation on LDEF was developed early in an LDEF Systems SIG investigation[1] as a series of ten exposures based on post-mission measurements and illustrated in figure 8-1. Minimizing contamination from ground operations prior to launch (exposure 1) and the launch environment (exposure 2) are critical to the initial performance of the systems in orbit. Early mission failures or problems may well have been the result of deficiencies during these phases of operation. Once on-orbit (exposure 3), outgassing and redeposition of molecular films were shown to degrade thermal control, optical, and solar energy systems. With the initiation of the retrieval activities, LDEF was exposed to new sources of contamination (exposures 4 through 10). The contaminants generated during retrieval activities were identified and backed out of the analysis to obtain the on-orbit contamination levels.

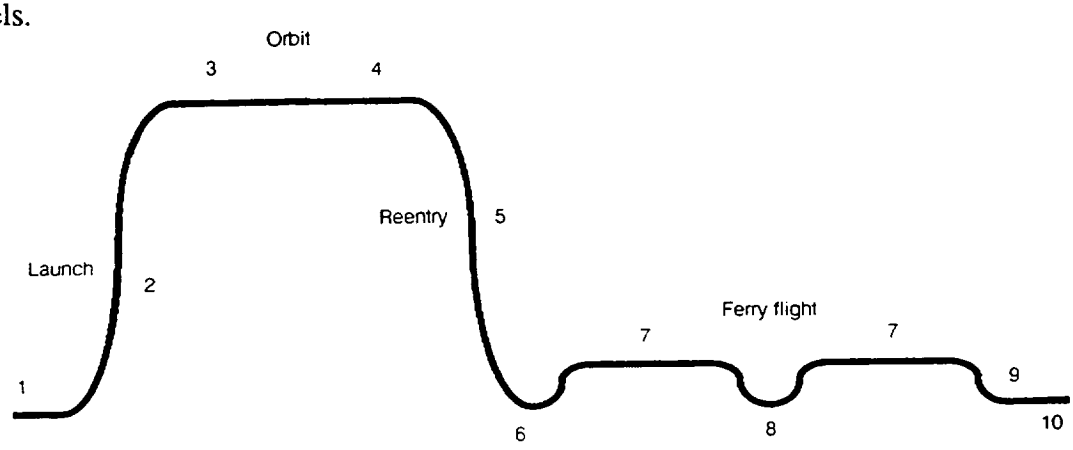

1. Condition of LDEF prior to launch: > MIL STD 1246B level 1000C for many trays.
2. During launch, many particulate contaminants are redistributed and Shuttle Bay debris is added.
3. Contaminants are modified and new contaminants are generated in the orbital environment.
4. Grappling causes some particles and films fragments to move, some may have relocated on LDEF.
5. During reentry, many particles and fragments of brittle molecular contaminant films relocate.
6. The Shuttle is exposed to the Edwards environment, accumulation of natural dusts.
7. High humidity, high gas flow velocities, thermal and pressure stresses occur.
8. HEPA filter fibers appear on tape lifts after exposure to new filters.
9. Ground operations prior to SAEF-2 include many manipulations to LDEF in complex environments.
10. SAEF-2 exposure

Figure 8-1 Contamination Exposure History of LDEF

8.1.1 Prelaunch Contamination

The LDEF was not designated as a contamination sensitive payload, consequently, formal measurements of prelaunch contamination values (particle level and molecular level) were not made. However, in most cases, it has been possible to derive estimates of prelaunch molecular and particulate levels, based on post-mission retrieval measurements of control samples and unexposed areas on LDEF.

8.1.1.1 Molecular Contamination

Molecular contamination of surfaces and systems can pose serious system degradation threats. Optical and thermal control systems are particularly vulnerable to contamination deposition. Optical systems can experience decreased performance due to contamination of specific elements. For example, molecular contamination on mirror surfaces can cause a decrease in reflectance and an increase in scattered light. Transmittance properties of lenses are greatly affected by layers of contaminant films. The presence of excessive contamination within an optical system can result in inaccurate imaging and unreliable detection of desired viewing targets. Thermal control surfaces, which are designed to effectively operate with specific thermal/optical properties, can be substantially degraded due to contamination deposition on the surfaces. This can potentially result in the loss of thermal control for a subsystem or spacecraft.

There were no specific prelaunch nonvolatile residue (NVR) measurements taken on LDEF surfaces. However, based on the post-mission NVR measurements, combined with assumptions regarding accumulations of additional molecular contamination from on-orbit materials outgassing, it has been estimated that the LDEF NVR level at launch was on the order of 2.5 mg/ft^2, corresponding to a MIL-STD-1246 Level C.[2] Molecular contamination found on the tray clamps and shims at numerous LDEF locations were measured post-mission. Front side (exposed) results were compared with back side (unexposed, control sample) to determine the LDEF prelaunch NVR levels. The amounts of molecular contamination measured on LDEF surfaces after the flight were much higher than the amount of contamination measured on the control samples, (back side of tray clamps and shims), suggesting that significant on-orbit deposition of outgassing by-products occurred.

8.1.1.2 Particulate Contamination

It can be inferred, by the types of particles identified, that most of the particulate contamination present in orbit was deposited on the surfaces of LDEF during ground exposure or the launch environment. The particles found on LDEF during post-mission examinations were characteristic of fabrication, assembly, and integration activities; some of the deposition patterns suggested that particles were redistributed due to launch forces or cross contamination. Particulate contamination can affect systems, both optically and mechanically. Particles may optically obscure, scatter, refract, diffract, and reflect light. They may also become infrared emitters. Scatter, refraction, diffraction and reflection all change the path of a ray of light. This effect introduces unwanted energy into the system decreasing the signal-to-noise ratio in an optical system, thereby decreasing a system's sensitivity.

As mentioned before, specific prelaunch surface cleanliness measurements were not taken on LDEF; consequently, a backtracking method of estimating the prelaunch particle cleanliness level was employed, based on post-retrieval LDEF surface inspections. The estimated particle cleanliness level of LDEF can be split into two ranges, based on particle diameter. For particles less than 250μm the estimated prelaunch cleanliness level was approximately a MIL-STD-1246 Level 1000. When considering those particles with larger diameters (less than 750 μm), the estimated particle cleanliness levels translates to roughly Level 2000 per MIL-STD-1246.[2]

8.1.2 Post-Mission Survey

Most experimenters had the opportunity to perform a post-mission inspection of the samples and experiments after retrieval of the LDEF. The following sections provide an overview of the more significant findings based on these surveys.

8.1.2.1 Molecular Contamination

The first, quick-look inspection of LDEF found an easily visible, brown discoloration on several LDEF surfaces. In fact, this discoloration was so obvious, it was noticed by the Space Shuttle Columbia crew as they approached the orbiting LDEF during the mission. This brown film was widely dispersed over the trailing rows of LDEF and at the space and Earth ends.[3] A closer examination and detailed analysis of the film was performed in the SAEF-2 facility at KSC following recovery.

After retrieval, inspections of the LDEF revealed a visible, thin, brownish molecular contaminant film on all exterior trailing surfaces and surfaces shielded from AO. While some areas of the film deposits had thicknesses in the range of a few hundred nanometers thick, other areas of the films were as much as a few hundred micrometers thick and were so thick that they were peeling from surfaces as large flakes.[3] The thickest brown films always formed on vents from the interior on the side facing into the ram direction.[3]

The LDEF structure, with the experiment trays removed, showed light and dark regions. The light regions were covered by tray clamps or the experiment tray edges; the dark regions were the contaminated regions. Several localized regions of additional contamination were also noted, especially around some electrical interconnects.[4] Thin polymer films were observed to be broken on experimental trays on rows 3, 6, 8, and 9 and on the space end of LDEF.[4] It is believed that on-orbit thermal cycling may have contributed to the polymer film degradation.[4]

When LDEF was first rotated in the SAEF-2 facility, a liquid began running from tray C-12. The FTIR spectrum of the liquid essentially matched that of the triocyl phosphate used as a fire retardant material in the plastic insulation around the fiber optic bundles on that tray. The brown film around tray C-12 contained very little silicones.[3]

FTIR analysis of molecular film samples indicated it was a polymer containing outgassing by-products from several different sources: silicones, urethane paint, and hydrocarbons.[3,5] Even though the leading edge trays were not discolored, FTIR analysis indicated the presence of silicate films; presumably, they are remnants of atomic oxygen reactions with the hydrocarbon/silicone film.[3] Many of the trays which reported extensive contamination contained samples which contributed to the contamination and were self-contaminating. Self contamination was the largest source of molecular contamination for virtually every tray.

To determine the molecular contaminant species which were launched with LDEF, the back side of numerous tray clamps and shims were evaluated. The molecular contamination from the back side of the tray E-06 clamp had the highest percentages of silicone components. Hydrocarbon levels increased closer to the edges of the clamp; at the clamp edges, the molecular film became very similar to the brown film found elsewhere.[3,5]

Close examination of the brown molecular contamination showed that it had been deposited cyclically with as many as 34 distinct layers.[3,4] These films do not change significantly from layer to layer which would suggest an initial LDEF contamination event.[3]

The LDEF molecular films could not be removed for analysis with alcohol wipes or other more aggressive solvents.[3]

Brown spots were found after retrieval, on a number of surfaces exposed to the Shuttle payload bay environment, and were identified as particulate matter, paint spheres, wear metals, fibers, and other debris. These spots had a significant concentration of sodium chloride, potassium chloride and other water soluble salts. These spots may be the residue of waste water dumps made either during deployment or after the retrieval of LDEF by the Shuttle.[3]

8.1.2.2 Particulate Contamination

Crutcher and Washer identified particles as residual matter from fabrication and assembly, cross-contamination from integration and prelaunch activities as well as the launch itself, orbit generated debris, and cross-contamination from retrieval and post-retrieval ground operations.[6] Particles present on-orbit acted to shield underlying surfaces from either atomic oxygen on ram surfaces or outgassing by-product depositions on trailing surfaces. This resulted in a characteristic shielding patterns that permitted investigators to distinguish particles present during the mission from those deposited during recovery or thereafter.[6] The types and sources of particles found on LDEF are summarized in table 8-1 .

Event	Generated Contamination
Fabrication and Assembly	Abrasives, abrasion generated metal, plastic, wood dust, spray paint, wear metals, etc. Cleanroom fallout and handling debris: skin flakes, paper and clothing fibers, natural minerals, etc.
Integration and Launch	Shuttle tile material and payload bay Beta Cloth materials
Orbit	Condensible outgassed material; micro-meteorites and debris impact generated particles: shattered LDEF materials and ejected molten metal; AO eroded materials produced: ash, thin metal foils, and free paint pigment particles
Reentry/Ground Operations prior to KSC	HEPA filter fiber
Post-Mission De-integration at KSC	Cleanroom fallout, especially paper fibers

Table 8-1. LDEF Particle Contamination

Specific particulate contamination has been identified as retrieval generated contamination. It is believed that this particulate contamination was stable on-orbit and was generated during retrieval activities. This particulate contamination included: thin metal foils that remained after the organic film on which they had been vapor deposited had been removed by AO exposure, fragments of partially eroded polymers, paint pigments, ash from a variety of composites, fragments of thick molecular film deposits, and both glass fibers and graphite fibers freed from AO eroded composite materials. Particles associated with the Shuttle, such as tile material, payload bay liner, and other solids, were distributed onto LDEF during exposures 2 and

4 through 9. Deintegration activities in SAEF-2 at KSC produced typical cleanroom fallout (pollens, natural mineral, clothing fiber, paper fiber, etc.).[1]

8.1.3 Contamination Summary of LDEF Materials, Structures and Components

Following are discussions concerning specific LDEF materials, structures and components and how they were either affected by contamination or contributed to the contamination residue on LDEF. Various degradation mechanisms and analytical results are also given.

8.1.3.1 Thermal Control Materials

LDEF carried a number of thermal control materials experiments in addition to the normal materials used for its own thermal control. With few exceptions, the changes in thermal performance were moderate or negligible.[7] As in other materials experiments, exposure to AO and UV light created the most significant changes to the material's appearance and performance. The synergistic effects of these two environments combined with surface contamination or outgassed contaminants often produced dramatically contrasting results in thermal performance. For example, the high erosion rates of some leading edge materials prevented surface layers from manifesting significant UV degradation. Consequently, such surfaces had near normal absorptance measurements, increased diffuse reflectance (due to the increased surface roughness), and slightly reduced emittance measurements due to reduced material thickness.

In contrast, surfaces that had erosion-preventative overcoats of silicones, did exhibit UV darkening and measurable changes in absorptance. More significant than this, was the interaction of the AO with the silicone to create a glassy silicon dioxide surface layer that redeposited on adjacent surfaces. This film coupled with UV degradation and hydrocarbon outgassing by-products resulted in absorptivity changes for materials on the leading and trailing edges.[8]

Thermal control materials and systems were the source of contaminants on several surfaces. Many of the experimenters hypothesized that AO interaction with the protective siloxane coatings was a significant contributing source to the dark, SiO_2 and hydrocarbon laden, thermally degrading film found on materials in the transition and trailing edges. Ground tests on the coatings recreated a film with similar constituents. Other contributing contaminants to these films were outgassing by-products of paints and, in particular, Chemglaze Z306.[9]

Thermal blankets manifested visibly dark orange films near the keyhole shaped vents. Silicone adhesives used in blanket construction were found to be the source of some of the depositions near vent holes. Adhesive release papers with siloxane coatings were found to be the source of silicone contamination on copper surfaces. Additionally, AO erosion of surfaces including selective erosion of binders or composite resins resulted in particle generating powder-like surfaces. This phenomenon was considered to be a major contributor to the particulate cloud that was observed entrailing LDEF prior to retrieval.[10]

As the majority of external spacecraft surfaces are thermal control surfaces, care must be taken in selecting these materials when they are to be used near contamination-sensitive optical or thermal surfaces.[10] Silicate paints (YB-71, Z93) and chromic acid anodized coatings proved to be the best materials from a standpoint of resistance to the UV and AO environments as well as generation of molecular or particulate contaminants.[7]

8.1.3.2 LDEF Structure

More than half of the exterior surfaces of LDEF were chromic acid anodized (CAA) aluminum. The CAA aluminum tray clamps were found on all LDEF rows and were exposed to all LDEF environments. Extensive optical testing provided a complete picture of the spaceflight environmental effects on this surface treatment. Comparison of front-side (exposed), backside (shielded) and control clamps showed slight changes in the optical properties.[7] However, the variations in absorptance and emittance have been attributed to the inherent variability in anodizing, to variations in measurements, and to the effects of on-orbit contamination deposited on tray clamp surfaces.[7]

8.1.3.3 LDEF Electronics

During cable harness inspection and removal, no degradation of dielectric components, interfacial seals or finishes was found. However, particle contamination was found on small electromechanical devices.

8.1.3.4 Optical Components

A decrease in the transmission of some optics was noted and has been attributed to the brownish molecular film. A change in some of the wavelength characteristics of coated optics was noted and has been initially attributed to the effect of an added thin film of contamination. Elemental analysis of the surface of some of these optics on the ram side of LDEF indicated a silica residue was present from the AO-degraded molecular film. Other optical effects included selective reflection due to sub-micron droplet size, decreased signal-to-noise ratio broadband, and increased background in the infrared. A comprehensive report of the results for the optical samples flown on LDEF is summarized in the *Long Duration Exposure Facility Space Optics Handbook*, Reference 11. A brief summary of the specific contamination effects found on the LDEF optics is provided in the following subsections.

IR Refractive Optics

There was a significant increase in optical scatter for the M0003-2 samples due to molecular contamination and particulate debris. Post-retrieval cleaning (alcohol drag) removed the contamination and reduced scatter by up to three orders of magnitude.[11] However, impact-induced cratering and cracking resulted in local scattering of up to five orders of magnitude above the background level.[11] Several of the M0003 samples were outfitted with covers which had been prelaunch programmed to close after 9 months in orbit. Comparison of the 9 and 69 month exposure samples found the same scatter levels, implying that the LDEF environment for the intervening 60 months produced a negligible increase in optical scatter.

Flight samples varied greatly in visible surface contamination and damage. A brown molecular film was visible on the S0050-1 and S0050-2 samples. The contamination found on the S0050-2 samples was easily removed using normal cleaning techniques. All samples had significantly reduced transmission due to molecular contamination. The fused silica and ULE samples returned to prelaunch flight values after cleaning.[11]

UV/Visible Refractive Optics

A significant decrease in transmission of the S0050-2 samples was seen due to molecular contamination. The fused silica and ULE samples were cleaned using standard techniques and returned to nearly prelaunch flight values. The density of the contaminant deposited on the sample varied between coatings and substrate materials. As an example, prior to cleaning, the transmission of the uncoated fused silica sample was reduced from 94 to 68 percent at 350 nm, while that of the ULE sample reduced from 94 to 45 percent.[11]

The transmission of the S0050-1 uncoated fused silica samples decreased by 30 to 50 percent from 200 nm to 700 nm. As with the samples from S0050-2, when the uncoated fused silica was cleaned, the transmission returned to the prelaunch flight value within 1 percent. The contaminant film found on the S0050-1 samples (MgF_2, CaF_2, and LiF windows) was measured using FTIR and found to be typical hydrocarbon contamination. The MgF_2 window molecular film had visible sharp edges, indicating that the film was brittle. Patterns on the film indicated the contaminant may be of low viscosity. The film on the LiF samples appeared to have a sprayed texture.[11]

A significant decrease in the transmission of CaF_2, MgF_2, LiF, Al_2O_3, and SiO_2 samples was due to molecular contamination. A comparison of the contaminated CaF_2 flight sample to the ground controlled sample showed the transmission monotonically increasing from zero at 200 nm to more than 50 percent at 380 nm. The higher transmission measured for the MgF_2 window relative to the CaF_2 and LiF windows was probably due to the fact that there was not a backing film on the MgF_2 window.[11]

IR Optical Coatings

For the M0003-7 Ag + $(Al_2O_3/Si)^3$ on polished Si sample, three small impact craters were observed surrounded by localized cracking on the exposed coating surface. The coating was cracked in spirals at the perimeter of the exposure area. The coating appeared to be blistered in the vicinity of the spiral cracks; flaking in the cracked region revealed a corroded and discolored residual substrate surface. A sample of electroplated Au on Ni/Al from the M0003-6 experiment, had a small quantity of debris on the surface, but no other changes were discernable.[11]

From experiments M0003-2 and M0003-7, a number of the IR coatings were contaminated and deteriorated in the space environment. The Ag + $(Al_2O_3/ZnS)^4$ coating on Mo appeared hazy and discolored on the exposed surface. Multiple zones of discoloration were apparent. The variation in discoloration was presumed to be the result of varying degrees of dendritic growth. The coating exhibited a high density of spots over its entire surface. Grain boundaries in the substrate were also apparent through the coating.[11]

For the Si/SiO_2 sample, a great deal of debris was found on the coating surface, yet, the surface remained highly specular. The PbF_2/SiO_2 sample had a large number of subsurface polishing scratches. Such coating features as bubbles, pinholes, or growth nodules in the coatings seemed to have formed preferentially along these scratches.[11]

The MgF_2 coating on SiO_2 was crazed on both the flight and control samples. A great deal of extraneous debris, including fibrous matter and metallic film fragments, was present on

the surface. There were three large spots of debris on the spaceward side of the sample where the coating was crazed more extensively. There were also blisters around these debris spots.[11]

The ZnS coating on the SiO_2 substrate was buckled in a regular pattern on two large areas of the surface. The entire coating was blistered. Large blisters, exhibiting many orders of interference fringes, were discernable on the surface of the sample at low magnification. In addition, a high density of very small blisters was apparent throughout the coating at magnifications of 200X and greater. The surface was, however, relatively clean of debris.[11]

UV/Visible Optical Coatings

The X-ray photoelectron spectroscopy (XPS) analysis of S0050-2 experiment samples found the substrates and coatings to be covered with a thin layer of polymer which contained silicon. The flight samples from experiment S0050-2 were measured for optical performance from 350 to 1200 nm. Of interest in the measurements is the fact that the optical density of the contaminant deposited on the sample varied between coatings and substrate materials. As an example, the transmission of the uncoated fused sample was reduced from 94 to 68 percent at 350 nm, while that of the uncoated ULE sample was reduced from 94 to 45 percent.[11]

For the case of an anti-reflection (AR) coating (SiO_2/TiO_2) also on S0050-2, the transmission decreased by up to 40 percent at 475 nm and 20 percent at 900 nm, but actually increased by 10 percent at 600 nm. These effects were due to a contamination layer. The contamination was not removable by normal solvent drag means. An attempt to remove the contamination using oxygen plasma for 3 hours only partially restored the transmission. The improvement was only about 10 percent and was limited to the wavelength range of 350 to 550 nm.[11]

For samples with a solar rejection coating, the post-flight transmission was almost identical to the prelaunch flight values, with a 3 percent decrease in the wavelength range of 1000 to 1150 nm. A high reflectance silver coated flight sample (with contaminant) and a control sample were measured for BRDF. A near order-of-magnitude increase in scattered light was measured above the 10° delta theta on the flight sample versus that of the control sample.[11]

For most of the experiment S0050-2 samples, the contaminant was silica-like in nature, but on the ULE substrate and the AR coating, the contaminant was visibly darker and appeared similar in structure to the silicone of the rubber gasket which was used to mount the optics. However, neither the relative atomic percentage nor the relative sizes of the silicon and oxygen peaks from the XPS conclusively prove that the contaminant is a residue from the mounting rubber gasket.[11]

Depth sputtering through the AR coating clearly shows the SiO_2/TiO_2 layers for both the control and flight samples. However the flight sample has a layer at the surface approximately 30 Angstroms thick, rich in carbon and silicon. The carbon content rises as the contamination layer is sputtered away and disappears at the contamination-AR layer interface. The total time required to sputter to the bottom of the SiO_2/TiO_2 layers was almost identical for both the flight and control samples. Since the hardness of the coating on both samples was assumed to be similar, the sputtering rates would have been equivalent, making the total coating thickness the same. This indicates that either the top surface of the flight coating has been removed and replaced with the silicon/carbon layer, or the silicon/carbon has fused into the SiO_2 layer.[11]

Optical Filters

A brownish molecular film was observed on optical filter surfaces. The most common responses for UV/Visible filters was a slight to significant reduction in transmittance accompanied by shifts in center wavelength toward the blue. The results of the high-performance IR filters indicate that the contamination was negligible. No significant changes were found either in transmission or spectral position of any hard coated II-VI/PbTe-based multi-layers on Ge substrates. The softer materials were adversely affected in their physical and optical properties by the long exposure in space; effects range from a reduced transmission to a complete opacity.[11]

Mirrors

All samples were hazed and discolored with corrosion spots on the surface. Degradation of the mirrors was due to the molecular film or oxidation of the silver film. Only the MgF_2/Al on Quartz sample did not experience deleterious effects on either the leading edge or trailing edge samples.

Second Surface Mirrors

Several second surface mirror (SSM) materials were flown. The SSM coatings were deposited in the configurations of the SSM/interference filter (IF) and SSM/IF/conductive layer (LS) and were characterized by analyzing the change in the coating's solar absorptivity (a) and emissivity (e). All the space-exposed surfaces showed increases in solar absorptivity of varying magnitudes. The magnitude of the solar absorptivity change due to contamination was negligible or slight. No appreciable change in thermal emissivity was seen.

Quartz Crystal Microbalance

The Quartz Crystal Microbalances (QCMs) flown on LDEF were of interest as contamination monitors for companion optics on experiments M0003 and S1002. Positions of the wavelength maxima and minima in the interference patterns were shifted negligibly. The QCMs measured approximately 8 nm of contamination during the entire mission. The major contaminant was silicon, which is consistent with other experiments. The level of contamination was found to be higher on the leading edge than on the trailing edge. Other lesser contaminants found on the crystals included Mg, Ca, K, Na, Cl, Sn, and Pb.[11]

8.2 COMPARISON OF RESULTS WITH LDEF ANALYTICAL MODEL

Several theories have been proposed for identifying the major source(s) of the molecular contamination observed on LDEF. These theories are presented without preferential ranking in Section 8.2.1. Analytical models were developed to determine the major sources of the molecular contamination and the models are discussed in Section 8.2.2. The conclusions from this modeling effort indicate the most probable source of contamination for the LDEF experiments.

8.2.1 Contamination Sources

8.2.1.1 Shuttle as a Source

Since the contaminant films consisted of methyl silicone and silica, one theory suggests that the primary source of the contamination was the Shuttle itself, prior to deployment of the LDEF. The two possible sources of the methyl silicone were DC-710 phenyl methyl silicone

found in the shuttle-bay-liner beta cloth and hexamethyldisilazane (HMDS) used as the shuttle tile waterproofing compound.[12,13] It has been hypothesized that HMDS produces silicone residues by the depolymerization of silicone sealants and potting compounds found on LDEF.[13] The absorption of HMDS vapor on surfaces during ground processing may have produced reaction products such as hexamethyldisiloxane.[13] It is further speculated that much of the silicone and silica contamination had come from ground operations and the orbiter.[12,13]

8.2.1.2 LDEF as a Source

It has also been proposed that the primary source of the LDEF molecular contamination was the Chemglaze Z306 paint used for thermal control in the LDEF interior surfaces.[2,14,15] The paint was not vacuum conditioned prior to launch and may have been the largest source of outgassing during the LDEF mission. Experience with other spacecraft has shown that non-vacuum baked Z306 is a significant source of on-orbit outgassing. Other sources were the RTV silicone materials used on many of the experiment trays.[2,15] Although the NVR level of the LDEF was estimated to be 2.5 mg/ft^2 at launch, this contamination was not considered to be a significant source of the molecular contamination found on LDEF after post-mission analysis.[2,4,15]

One theory, supported by most observations, involves a complex contamination mechanism of outgassing from LDEF materials followed by re-deposition of these outgassed species back onto LDEF. The outgassing from the Chemglaze Z306, the RTV silicones, and the experiment tray sample materials was temperature driven and it is speculated that re-deposition of these contaminants onto LDEF was influenced by temperature and UV light exposure.[2,4,14,15] Although there is basic agreement on the contamination mechanism for the outgassed molecular contamination, there is considerable debate regarding the duration of the outgassing and the extent of influence of the UV radiation in determining the thickness of contamination deposition.

Several theories have suggested that the contamination sources were outgassing uniformly over the LDEF mission, producing deposition layers which do not differ in composition from layer to layer.[2,15,16] Other theories have suggested a large outgassing source at the start of the LDEF mission, diminishing throughout the mission as the source outgassing rate tapered off.[3]

UV light exposure was required to "fix" the deposited film as is indicated by the distribution of the films on interior surfaces and the thickness of the films at the vent locations. Thermal conditions at the time of exposure to UV light seems to be an important factor in the thickness of the deposit. Ram direction surfaces always had the thicker films. These were the coldest surfaces at the time of their exposure to UV light.[15]

One theory has the initial contaminant film "fixed" by subsequent exposure to AO which appears to have oxidized the silicones into silicates. This contamination was generally lighter in color on the surfaces which were exposed to the highest AO fluences. This observation may indicate that, later in the LDEF mission, the contamination cloud was less dense or had dissipated completely so that continuing AO exposure eroded the silicate surface of the contamination.[3]

Another theory explores the possibility that all of the processes discussed above were competing and produced a site-specific contamination environment during the mission. Removal of the contaminant film was made possible by thermal cycling and oxidation of the film to volatile species. Simultaneously, the contaminant species were photo-polymerized, cross-linked and oxidized to nonvolatile species.[17]

8.2.2 Contamination Modeling Results

Contamination models were developed using the Integrated Spacecraft Environments Model (ISEM) to determine the flux of the contaminant species on LDEF surfaces and to determine the site specific molecular contamination.[18,19,20] ISEM is a collisional molecular transport code which computes molecular density and flux in a three dimensional modeling volume for any number of user defined molecular species.[18] The LDEF geometry used for this modeling study is shown in figures 8-2 and 8-3. Additional specific model descriptions can be found in Reference 19. The LDEF mission was modeled using three different time periods, representative of the beginning, middle and end of the mission, corresponding to orbital altitudes of 463 km, 417 km, and 333 km, respectively. The ambient environment background was predicted using MSIS86.[20]

The outgassing and erosion rates used for the modeling of the beginning (463 km) and ending (333 km) mission phases are shown in table 8-2. External surfaces were modeled as having an average uniform outgassing rate which decreased with time. The initial outgassing rates were based on test data and the percentages of various materials present. Outgassing from internal surfaces was allowed to escape to the external environment via the numerous holes around the experiment trays. The average erosion rate was assumed to be 15 percent of that of Kapton for all surfaces.[20]

Rate, $gcm^{-2}s^{-1}$	463 km, April 1984	333 km, January 1990
External	2.0×10^{-9}	1.4×10^{-12}
Internal	2.0×10^{-10}	4.8×10^{-13}
Erosion	6.3×10^{-11}	2.2×10^{-9}

Table 8-2. LDEF Model Outgassing and Erosion Rates

The total density value is the sum of the ambient species, surface re-emitted ambient species, internal and external outgassed species, and the scatter portions of all species. The total iso-density contours for the early mission case at an altitude of 463 km, shown in figure 8-4. show a slight ram buildup in front of the LDEF, but the density around LDEF is dominated by the outgassing. Total iso-density contours for the late mission case at an altitudes of 333 km, shown in figure 8-5, show a strong density buildup in the front of LDEF due to ambient and erosion products. The wake is well defined, and although the overall densities are much less than those on the ram side, the density in the wake region is still dominated by the outgassing species.[20]

The modeling results were consistent with observations on LDEF and do provide some insight into the overall environment and the environment/satellite interaction to produce contamination. The modeling provided a method for determining whether the observed post-mission contamination was caused by materials outgassing or by a synergistic interaction between deposited outgassed material and AO or UV radiation. Early in the mission, the

environment is dominated by outgassing of the LDEF itself. Outgassing dominated the wake region density for the entire mission. Later in the mission, the ram side density was many times that of the ambient. This was caused by a combination of accommodation and emission of AO, emission of reaction products, and scattered molecules. The flux to the surface is dominated by direct AO impingement, but a significant flux can be observed at angles up to 180. The return flux of erosion species near the end of the mission was an order of magnitude greater than the return flux of outgassed products early in the mission.[20]

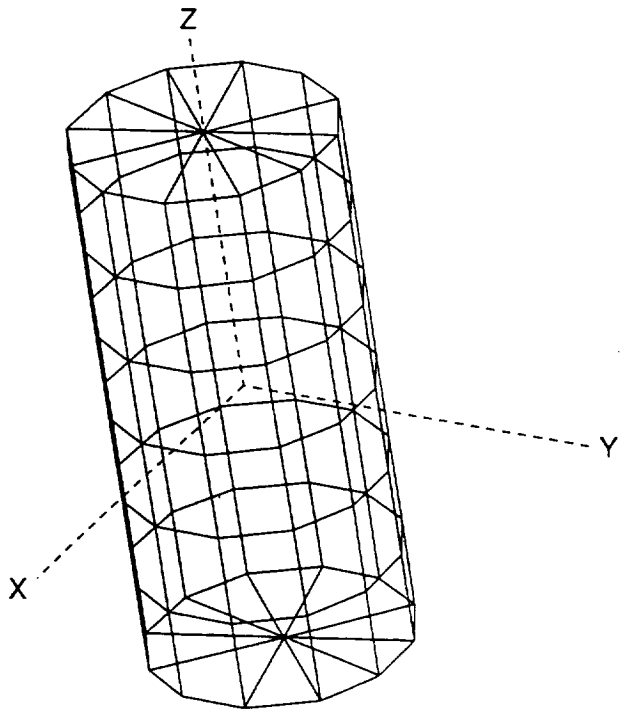

Figure 8-2. LDEF Geometry Model

Q-2

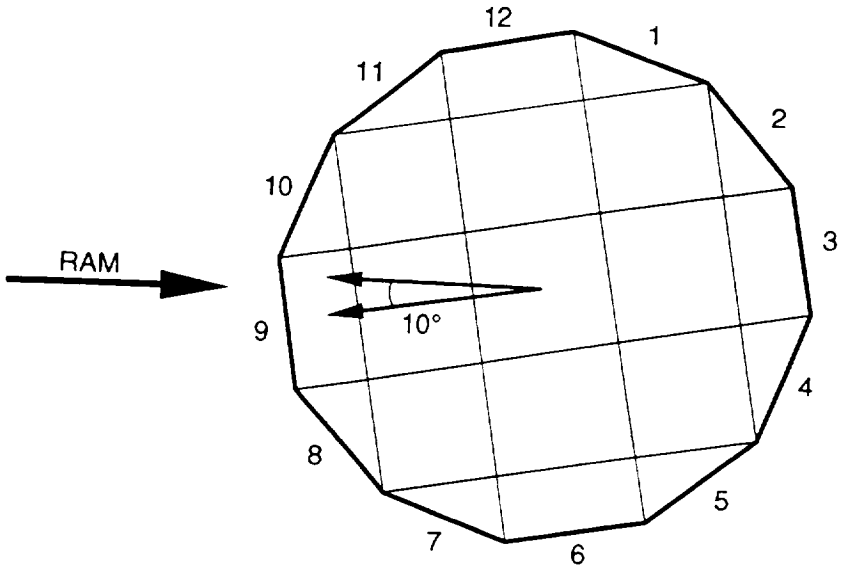

Figure 8-3. LDEF Geometry Model with Respect to Ram Direction

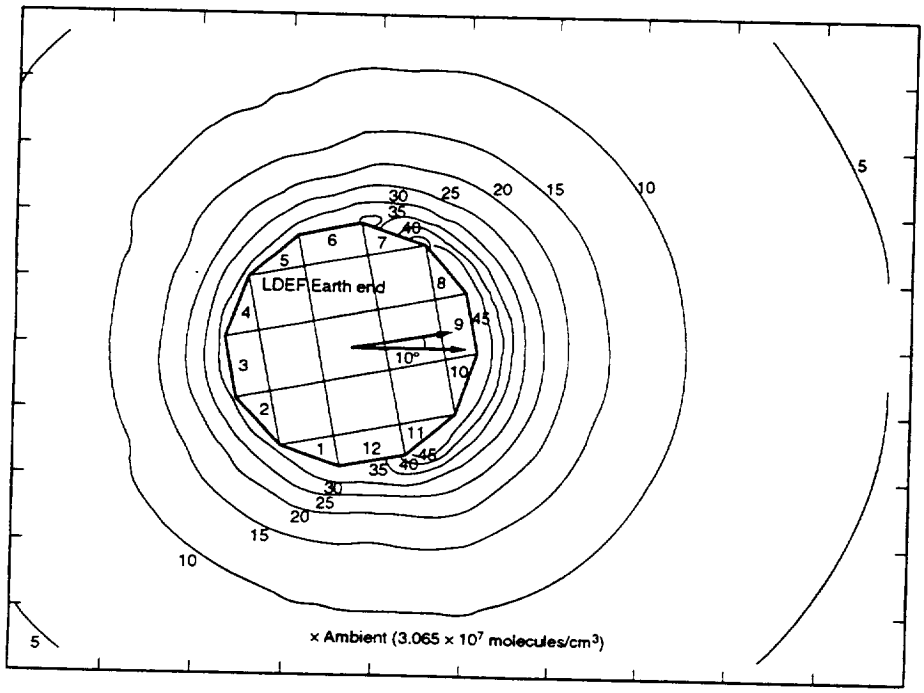

to left Figure 8-4. Total Density at 463 km. (Note that ram is from right)

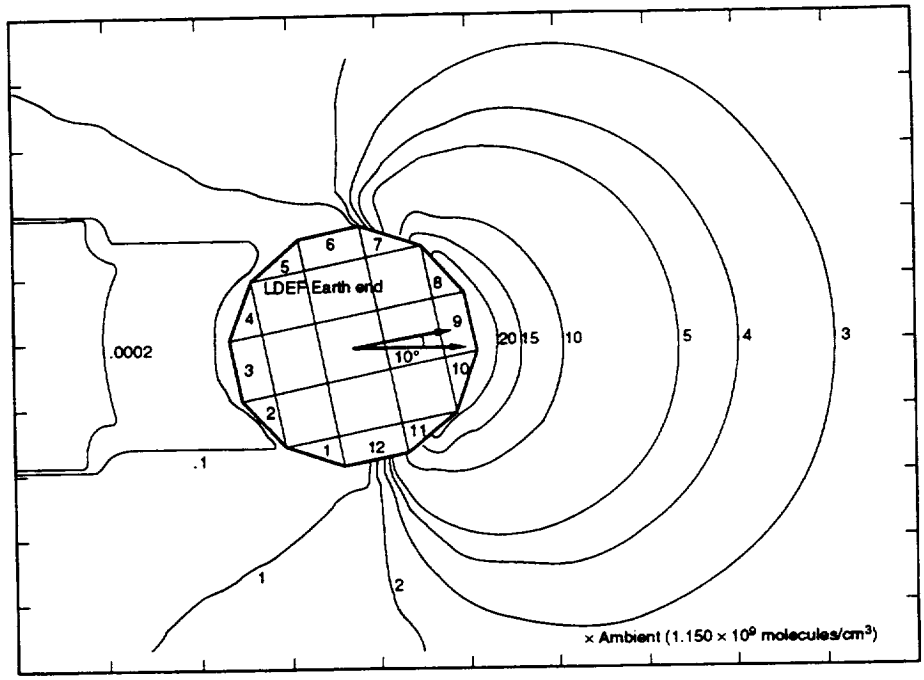

Figure 8-5. Total Density at 333 km. (Note that ram is from right to left)

To determine if the contamination observed on LDEF was tray dependent, the A0171 (A8) tray was modeled. The analysis determined the local environment of the tray due to the materials on the tray itself and their collisional interaction with the ambient atmosphere.[19] The modeling results indicate that each tray on LDEF was a contamination microenvironment within the overall contamination environment of LDEF. This contamination microenvironment was dependent on the materials used on that tray. High outgassing materials would produce a higher flux in the tray microenvironment and cause greater contamination effects for that tray.

To examine the incident molecular flux through a small aperture and the resulting incident flux on an internal surface, incident AO was modeled as entering the aperture and then allowed to expand due to its thermal distribution. The AO pattern incident on the side of an experiment tray was consistent with the deposition pattern observed on the side of the tray. Also, rivet and bolt heads shadowed portions of the experiment tray from AO impingement and no deposition was observed. The modeling results are consistent with the view that outgassing products from the inside the LDEF were adsorbed onto surfaces. Where AO was able to flow through the vents and apertures and impinge on these surfaces, the resulting chemical interaction formed a permanent deposit.[20]

Typically, a spacecraft is modeled with the modeling input (actual outgassing rates) from test data of subsystem components. However, for LDEF, the majority of subsystem components or experiments were not vacuum exposed prior to launch. If the subsystems were vacuum exposed prior to launch, the outgassing rates were not measured because LDEF was not designated a contamination sensitive payload. Thus, assumptions were made for the outgassing characteristics of the LDEF materials. Typically, TML and CVCM values from ASTM E595 materials testing, weighted for actual on-orbit temperature, are used as input for outgassing. However, it has been shown that the outgassing rates may be several orders of magnitude higher or lower than directly measured outgassing rates.

This model assumed an average uniform outgassing rate for all external surfaces. Approximately 60 percent of LDEF's exterior surface was aluminum and did not contribute uniformly to the outgassing. This assumption was made to limit computational time, but provide credible results. While this implies that the modeling was not conservative, the modeling results did correlate well with the observed contamination and contamination patterns seen on individual trays. Thus this assumption proved to be a good assumption for LDEF.

8.2.3 Conclusions

The LDEF spacecraft served to provide an enormous amount of new data regarding materials behavior in a space environment. In addition, many significant observations and phenomena related to contamination behavior and effects were seen. It is important to interpret and understand the contamination effects experienced by LDEF in an attempt to improve future spacecraft design and performance.

While there is, to date, no definitive conclusion regarding the LDEF contamination sources, transport mechanisms, and resulting effects of the depositions, it is clear that there are probably a number of physical, chemical, and space environmental mechanisms at work. The analytical modeling results correlate well and in many cases confirm actual effects shown on many of the LDEF experiments, as was shown with the A0171 microenvironment modeling.

There were many theories proposed to explain the sources and mechanisms of the contamination observed on LDEF. While no one theory has explained all the contamination effects observed on LDEF, many of the theories correlate well with the modeling results to explain the sources of contamination on LDEF and the effects of AO and UV radiation. The actual contamination observed on LDEF is due to complex interactions with the space environment and LDEF materials.

8.3 SPACECRAFT DESIGN CONSIDERATIONS

The spacecraft design considerations to minimize contamination are related to the choice of materials and workmanship. LDEF is a good example of the types and amounts of contamination which can be generated on-orbit when the selection of materials is not controlled. Much is available in the literature discussing materials choices for a variety of spacecraft designs and performance characteristics. Low outgassing materials should be chosen to minimize contamination. These materials should also not generate particles. Selection criteria based on ASTM E-595 materials testing results of TML less than 1.0 percent and CVCM less than 0.10 percent is usually sufficient for most payloads. When a specific material will be used near a critical surface, additional testing to determine its specific outgassing characteristics should be performed. Contamination modeling, such as that performed for LDEF, provides a good engineering tool for determining if a spacecraft will meet its performance requirements.

While the choice of materials is generally tightly controlled for contamination sensitive spacecraft, workmanship varies between vendor, manufacturer and integrator. It becomes the role of the contamination engineer in conjunction with the mechanical and electrical engineers and technicians to verify that the workmanship of subassemblies and assemblies meet the requirements for the specific spacecraft. While general workmanship standards can be applied to all spacecraft, specific standards need to be tailored and implemented for contamination sensitive spacecraft.

8.4 REFERENCES (FOR SECTION 8)

1. H. W. Dursch, W. S.Spear, E. A. Miller, G. L. Bohnhoff-Hlavacek, and J. Edelman, "Analysis of Systems Hardware Flown on LDEF - Results Of The Systems Special Investigation Group," NASA CR-189628, Contract No. NAS1-19247, April (1992).

2. E. R. Crutcher, L. S. Nishimura, K. J. Warner, and W. W. Wascher, "Quantification of Contaminants Associated with LDEF", *LDEF-69 Months in Space First Post-Retrieval Symposium*, NASA CP-3134, Part 1, 1992, pp. 141-154.

3. E. R. Crutcher and K. J. Warner, "Molecular Films Associated with LDEF", *LDEF-69 Months in Space First Post-Retrieval Symposium*, NASA CP-3134, Part 1, 1992, pp. 155-177.

4 B. A. Stein and H. G. Pippin, "Preliminary Findings of the LDEF Materials Special Investigation Group", *LDEF-69 Months in Space First Post-Retrieval Symposium*, NASA CP-3134, Part 2, 1992, pp. 617-641.

5. B. K. Blakkolb, L. E. Ryan, H. S. Bowen, and T. J. Kosic, "Optical Characterization of LDEF Contaminant Film", LDEF-69 Months in Space Second Post-Retrieval Symposium, NASA CP-3194, Part 3, 1993, pp. 1035-1040.

6. E. R. Crutcher and W. W. Wascher, "Particle Types and Sources Associated with LDEF", *LDEF-69 Months in Space First Post-Retrieval Symposium*, NASA CP-3134, Part 1, 1992, pp. 101-119.

7. J. B. Mason, H. Dursch, and J. Edelman, "Overview of the Systems Special Investigation Group Investigation", *LDEF-69 Months in Space Second Post-Retrieval Symposium*, NASA CP-3194, Part 4, 1993, pp.1257-1268.

8. B. A. Banks, J.A. Dever, L. Gebauer, and C. M. Hill, "Atomic Oxygen Interactions with FEP Teflon and Silicones on LDEF", *LDEF-69 Months is Space First Post-Retrieval Symposium*, NASA CP-3134, Part 2 , 1992, pp. 802-815.

9. J. L. Golden, "Z306 Molecular Contamination Ad Hoc Committee Results", *LDEF Materials Workshop '91*, NASA CP-3162, Part 1, 1992, pp. 115-140.

10. G. Pippin and R. Crutcher, "Spacecraft Contamination Issues from LDEF: Issues for Design", *LDEF Materials Results for Spacecraft Applications*, CP-3257, 1993, pp. 97-103.

11. W. T. Kemp, E. Taylor, C. Bloemker, F. White, G. Resner, and A. Watts, *Long Duration Exposure Facility Space Optics Handbook*, PL-TN-93-1067, 1993.

12. G. A. Harvey, "Sources and Transport of Silicone NVR", *LDEF Materials Workshop '91*, NASA CP-3162, Part 1, 1992, pp. 175-184.

13. G. A. Harvey, "Silazane to Silica", *LDEF-69 Months in Space Second Post-Retrieval Symposium*, NASA CP-3194, Part 3, 1993, pp. 797-810.

14. G. A. Harvey, "Organic Contamination of LDEF", *LDEF-69 Months in Space First Post-Retrieval Symposium*, NASA CP-3134, Part 1, 1992, pp.179-196.

15. E. R. Crutcher and K. J. Warner, "Molecular Films Associated with LDEF", *LDEF-69 Months in Space First Post-Retrieval Symposium*, NASA CP-3134, Part 1, 1992, pp. 155-177.

16. E. R. Crutcher, L. S. Nishimura, K. J. Warner, and W. W. Wascher, "Migration and Generation of Contaminants from Launch Through Recovery: LDEF Case History", *LDEF-69 Months in Space First Post-Retrieval Symposium*, NASA CP-3134, Part 1, 1992, pp. 121-140.

17. G. Pippin, R. Crutcher, "Contamination on LDEF: Sources, Distribution, and History", *LDEF-69 Months in Space Second Post-Retrieval Symposium*, NASA CP-3194, Part 3, 1993, pp. 1023-1031.

18. T. Gordon and R. Rantanen, "Long Duration Exposure Facility (LDEF) Contamination Modeling", *LDEF Materials Workshop '91*, NASA CP-3162, Part 1, 1992, pp. 141-157.

19. R. Rantanen and T. Gordon, LDEF Experiment A0171 Contamination Modeling Final Report, ROR-MSFC-1-93, 1993.

20. M. R. Carruth, R. Rantanen, and T. Gordon, "Modeling of LDEF Contamination Environment", *LDEF Materials Results for Spacecraft Applications*, CP-3257, 1993, pp. 87-95.

APPENDIX A - EXECUTIVE SUMMARY EXCERPTS FROM THE 1992 SYSTEMS SIG SUMMARY REPORT

The following paragraphs summarize the major Systems findings through 1991. All of these findings are discussed in much greater detail in the April 1992 report which available through the LDEF Archive Office.

General Observations:

LDEF carried a remarkable variety of mechanical, electrical, thermal, and optical systems, subsystems, and components. A total of 19 of the 57 experiments flown on LDEF contained functional systems that were active on-orbit. Almost all the other experiments possessed at least a few specific components of interest to the Systems SIG (adhesives, seals, fasteners, optical hardware, etc.).

No system anomalies occurred that indicate any new fundamental limitations to extended mission lifetimes in LEO. However, shielding from the effects of atomic oxygen, micrometeoroids, space debris, and ultraviolet radiation must be considered.

There were several major system anomalies. However, the analysis to date has indicated that none of these can be solely attributed to the long-term exposure to LEO. Design, workmanship, and lack of pre-flight testing have been identified as the primary causes of all system failures.

The combination of any of the individual low Earth orbit environmental factors such as UV, atomic oxygen, thermal cycling, meteoroid and/or debris impacts and contamination can produce synergistic conditions that may accelerate the onset and rate of degradation of space exposed systems and materials

The most detrimental contamination process during LDEF's mission was the outgassing and redeposition of molecular contaminants which resulted in a brown film on the surfaces of LDEF. This brown film was widely dispersed over the trailing rows and both the Earth and space ends. Thermal control surfaces, optics hardware and solar cells were most susceptible to this contamination. Ram facing surfaces appeared "clean" due to atomic oxygen attack (i.e., cleaning) of the brown film.

Atomic oxygen erosion was observed on exterior surfaces at up to 100 degrees from the ram direction. This was due to the thermal component of the oxygen molecular velocity plus the effects of co-rotation of the atmosphere. Roughly 54 percent of the atomic oxygen exposure was accumulated during the last 6 months of the LDEF mission. The rapid increase in atomic oxygen fluence at the end of the mission was a result of both increasing solar activity and decaying orbit altitude.

Mechanical:

The LDEF deintegration team and several experimenters noted severe fastener and hardware removal difficulties during post-flight activities. The Systems SIG has investigated all reported instances, and in all cases the difficulties were attributed to galling during installation or post-flight removal. To date, no evidence of coldwelding has been found. Correct selection of materials and lubricants as well as proper mechanical procedures are essential to ensure successful on-orbit or post-flight installation and removal of hardware.

The finding of no coldwelding indicated a need to review previous on-orbit coldwelding experiments and on-orbit spacecraft anomalies to determine whether the absence of coldwelding

on LDEF was to be expected. The results of this investigation showed that there have been no documented cases of a significant on-orbit coldwelding event occurring on U.S. spacecraft. There have been a few documented cases of seizure occurring during on-orbit coldwelding experiments. However, the seized materials had been selected for the experiment because of their susceptibility to coldweld during vacuum testing on Earth. This susceptibility was enhanced by effective pre-flight cleanliness procedures.

The majority of seals and lubricants used on LDEF were designed as functioning components of experiments and were, therefore, both shielded and hermetically sealed from exposure to the LEO environment. Post-flight testing has shown nominal behavior for these seals and lubricants. However, several lubricants were exposed to the LEO environment as experiment specimens. Post-flight analysis showed a range of results for these specimens ranging from nominal behavior to complete loss of lubricant, depending on the particular lubricant and its location on LDEF.

With few exceptions, adhesives performed as expected. Several experimenters noted that the adhesives had darkened in areas that were exposed to UV. The most obvious adhesive failure was the loss of four solar cells bonded to an aluminum substrate using an unfilled epoxy. Two cells were on a leading edge tray and the other two were bonded on a trailing edge tray. No adhesive remained on the two leading edge tray but some remained on the trailing edge tray. This indicated that the bond failed at the cell/adhesive interface and then the adhesive was attacked by atomic oxygen. Possible causes of failure include poor surface preparation and/or thermal expansion mismatch between the solar cell substrate and the aluminum mounting plate.

The viscous damper, used to provide stabilization of LDEF from deployment caused oscillations, performed as designed and exhibited no signs of degradation. The damper has undergone extensive post-flight testing and has been returned to NASA LaRC in a flight ready condition.

Both the rigidize-sensing grapple, used by the RMS to activate the active experiments prior to deployment, and the flight-releasable grapple, used by the RMS to deploy and retrieve LDEF, worked as designed. The grapples are currently awaiting functional testing to determine their post-flight condition *(as of 3/15/95, the grapples have not undergone functional testing).*

The most significant finding for the fiber-reinforced organic composites was the atomic oxygen erosion of leading edge specimens. While the measured erosion was not unexpected, the detailed comparison of ground based predictions vs actual recession rates has not been completed. A thin protective coating of nickel and SiO_2 was used on leading edge specimens to successfully prevent this erosion.

Electrical:

Electrical/mechanical relays continue to be a design concern. Two of the most significant LDEF active system failures involved relay failures. The Interstellar Gas Experiment was one of the more complex experiments on LDEF, with seven "cameras" located on four trays. Each camera contained five copper-beryllium foil plattens, which were to sequentially rotate out of their exposed position at pre-determined intervals. This experiment was never initiated due to a failure of the experiment's master initiate relay. The Thermal Control Surfaces Experiment recorded on-orbit optical properties of various thermal control coatings using a four-track Magnetic Tape Module. The latching relay which switched track sets failed to operate when switching from track 3 to track 4. Consequently, portions of the early flight data on track 1 were overwritten and lost.

The Experiment Initiate System (EIS) provided the initiate signal to the active experiments which directed them to turn on their power and begin their operational programs. Post-flight inspection and testing, using the original ground support equipment, showed the condition of the EIS to be nominal.

NASA supplied seven Experiment Power and Data Systems (EPDS) to record on-orbit generated data. All EPDS units were similar, consisting of a Data Processor and Control Assembly (DPCA), a tape recorder (the Magnetic Tape Module), and two $LiSO_2$ batteries, all of which were attached to a mounting plate designed to fit into the backside of the experiment tray. The EPDS components were not directly exposed to the exterior environment, being protected by their mounting plate and by external thermal shields. Although simple compared with today's data systems, the EPDS contained many elements common to most such systems, including various control and "handshake" lines, programmable data formats and timing, and a data storage system. EPDS electronic components were procured to MIL-SPEC-883, Class B standards, and were not rescreened prior to installation. Data analysis and post-flight functional testing showed that all EPDS functioned normally during and after the LDEF flight.

Three different types of batteries were used on LDEF: lithium-sulfur-dioxide ($LiSO_2$), lithium carbon monofluoride (LiCF), and nickel-cadmium (NiCd) batteries. NASA provided a total of 92 $LiSO_2$ batteries that were used to power all but three of the active experiments flown on LDEF. Ten LiCF batteries were used by the two active NASA MSFC experiments. One NiCd battery, continuously charged by a four-array panel of solar cells, was used to power an active experiment from NASA GSFC. A loss of overcharge protection resulted in the development of internal pressures which caused bulging of the NiCd cell cases. However, post-flight testing showed that the battery still has the capability to provide output current in excess of the cell manufacturer's rated capacity of 12.0 ampere-hours. All the LiCF and $LiSO_2$ batteries met or exceeded expected lifetimes.

LDEF provided valuable knowledge concerning the viability of using various solar cells and solar cell encapsulants (adhesives and coverglass materials). Coverglass materials such as ceria doped microsheet and fused silica withstood this particular environment. Measurable degradation of some widely used antireflection coatings was observed. Results from some low cost materials such as silicone, Teflon, and polyimide indicated that these materials will require additional research before full-scale replacement of the conventional encapsulants (fused silica coverglass and DC 93500 adhesive) is justified. Micrometeoroid and debris impacts will continue to be a significant solar cell performance degradation mechanism. Solar cell performance degradation due to the deposition of contamination on the surfaces was also well documented. However, the majority of electrical characterization and analysis of on-orbit data remains to be completed.

Pyrotechnic devices, flown on Experiment A0038, were successfully fired during post-retrieval ground testing.

Thermal:

The change in performance of a wide variety of thermal control coatings and surfaces was moderate, with a few exceptions. A significant amount of these changes has been attributed to contamination effects. Certain metals (esp. chromic acid anodize aluminum), ceramics, coatings (YB-71, Z-93, PCB-Z), aluminum coated stainless steel reflectors, composites with inorganic coatings (Ni/SiO_2), and siloxane-containing polymers exhibited spaceflight environment resistance that is promising for longer missions. Other thermal control and silicone based conformal coatings, uncoated polymers and polymer matrix composites, metals (Ag, Cu) and silver Teflon thermal control blankets and second surface mirrors displayed significant

environmental degradation. In addition, post-flight measurements may be optimistic because of bleaching effects from the ambient environment.

The results of thermal measurements on different samples of the same materials made at different laboratories have proven to be remarkably consistent and in agreement, lending additional credibility to the results. Confidence in designers' thermal margins for longer flight missions has been increased.

One of the most notable observations made during the on-orbit photo survey was the loose silverized Teflon thermal blankets located on a space end experiment. Tape was used to hold the edges of the thermal blankets to the experiment tray frame. The blankets apparently shrunk in flight causing the blankets to detach from the frame. Portions of the tape were attached to both the blanket and frame, indicating that the tape had failed in tension. Post-flight adhesion testing showed that the tape retained adequate adhesive properties.

Initial functional tests were performed for each of the three heat pipe experiments flown on the LDEF, and the heat pipe systems were found to be intact and fully operational. No heat pipe penetration occurred due to micrometeoroid or debris impact.

Actual measured temperatures within the interior of the LDEF ranged from a low of 39°F to a maximum of 134°F and were well within design specifications. External thermal profiles varied greatly, depending on orientation, absorptance/emittance, and material mounting and shielding. The thermal stability of the LDEF adds to the accuracy of existing thermal models and enhances our ability to model the LDEF thermal history, as well as other spacecraft.

The loss of specularity of silver Teflon thermal blankets, one of the earliest observations noted at the time of retrieval, was determined to have had no significant effect on the thermal performance of those materials. This loss of specularity is the result of first surface erosion and roughening by atomic oxygen.

The thermal performance (absorptance/emittance) of many surfaces was degraded by both line-of-sight and secondary contamination. The specific contamination morphology in various locations was affected by ultraviolet radiation and atomic oxygen impingement. Overall, the macroscopic changes in thermal performance from contamination appear to be moderate at worst. Limited measurements on surfaces from which the contamination was removed post flight suggest that the surfaces beneath the contamination layers have undergone minimal thermal degradation.

Over 50 percent of all LDEF's exterior surfaces were chromic acid anodized (CAA) aluminum. Extensive optical testing of LDEF's CAA aluminum tray clamps was performed because of their wide distribution around the LDEF and representation of a complete spectrum of spaceflight environmental exposures. The tray clamps provided a complete picture of the spaceflight environmental effects on this surface treatment. Comparison of front-side (exposed), backside (shielded) and control clamps showed slight changes in the optical properties. However, the variations in absorptance and emittance have been attributed to the inherent variability in anodizing, to variations in measurements, and to the effects of on-orbit contamination deposited on tray clamp surfaces.

Betacloth which was exposed to the atomic oxygen flux was seen to have been cleansed of the many minute fibers that normally adorn its surface. This has been observed to have no measurable effect on the thermal performance of the betacloth, although some associated contamination issues are raised.

Optical:

Contaminant films and residue were widespread in their migration over LDEF and onto optical experiment surfaces, especially due to the decomposition and outgassing of several materials, at least two possible sources being identified as those from the vehicle itself, as well as those materials used in some of the experiments.

Four experiments flew fiber optics and a fifth experiment evaluated fiber optic connectors. Four of these five experiments recorded on-orbit data using the NASA provided EPDS. Overall the fiber optics performed well on-orbit, with little or no degradation to optical performance. Most environmental effects were confined to the protective sheathing. However, one fiber optic bundle was struck by a meteoroid or debris particle causing discontinuity in the optical fiber. Preliminary data has indicated the need for additional study of the temperature effects on fiber optical performance. Post-flight testing performed on fiber optics flown on the Fiber Optic Exposure Experiment showed an increase in loss with decreasing temperature, becoming much steeper near the lower end of their temperature range.

Four LDEF experiments contained a variety of detectors. Most detectors were not degraded, with one exception. The triglycine sulfide had a 100 percent detectivity failure rate on both the control and flight samples.

Several types of optical sources were flown on LDEF including solid and gas lasers, flashlamps, standard lamps, and LEDs. To date, the results indicate that most optical sources operated nominally except for two gas lasers (HeNe and CO_2) which would not fire during post-flight testing and a flickering deuterium lamp arc. During post-flight testing of the two gas lasers, no laser action could be obtained from the tubes. The characteristics of the tubes suggested that the mixture of fill gas had changed during the period between pre-flight and post flight tests. This result is consistent with changes expected due to gas diffusion through the glass tube. The tubes were in good physical condition, and survived the launch and recovery phases without apparent degradation.

Micrometeoroid and debris impacts on optical surfaces caused localized pitting, punctures, cracking, crazing, and delaminations.

Spectral radiation from both solar and Earth albedo sources was indicated in the modifications of surface coating materials (chemical decomposition caused by ultraviolet radiation). This was particularly noticeable on an experiment located on the trailing edge where the holographic gratings had a 30 percent to 40 percent degradation of reflectivity from exposure to solar radiation and cosmic dust. Experimenters also noted that changes to coating interfaces as a result of infrared absorption may have contributed to mechanical stresses and failures from thermal cycling.

Atomic oxygen had a major effect in the oxidation of many physically "soft" materials, including optical coatings and thin films, as well as oxidation of uncoated, metallic reflective coatings (copper and silver). In general, "hard" uncoated optical materials were found to be resistant to the LEO environment.

Synergistic conditions of degradation resulted from the multiple and combined effects of environmental factors; for instance, UV and atomic oxygen attacked, changed, or even eroded away some of the overlaying contamination, modifying the broadband and spectral content of optical inputs to the sample beneath.

An LDEF Optical Experiment Database was created (using Filemaker Pro database software) that provides for quick and easy access to available experimenter's optic's related findings. The database contains a file for each of the LDEF experiments that possessed optical hardware (database currently contains 29 files). Each file contains various fields that identify the optical hardware flown, describe the environment seen by that hardware, summarizes experimenter findings and list references for additional information.

REPORT DOCUMENTATION PAGE

Form Approved
OMB No. 0704-0188

1. AGENCY USE ONLY (*Leave blank*)	2. REPORT DATE	3. REPORT TYPE AND DATES COVERED
	September 1995	Contractor Report

4. TITLE AND SUBTITLE
Analysis of Systems Hardware Flown on LDEF - New Findings and Comparison to Other Retrieved Spacecraft Hardware

5. FUNDING NUMBERS
C NAS1-19247
TA 18
WU 233-03-02-02

6. AUTHOR(S)
Harry Dursch, Gail Bohnhoff-Hlavacek, Donald Blue, Patricia Hansen

7. PERFORMING ORGANIZATION NAME(S) AND ADDRESS(ES)
Boeing Defense & Space Group
P.O. Box 3999
Seattle, WA 98124-2499

8. PERFORMING ORGANIZATION REPORT NUMBER

9. SPONSORING / MONITORING AGENCY NAME(S) AND ADDRESS(ES)
National Aeronautics and Space Administration
Langley Research Center
Hampton, VA 23681-0001

10. SPONSORING / MONITORING AGENCY REPORT NUMBER
NASA CR-4693

11. SUPPLEMENTARY NOTES
Contracting Officer's Technical Monitor: Joan G. Funk
Technical Monitor: James Mason (NASA-GSFC)

12a. DISTRIBUTION / AVAILABILITY STATEMENT
Unclassified - Unlimited
Subject Category 18

12b. DISTRIBUTION CODE

13. ABSTRACT (*Maximum 200 words*)

The Long duration Exposure Facility (LDEF) was retrieved in 1990 after spending 69 months in low-Earth-orbit (LEO). A wide variety of mechanical, electrical, thermal, and optical systems, subsystems, and components were flown on LDEF. The Systems Special Investigation Group (Systems SIG) was formed by NASA to investigate the effects of the 60 month exposure on systems related hardware and to coordinate and collate all systems analysis of LDEF hardware. This report is the Systems SIG final report which updates earlier findings (published in April 1992, NASA CR-189628) and compares LDEF systems findings to results from other retrieved spacecraft hardware such as Hubble Space Telescope. Also included are sections titled; 1) Effects of Long Duration Space Exposure on Optical Scatter, 2) Contamination Survey of LDEF, and 3) Degradation of Optical Materials in Space.

14. SUBJECT TERMS
LDEF, low Earth orbit, spacecraft systems, Optical scatter, Contamination, Space4craft optics, Hubble Space Telescope

15. NUMBER OF PAGES
106

16. PRICE CODE
A06

17. SECURITY CLASSIFICATION OF REPORT	18. SECURITY CLASSIFICATION OF THIS PAGE	19. SECURITY CLASSIFICATION OF ABSTRACT	20. LIMITATION OF ABSTRACT
Unclassified	Unclassified	Unclassified	UL